

THE EFFECT OF TEMPERATURE ON CONSOLIDATION BEHAVIOR OF CLAY

FOR REFERENCE

REMOVED FROM THIS ROOM

Thesis by

MUHAMMET AHMET TUNCAN

B.S. in C.E., Esk.D.M.M.Akademisi, 1981

Submitted to the Institute for Graduate Studies in
Science and Engineering in partial fulfillment of
the requirements for the degree of

Master of Science

in

Civil Engineering

Bogazici University Library



39001100374464

14

Boğaziçi University

Bebek - Istanbul

July - 1984

ACKNOWLEDGEMENT

I would like to express my sincere gratitude to Doç. Dr. Erol Güler, for his very kind interest and help in the planning and running the stages of experiments, and in the evaluation of results.

I also would like to thank Mr. Isa Kul, and Mr. Mustafa Tuncan for helping me preparing the test apparatus.

Finally, I would like to give my special thanks to Mr. Mustafa Şen for his undertaking the difficulty of typing the manuscript.

M. Ahmet Tuncan

A B S T R A C T

THE EFFECT OF TEMPERATURE ON CONSOLIDATION BEHAVIOR OF CLAY

The influence of increasing the temperature in a consolidating soil is examined by consideration of the thermal energy input from the temperature change. This energy provides the potential necessary to cause flow through physical changes in the pore water and the soil-water interface. A consolidometer was designed to provide temperature changes through a heating element and the temperatures being measured by a thermostat in the water. The level of temperatures were chosen as 20°C, 40°C, 60°C, and 80°C. Each temperature level was allowed to remain on the specimen for 24 hours.

It was observed that the magnitude of the resulting deformation depended directly on the magnitude of the temperature increase. Void ratio is effected by change in temperature between the range of 20°C to 40°C the most. Changes between the range of 40°C to 60°C, and 60°C to 80°C have lesser effects respectively. The coefficient of consolidation increases with temperatures in the range of 20°C to 40°C and 40°C to 60°C, but decreases at temperatures in the range of 60°C to 80°C.

Ö Z E T

Konsolide bir zeminde sıcaklık artışının etkisi sıcaklık değişmesinden dolayı termal enerji girişinin dikkate alınması ile gözlenir. Bu enerji zemin-su yüzeyinde ve boşluk suyundaki fiziksel değişmelerden dolayı akışa sebep olan gerekli potansiyeli sağlar. Bir ısı elemanı vasıtasıyla sıcaklık değişmelerini sağlamak ve su içindeki bir termostat ile sıcaklık derecelerini ölçmek için bir konsolidometre tertip edildi. Sıcaklık seviyeleri 20°C, 40°C, 60°C ve 80°C olarak seçildi. Her sıcaklık seviyesinin numuneye uygulanmasına 24 saat mücade edildi.

Sonuç deformasyon büyüklüğünün direk olarak sıcaklık artışının büyüklüğüne bağlı olduğu gözlemlendi. Boşluk oranı en fazla 20°C ile 40°C arasındaki sıcaklık değişmesi ile etkilenir. 40°C ile 60°C ve 60°C ile 80°C arasındaki değişikliklerde sırasıyla daha az etkiye sahiptirler. Konsolidasyon katsayısı 20°C ile 40°C ve 40°C ile 60°C arasındaki sıcaklıklarda artar, fakat 60°C ile 80°C arasındaki sıcaklıklarda azalır.

TABLE OF CONTENTS

Acknowledgement	iii
Abstract	iv
Özet	v
List of Figures	viii
List of Tables	xii
List of Symbols	xiii
Chapter 1 INTRODUCTION	1
Chapter 2 PREVIOUS RESEARCH	3
A. STRUCTURE OF CLAYS	3
1. Definition	3
2. Shape and Surface Area	3
3. Adsorb Water	5
4. Double Ionic Layer	7
5. Compression and Swelling of Clay	7
B. CONSOLIDATION THEORY	10
1. Definition	10
2. Assumptions Made	10
3. The Coefficient of Consolidation	13
C. EVALUATION OF HEAT FLOW-CONSOLIDATION EFFECT	21
Chapter 3 TESTING PROCEDURE	36
A. MATERIAL	36
1. Clay with Low Plasticity	36
2. Clay with High Plasticity	36

B. MINEROLOGICAL PROPERTIES OF CLAY USED ...	37
G. EQUIPMENT	39
D. MATERIAL AND SAMPLE PREPARATION	44
1. Grain Size Distribution Diagrams	45
E. TESTING	48
F. EVALUATION OF TEST RESULTS	49
1. Calculation of Void Ratio	49
2. Calculation of Coefficient of Consoli- dation	50
3. Expansion of Brass Ring	53
Chapter 4 TEST RESULTS	55
A. CLAY WITH LOW PLASTICITY	55
B. CLAY WITH HIGH PLASTICITY	79
C. INTERPRATATION OF TEST RESULTS	103
Chapter 5 CONCLUSIONS	112
REFERENCES	113

LIST OF FIGURES

FIGURE

- 2.1 Edge-View Sketches to Show Relative Size and Shape of Clay Particles.
- 2.2 Distribution of Attractive Forces within the Adsorbed Water Layer.
- 2.3 Schematic Diagram of Clay Particle with Adsorbed Water Layer and Some Cations at the Surface, and the Remainder of the Exchangeable Cations in the Diffuse Ion-layer.
- 2.4 Particle Surrounded by a Double Diffuse Layer.
- 2.5 Settlement of a Soil Sample.
- 2.6 Idealization of Soil and Fluid Flow for Development of the One-dimensional Theory of Consolidation.
- 2.7 Excess Pore Pressure Distribution Assumptions for an Increased Effective Stress within a Stratum and Qualitative Pore Pressure Distribution as a Function of Elapsed Time.
- 2.8 Effect of Temperature on Coefficient of Consolidation.
- 2.9 Effect of Temperature on Coefficient of Consolidation.
- 2.10 Effect of Temperature on the Compression Curve.
- 2.11 Schematics of a Temperature Controlled Consolidometer.
- 2.12 Strain vs. Time: Long Time--Low Temperature Rise.
- 2.13 Strain vs. Time: Long Time--High Temperature Rise.
- 2.14 Strain vs. Time: High, Rapid Temperature Rise.
- 3.1 Schematic of a Temperature Controlled Consolidometer.

- 3.2 Consolidometer.
- 3.3] Consolidometer and Loading Device.
- 3.4]
- 3.5 Grain Size Distribution Diagram for Topser-Yellow.
- 3.6 Grain Size Distribution Diagram for Boğazköy-Grey.
- 3.7 Plot of Strain vs. Log Time.
- 3.8 Expansion of the Ring.
- 4.1]
- 4.2] Plot of DR. vs. Log time (min) for 1.00 kg/cm² (Topser-
- 4.3] Yellow)
- 4.4]
- 4.5 Effect of Temperature on Coefficient of Consolidation,
for 1.00 kg/cm². (Topser-Yellow)
- 4.6 Effect of Temperature on Void Ratio, for 1.00 kg/cm².
(Topser-Yellow)
- 4.7 Effect of Temperature on the Compression Curve, For
1.00 kg/cm². (Topser-Yellow)
- 4.8]
- 4.9] Plot of DR. vs. Log time (min), for 2.00 kg/cm².
- 4.10] (Topser-Yellow)
- 4.11]
- 4.12 Effect of Temperature on Coefficient of Consolidation,
for 2.00 kg/cm². (Topser-Yellow)
- 4.13 Effect of Temperature on Void Ratio, for 2.00 kg/cm².
(Topser-Yellow)
- 4.14 Effect of Temperature on the Compression Curve, for
2.00 kg/cm². (Topser-Yellow)

4.15
4.16
4.17
4.18

Plot of DR. vs. Log time (min) for 4.00 kg/cm².
(Topser-Yellow)

- 4.19 Effect of Temperature on Coefficient of Consolidation, for 4.00 kg/cm². (Topser-Yellow)
- 4.20 Effect of Temperature on Void Ratio, for 4.00 kg/cm². (Topser-Yellow)
- 4.21 Effect of Temperature on the Compression Curve, for 4.00 kg/cm². (Topser-Yellow)

4.22
4.23
4.24
4.25

Plot of DR. vs. Log time (Min), for 1.00 kg/cm².
(Boğazköy-Grey)

- 4.26 Effect of Temperature on Coefficient of Consolidation, for 1.00 kg/cm². (Boğazköy-Grey)
- 4.27 Effect of Temperature on Void Ratio, for 1.00 kg/cm². (Boğazköy-Grey)
- 4.28 Effect of Temperature on the Compression Curve, for 1.00 kg/cm². (Boğazköy-Grey)

4.29
4.30
4.31
4.32

Plot of DR, vs. Log time (min), for 2.00 kg/cm².
(Boğazköy-Grey)

- 4.33 Effect of Temperature on Coefficient of Consolidation, for 2.00 kg/cm². (Boğazköy-Grey)
- 4.34 Effect of Temperature on Void Ratio, for 2.00 kg/cm². (Boğazköy-Grey)

- 4.35 Effect of Temperature on the compression Curve, for
2.00 kg/cm². (Boğazköy-grey)
- 4.36]
4.37] Plot of DR. vs. Log time (min), for 4.00 kg/cm².
4.38] (Boğazköy-Grey)
4.39]
- 4.40 Effect of Temperature on Coefficient of Consolidation,
for 4.00 kg/cm². (Boğazköy-Grey)
- 4.41 Effect of Temperature on Void Ratio, for 4.00 kg/cm².
(Boğazköy-Grey)
- 4.42 Effect of Temperature on the Compression Curve, for
4.00 kg/cm². (Boğazköy-Grey)
- 4.43 The Family of Temperature-Void Ratio Curves, for
Topser-Yellow.
- 4.44 The Family of Temperature-Coefficient of Consolidation
for Topser-Yellow.
- 4.45 The Family of Temperature-Void Ratio Curves, for
Boğazköy-Grey.
- 4.46 The Family of Temperature-Coefficient of Consolidation
for Boğazköy-Grey.

LIST OF TABLES

TABLE

- 2.1 Time Factor for Identical Pressure Distribution.
- 4.1 Results of Tests Conducted on Topser Yellow Clay.
- 4.2 Results of Tests Conducted on Boğazköy Grey Clay.

LIST OF SYMBOLS

SYMBOL

A (cm^2)	= Area of the oedometer ring.
a_v (cm^2/kg)	= Coefficient of compressibility.
C_s	= Heat capacity of water.
C_v (cm^2/sn)	= Coefficient of consolidation.
C_w	= Heat capacity of water.
D (cm)	= Diameter of the ring.
D_0	= Initial dial reading.
D_1, D_2	= Constant.
D_{50}	= Dial reading corresponding to 50 percent consolidation.
D_{100}	= Dial reading corresponding to 100 percent consolidation.
Δd	= The increase in diameter.
e	= Void ratio.
Δe	= Increment of void ratio.
H (cm)	= Average length of the longest drainage path during the given load increment.
H_d (cm)	= Average drainage length.
H_s	= Height of soil solids.
H_v	= Height of voids.
ΔH	= Increment of the drainage length.
h	= Hydraulic head.
i	= Hydraulic gradient.

k	= Coefficient of permeability.
L.L	= Liquid limit.
M_v (cm^2/kg)	= The coefficient of volume compressibility.
n	= Porosity.
p (kg/cm^2)	= Consolidation pressure.
P.L	= Plastic limit.
P.I	= Plasticity index.
Δp	= Increment of load.
Q, Q_1, Q_2	= Heat energy added to system, caused by temperature change, ΔT .
Q_{soil}	= Heat energy absorbed by soils, caused by temperature change, T .
Q_{tot}	= Total heat energy absorbed by soils water system, caused by temperature change, T .
Q_{water}	= Heat energy absorbed by pore water, caused by temperature change, T .
S	= Settlement of soil sample.
T_v	= Time factor.
ΔT	= Temperature difference.
t	= Time for the corresponding time factor T_v .
Δt	= The increase in temperature.
$U \%$	= Average percentage of consolidation.
u	= Pore - pressure.
V_s	= Volume of solids.
V_v	= Volume of voids.
V	= Velocity of water.
w	= Water content.
w_d	= Dry weight of soil.

w_{wi}	= Weight of wet soil.
x, y, z	= Rectangular co-ordinates.
z	= Depth in soil sample.
α	= Proportionality constant.
γ_s	= Unit weight of soil grains.
γ_w	= Unit weight of water.
ρ_s	= Mass density of soil.
ρ_w	= Mass density of water.
C_{vt}	= The C_v value obtained from the settlement vs time relation at an increase in temperature.

CHAPTER I INTRODUCTION

In the solution of many engineering problems it is necessary to improve the properties of soil, whether as a foundation material or as a material of construction in embankments, dams, and other artificial works. With this research we wanted to investigate whether it is possible to improve the mechanical behaviour of soft clay layers by heating them. Any foundation subject to sudden or continued temperature rises would be affected by an increase in strain if it is resting upon soft clay layer. Such structures as kilns, ovens, boilers, power plants, and liquified natural gas storage, all create temperature changes in the foundation soil. Thus, the soil beneath them would have to be investigated with respect to the effect of the temperature changes.

The theory that a consolidating soil is affected by temperature changes is known since a long time. Research papers on this subject fall into two general categories:

a - Consolidation of soil, assuming a fixed soil-water temperature.

b - Heat flow through a static soil-water system.

In addition to existing researches, we wanted to investigate the influence of changing soil-water temperature under constant load.

To investigate the probable settlement under the effect of temperature increase, we performed a series of consolidation tests on clay samples.

The consolidation tests were performed on two kind of laboratory prepared clay samples. The constant vertical loads applied to the specimens were 1.00, 2.00, 4.00 kg. per. sq. cm. For each load, the behaviour has been investigated for the following temperatures: 20, 40, 60, and 80°C. Each temperature level was allowed to remain on the same temperature for 24 hours.

CHAPTER 2 PREVIOUS RESEARCH

A. STRUCTURE OF CLAYS

1. Definition:

Clay particles are usually of small size less than two microns and most clay minerals are thin flat plates. all are extremely fine grained, with large surface areas per unit mass. Particles with a diameter smaller than 0.001 mm. but larger than molecular size (10^{-6} mm) are classified as colloids. Clay particles fall into this range. Nearly all clay particles are colloidal even though the maximum particle dimensions of several of the clay minerals is greater than 0.001 mm. (1)

2. Shape and Surface Area:

A schematic comparison of the size, shape, and surface area of several clay minerals is shown in fig. 2.1. Plate-shaped particles are the result of layer-lattice structure due to strong bonding along two axes, but weak bonding between layers. The clay particles thickness depends on the magnitude of the forces of attraction between the layers. The variation in specific surface area is due to different thickness of the plate-shaped particles. Montmorillonite layer is in the average (10 \AA) thick. Usually a clay particle was several layers. Variation in the other two dimension of clay particles is related to degree of crystallinity

of the clay minerals. A well-crystallized kaolinite has large particles; if it is poorly crystalline the particles has no larger than those of montmorillonite. In general, the smallest surface area is that of kaolinite (about $15 \text{ m}^2 / \text{g}$). Illite has a higher specific surface area and a higher activity. Montmorillonite has the highest specific surface area and activity. (1)

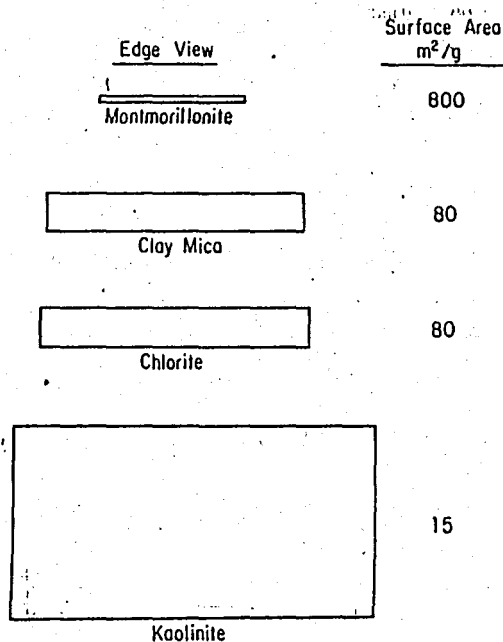


Fig. 2.1 - Edge-View Sketches to Show Relative Size and Shape of Clay Particles; Dimension Not Shown Is Equal to Length.

3. Adsorb Water:

The property of attracting and holding solvent materials, ions, gas and water on the surfaces of the particles is termed adsorption. Clay particles in soils are always surrounded by layers of water molecules called adsorbed water. Plasticity, compaction, interparticle bonding and water movement in soils are all influenced by the water layers. The forces holding water molecules to the clay surface arise between water and clay. Water is a dipolar molecule, with a separation of centers of positive and negative charge. This means that water will be attracted by the charges on the clay surface. Further, the hydrogen bonds of water will lead to hydrogen bonding of water molecules to the exposed oxygen atoms of the clay mineral surface. Hence the clay contributes both the negative charge and oxygen or hydroxyl surface to attract water molecules. Cations in water are always hydrated. The main force bonding water to the surface is due to the hydrogen bond. This is a very important bond in many natural materials. The first layer of water molecules is held by hydrogen bonding to the clay surface. The second water layer is held to the first, again by hydrogen bonding, but the force becomes weaker with distance as the orienting influence of the surface on the water close to the clay surface differ from those of free water. The density of adsorbed water is higher than that of free water. The viscosity of this water is greater than that of free water. The adsorbed water is very strongly attracted to the surface of the soil particles.

Within the adsorbed water layer, water molecules are orientated in such a manner that the positive poles are facing the anions on the surface of the particles, and the negative poles are facing the cations present in the adsorbed water layer. The clay particle with its layer of adsorbed water and diffuse layer of exchangeable cations can be illustrated in fig. 2.2 and fig. 2.3. (2)

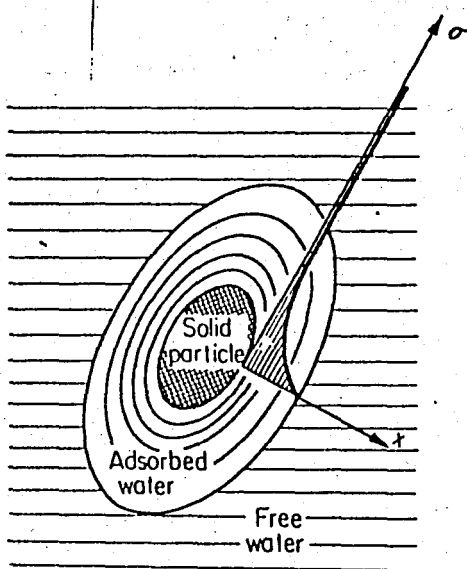


Fig. 2.2 - Distribution of attractive forces within the adsorbed water layer: σ , attractive forces; x , distance from the particle surface.

4. Double Ionic Layer:

Because a solid particle is surrounded by the oriented water dipoles, the electric charge of the surface ions is not electrostatically balanced. To achieve the balance, ions must be adsorbed from the water solution present in the pores. However, the attracted cations cannot form a single layer around a particle, because they themselves are surrounded by water molecules which prevent them from packing closely together, and hence they are distributed (diffused) through a certain layer, with the greatest concentration close to the particle surface, gradually decreasing until the normal concentration of the pore water solution is reached. This layer is known as a diffuse layer. Fig. 2.4. The diffuse layer of cations together with the surface layer of anions is called a double diffuse layer. (2)

5. Compression and Swelling of Clay:

The physico-chemical properties of clay minerals are of great value in understanding the mechanical behavior of clay on the macro-scale. A number of interesting investigations have illuminated the compression and swelling of clays. Considering consolidation test in which the applied stress is steadily increased, the increasing stress compresses the clay. If the clay particles are perfectly parallel to each other, the compression results in pushing the clay particles closer and closer together.

As the stress is gradually reduced, the clay swells as the particles move apart. The mechanism of compressibility and swelling is related to the equilibrium of water content in the soil. The phenomenon of compressibility is accompanied not only by the change in water content but also by the decrease in the distance between the soil particles and hence by the change in the magnitude of the attractive forces between soil particles which result further compression. (3)

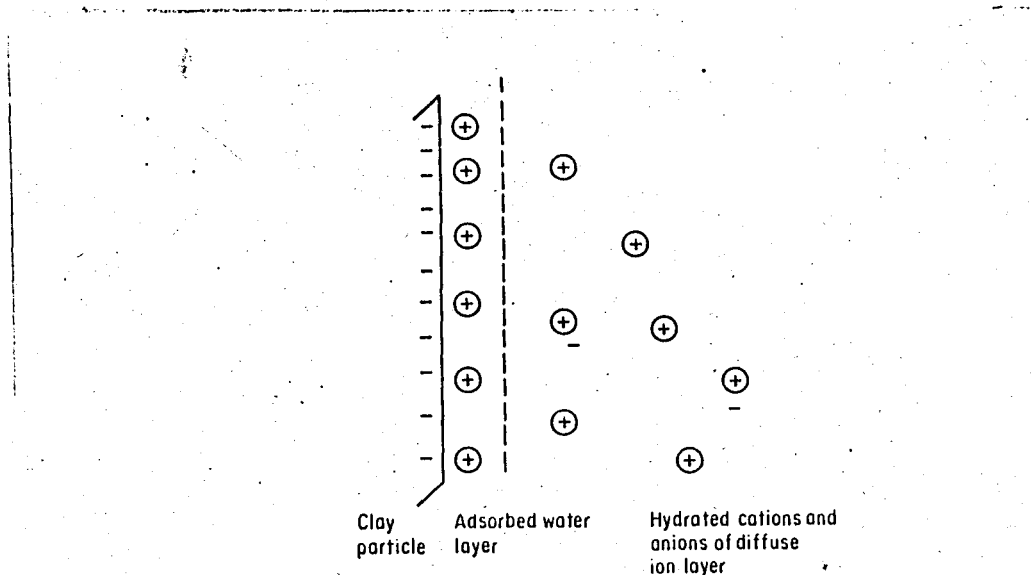


Fig. 2.3 - Schematic Diagram of Clay Particle with Adsorbed Water Layer and Some Cations at the Surface, and the Remainder of the Exchangeable Cations in the Diffuse Ion-Layer.

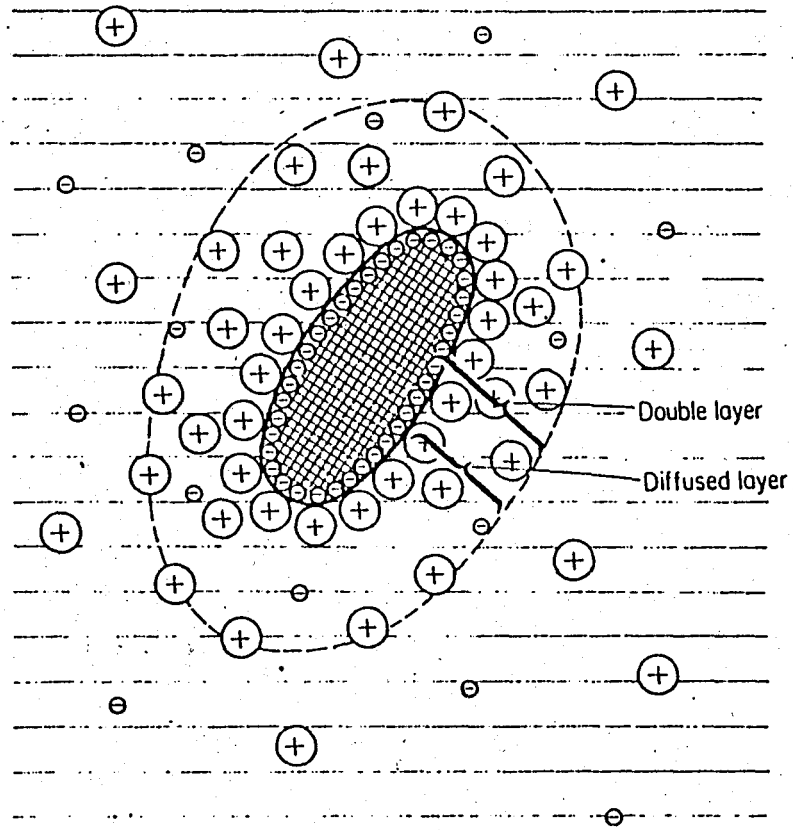


Fig. 2.4 - Particle surrounded by a double diffuse layer.

B. CONSOLIDATION THEORY

1. Definition:

The compression of soil occurs mainly as a function of a decrease of the volume of the voids. If the voids of a soil are entirely filled with water, measurable compression can occur only as a result of the escape of excess water from the voids. Gradual compression of a soil under such conditions, when induced by static forces of gravity, such as the weight of the soil itself or of structures erected upon it, is termed consolidation. If the saturated soil is a clay with low permeability, its consolidation will be quite slow, since any excess water in the voids will take time to be squeezed out toward pervious boundaries of the clay layer. The consolidation of saturated clay under load can be divided into two parts. Primary consolidation during which free water is squeezed out the void spaces, and secondary consolidation during which some of the highly viscous water between the points of contact is squeezed out from between the grains. (4)

2. Assumptions Made:

The theoretical concept of the consolidation process for saturated clays under load was stated and a mathematical statement for the progress of consolidation was developed by Terzaghi and Frölich during the decade between 1910 and 1920 while at the University of Vienna. In consolidation theory the following assumptions are made: (5,6)

- 1- The soil is completely saturated.
- 2- Water and soil grains are incompressible.
- 3- Darcy's law is valid ($V = k \cdot i$)
- 4- consolidation is one dimensional (Vertical), that is, there is no lateral flow of water or soil movement.
- 5- There is a constant temperature. A change in temperature from about 10 to 20°C (typical field and laboratory temperature, respectively) results in about a 30 percent change in the viscosity of water.

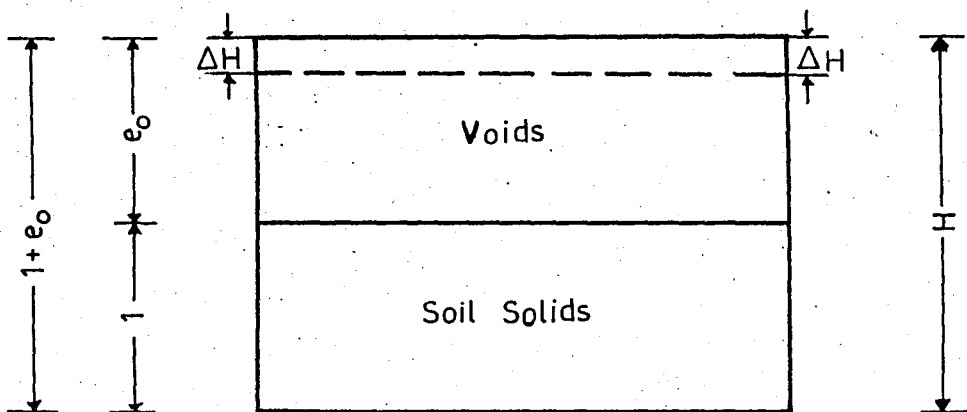


Figure 2.5. Settlement of a soil sample.

The degree of compressibility of a soil is expressed by the compressibility coefficient a_v .

$$a_v = \frac{\Delta e}{\Delta p} = \frac{e_0 - e}{p - p_0} \quad \text{cm}^2/\text{kg} \quad (1)$$

If $P > P_0$, a_v is a compressibility coefficient.

If $P < P_0$, a_v is a swelling coefficient.

The decrease in volume is the settlement of the soil.

Hence the void ratio also varies with the load. The time-dependent settlement of a layer of soil can be computed using consolidation parameters (refer to fig.2.5.) as follows:

By proportion,

$$\frac{\Delta H}{H} = \frac{\Delta e}{1 + e_0} \quad (2)$$

or the settlement,

$$\Delta H = \frac{\Delta e}{1 + e_0} \times H$$

$$\Delta H = \frac{e_0 - e_1}{1 + e_0} \times H$$

$$\Delta H = \frac{a_v}{1 + e_0} \times \Delta P \times H \quad (3)$$

Another coefficient, the modulus of volume change M_v , is frequently used.

$$M_v = \frac{a_v}{1 + e_0} \quad \text{cm}^2/\text{kg} \quad (4)$$

3- The Coefficient of Consolidation:

The second consolidation parameter of interest at a consolidation test is the coefficient of consolidation C_v . The equation for C_v is developed based on one-dimensional flow and saturated soil conditions. Since consolidation under these conditions is directly dependent on the extrusion of pore water from the soil voids, one may develop the needed equations by considering continuity of flow (fig.2.6.) as (6)

$$Q_{in} = V_y \times dx \times dz \times dt$$

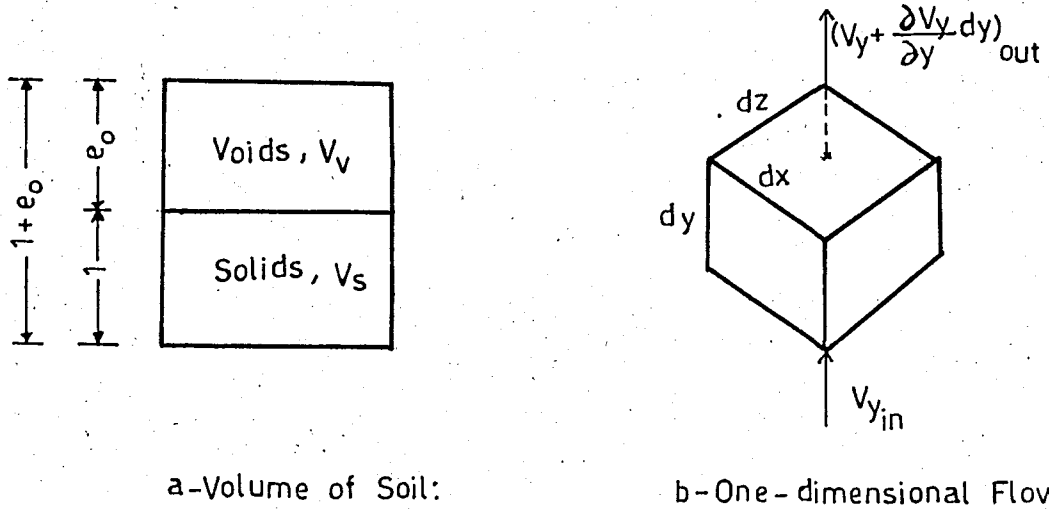
$$Q_{out} = (V_y + \frac{\partial V_y}{\partial y} dy) dx \times dz \times dt$$

and the volume change as a rate process is

$$\text{Volume Change} = \frac{\partial V}{\partial t} dt = Q_{out} - Q_{in}$$

Equating as indicated, one obtains

$$\frac{\partial V_y}{\partial y} dy dz dx dt = \frac{\partial V}{\partial t} dt \quad (a)$$



a-Volume of Soil:

b-One-dimensional Flow:

Figure: 2.6. Idealization of soil and fluid flow for development of the one-dimensional theory of consolidation.

Since the soil grains and water are incompressible for all practical purposes and for the pressures involved, the change in volume must be due to a change in the volume of soil voids, or,

$$\frac{\partial v}{\partial t} = \frac{\partial V_V}{\partial t} \quad (b)$$

The definition of void ratio gives

$$V_V = e \times V_S$$

and differentiating with respect to time and using the product rule, obtain

$$\frac{\partial V_V}{\partial t} = e \frac{\partial V_S}{\partial t} + V_S \frac{\partial e}{\partial t}$$

Observing that $e(\partial V_S / \partial t) = 0$, since there is no change in the volume of soil grains, we have

$$\frac{\partial v_v}{\partial t} = v_s \frac{\partial e}{\partial t} \quad (c)$$

From fig.2.6. note that $V_s / V = 1/1+e$, and solving for V_s , obtain

$$V_s = \frac{V}{1+e} = \frac{dx dy dz}{1+e} \quad (d)$$

Substituting Eq.(d) into Eq.(c) and multiplying by dt,

$$\frac{\partial V}{\partial t} dt = \frac{dx dy dz}{1+e} \times \frac{\partial e}{\partial t} dt \quad (e)$$

Substituting Eq.(e) into Eq.(a) and cancelling the product of the four differentials, obtain

$$\frac{\partial v_y}{\partial y} = \frac{1}{1+e} \frac{\partial e}{\partial t} \quad (f)$$

There is a linear relationship between applied pressure and volume change, and noting that volume change depends on pore water extrusion from the soil voids when the soil is saturated, obtain

$$\frac{\partial e}{\partial t} = \frac{\partial e}{\partial p} \times \frac{\partial u}{\partial t} = a_v \times \frac{\partial u}{\partial t} \quad (g)$$

Where: $a_v = \frac{\partial e}{\partial p}$, the coefficient of compressibility.

U = pore water pressure.

From Darcy's law, the velocity of water is $v = k.i$, and with the total head $h = u/\gamma_w$, we have

$$\frac{\partial v_y}{\partial y} = \frac{k}{\gamma_w} \times \frac{\partial^2 u}{\partial y^2} \quad (h)$$

Where $n =$ any integer.

$y =$ depth into a stratum of length of drainage path H .

$H =$ length of longest drainage path in soil sample.

$T =$ dimensionless number termed a time factor, or

$$T = \frac{C_v \times T_i}{H^2} \quad (8)$$

For the case of constant (actually any linear variation) initial hydrostatic pressure Eq.(7) simplifies to

$$U = \sum_{m=0}^{\infty} \frac{2u_i}{M} \sin \frac{My}{H} \exp - M^2 T \quad (9)$$

Where $U_i =$ initial pore pressure distribution; use constant, linear variation, sine wave or $u_i = u_0 + u_1(H-y/H)$ as in fig.2.7.

$M = \frac{1}{2} \pi (2m+1)$, where m is any integer from 0 to ∞

Referring to fig.2.7. if we apply a pressure increment P to a fully saturated soil which has fully consolidated ($u=0$) under the existing pressure P_1 , the new total pressure is $P_2 = P_1 + P$. The pore water carries the load at $t=0$ (fig.2.7.a) since drainage is not instantaneous, and $u_i = P$ for $S=100$ percent. At $t=0$ the consolidation has just begun, or the percent consolidation $u = 0$ percent. At some times t_i (fig.2.7.b), the pore pressure patterns (isochrones) due to drainage being more rapid at or near the free surfaces are at, or approaching, zero as shown. At the free surfaces, $u=0$ and consolidation is complete ($u=100$ percent). At interior points the consolidation U_y would, by inspection of fig.2.7.b, be

$$U_y = \frac{u_e - u_i}{u_o} = 1 - \frac{u_i}{u_o} \quad (10)$$

$$U_y = 1 - \sum_{m=0}^{\infty} \frac{2}{M} \sin \frac{M \cdot y}{H} \exp -M^2 T \quad (11)$$

Eq. (10) is obtained by dividing Eq.(8) by u_o and subtracting 1, as indicated in Eq.(9). It is necessary to integrate u_y for the entire stratum thickness as

$$U = 1 - \frac{\int_0^{2H} u_i}{\int_0^{2H} u_o} \quad (12)$$

Substituting Eq.(8) in the numerator and u_o constant in the denominator of Eq.(12) gives.

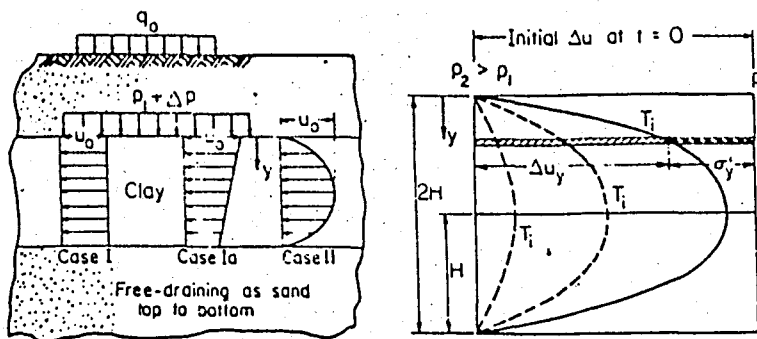
$$U = 1 - \sum_{m=0}^{\infty} \frac{y}{M^2} \exp -M^2 T \quad (13)$$

Often the first term (with $m=0$) provides a solution of sufficient precision for all in terms of percent consolidation U versus T by rearranging and solving Eq.(13) for T , to obtain

$$T \cong \frac{\ln(2/M^2) - \ln(1-U)}{M^2}$$

Note that the time factor T is not defined when $U = 1.00$, since the logarithm of 0 is ∞ . Selected solution of Eq.(13) are given in Table 2.1 (with $m > 0$) for several assumed initial pore-pressure distributions caused by a stress increased ΔP as shown.

Superposition of cases I and II or cases Ia and II provide solution for other pore pressure distributions. (6)



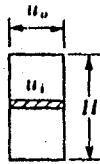
(a) Excess pore pressure distribution assumptions in consolidating clay layer with foundation load q_0 causing a stress increase from p_1 to $p_1 + \Delta p$.

(b) Pore pressure distribution with times T_i (noting $T = f(\text{time})$) and depth in stratum.

Fig. 2. 7 - Excess pore pressure distribution assumptions for an increased effective stress within a stratum and qualitative pore pressure distribution as a function of elapsed time.

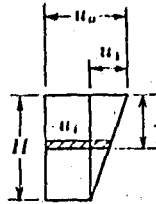
Table 2-1 Time Factors for Indicated Pressure Distribution

U(%)	Case I- I a	Case II
0	0.000	0.000
10	0.008	0.048
20	0.031	0.090
30	0.071	0.115
40	0.126	0.207
50	0.197	0.281
60	0.287	0.371
70	0.403	0.488
80	0.567	0.652
90	0.848	0.933
100		



$$u_i = u_u$$

Case I



$$u_i = u_u - u_i \frac{z}{H}$$

Case Ia



$$u_i = u_u \sin \frac{\pi z}{H}$$

Case II

Pore-pressure distribution for case I usually assumed for case Ia.

Table 2.1 - Time Factors for Indicated Pressure Distribution.

C- EVALUATION OF HEAT FLOW- CONSOLIDATION EFFECT

The first law of thermodynamics relates the change in heat energy to the change in internal energy of a substance and to the work done. In this way an energy balance and an evaluation of heat can be obtained for a given substance. To have a change in heat energy, either the result of process or the cause of one, it is necessary to apply some type of driving force or potential. One type of potential is a temperature difference defined by

$$\Delta T = T_i - T_j \quad (14)$$

Where $T_i \neq T_j$, ΔT = temperature difference, and T_i and T_j = temperature either at any two points in the body, or at one point at two different times. When this temperature difference, ΔT , occurs either over a particular sample distance, x , over a period of time, t , a temperature gradient ($\Delta T/x$ or $\Delta T/t$) is established. The heat energy, Q_{tot} , absorbed in a saturated soil of porosity, n , can be expressed in terms of an externally applied temperature source, ΔT , as

$$Q_{tot} = Q_{water} + Q_{solids} \quad (15)$$

Because

$$Q_{water} = c_w \cdot \rho_w \cdot n \cdot \Delta T \quad (16a)$$

and
$$Q_{\text{soil}} = c_s \cdot \rho_s \cdot (1-n) \Delta T \quad (16b)$$

then
$$Q_{\text{tot}} = (c_w \cdot \rho_w \cdot n + c_s \cdot \rho_s \cdot (1-n)) \Delta T \quad (17)$$

where:

- c_w = heat capacity of water,
- c_s = heat capacity of soil,
- ρ_s = Mass density of soil,
- ρ_w = mass density of water,
- n = porosity.

In this way it would be possible to determine the heat energy absorbed from a given temperature gradient for a soil whose physical characteristics are known.

In a consolidating soil, however, n would be changing and ΔT might also vary. It is evident that as the temperature gradient is increased, the heat input is increased. The porosity decreases, the heat absorbed by the system decreases. This is caused by the relatively high specific heat of water. During the consolidation process, the heat energy absorbed for a constant ΔT would decrease. Because the void decrease is a decay phenomena, and as indicated by Eq.(17), q is a linear function of n , then $Q(n(t))$ would also decrease with time for a constant ΔT . An applied temperature gradient causes a flow of water out of the system, which by nature and definition is a consolidation process. Basically, as the water becomes two major factors increase the rate of consolidation. First, the viscosity of the free pore-water decreases exponentially with T as

$$\mu = A \times e^{B/T} \quad (18)$$

With a smaller value of viscosity there is a decreased internal resistance to flow at points of higher temperatures. Secondly, the increase in heat energy will cause an increase in ionic movement of the adsorbed water films at the soil particle-water interface. To interpret the effects at temperature on consolidation, it is necessary to examine the physical changes in the soil as the voids decrease during a specific heat input. If the applied temperature difference is ΔT , and porosity at a given instant is n , using Eq.(17), let.

$$D_1 = c_w \cdot \rho_w \quad (18a)$$

$$D_2 = c_s \cdot \rho_s \quad (18b)$$

and
$$Q_{tot} = (n D_1 + (1-n) D_2) \Delta T \quad (19)$$

for
$$Q = \text{constant}$$

$$Q_1 = Q_2 = Q_c \quad (20)$$

$$(n_1 D_1 + (1-n_1) D_2) \Delta T_1 = (n_2 D_1 + (1-n_2) D_2) \Delta T_2 \quad (21)$$

and

$$\frac{\Delta T_1}{\Delta T_2} = \frac{n_2(D_1 - D_2) + D_2}{n_1(D_1 - D_2) + D_2} \quad (22)$$

From the above equations, D_1 and D_2 are constant, it can be seen that a decrease in voids, n , would necessitate an increase in temperature on the system to sustain the constant heat energy, Q , which results in the consolidation of the system. From (22), for a smaller porosity a greater temperature increase must be established to maintain a constant heat energy.

input. If the temperature is not increased as the voids decrease, i e., if the heat energy is not sustained, the potential necessary to continue the flow of water decreases. A sudden increase in potential (mechanical or thermal) would create an increase on the amount and rate of consolidation. However, as the energy level of the system becomes constant, the soil voids (and permeability) are decreasing.

This decay phenomenon would to the primary consolidation, where bulk flow through the voids predominated. However, in secondary consolidation changes in the soil-water behavior would also contribute to consolidation and a certain amount of energy will be dissipated at the soil-water interface. Whereas primary and secondary consolidation occur simultaneously, the first phases of pore pressure dissipation under large gradients might occur as a predominantly phase, whereas secondary consolidation may become a greater factor over large time periods. It might be possible to examine the effects of heat on secondary consolidation if the heat is increased and the nature of the change noted. The thermal energy applied would be changing the viscosity of the water and energy at the soil-water boundaries. However, because at this time hydrodynamic consolidation approaches 100 % and the pore-water pressure approaching zero, increase in consolidation would be mainly caused by an increase in ionic movement at the soil water interface, coupled with the decreased water viscosity. The result would be a decreased shearing resistance of the system as a whole.

whereas the exact nature of the influence of heat on a consolidating soil is difficult to define, the effect of such energy application can be measured as a gross effect or the total strain response to the temperature gradient.(7)

A number of studies have established that the engineering properties of soils can be influenced significantly by temperature variations. FINN (8) and PAASWELL (7) have investigated the effect of temperature on consolidation.

Finn has investigated the effect of temperature on the consolidation characteristics of remolded clay.

The consolidation tests have been performed in the laboratory where temperatures have been varied from 4.5°C to 27°C . The consolidation characteristics of a soil are evaluated by application of the Terzaghi theory of primary consolidation, which is based on a number of simplifying assumptions and approximations. To study the effect of temperature on the consolidation characteristics of clay, nine consolidation tests were performed by Finn; three tests at 20°C and two each at 4.5 , 10 , and 27°C . The limit space available in temperature controlled rooms made it necessary to use a relatively small and portable consolidometer. The soil used for the consolidation tests have a liquid limit of 64 percent and a plastic limit of 38 percent. The loads applied to the specimens develop pressures of 0.25, 0.50, 1.00, 2.00, 4.00, and 8.00 tons per sq ft and each load is allowed to remain on the specimen for 24 hours. Fig. 2.8. and fig.2.9. show the effect of temperature on the coefficient of consolidation. From these curves it can be seen that tests made at 20 and 27°C result

in coefficients of consolidation which are, for practical purposes, the same. Results of tests performed at temperatures of 10 and 4.5°C indicate a definite decrease in coefficient of consolidation as compared to 20°C values.

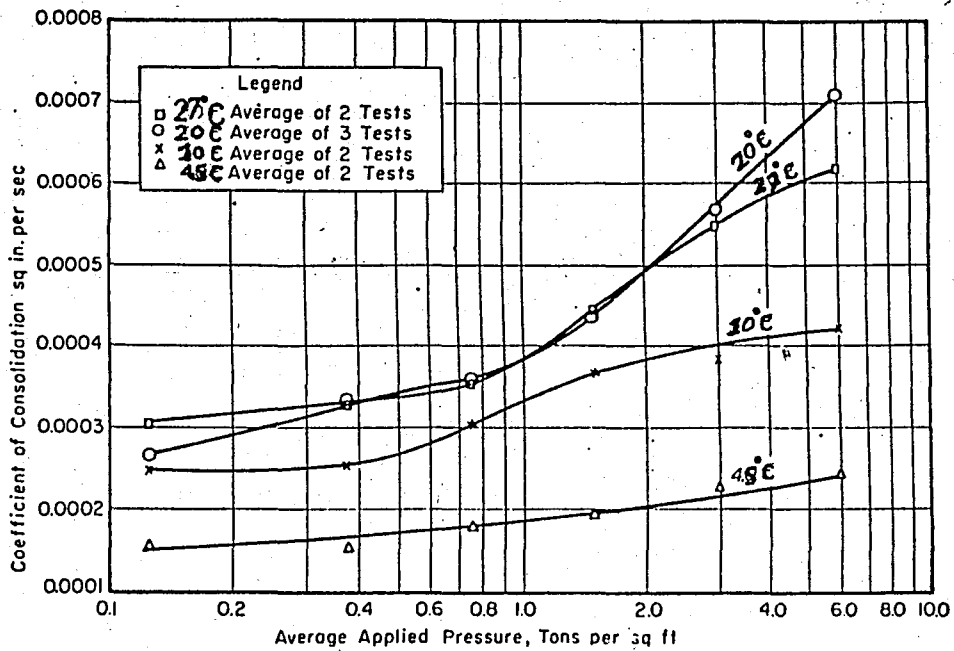


Fig. 2.8 - Effect of Temperature on Coefficient of Consolidation.

Fig. 2.9. indicates clearly that the temperature effect is more pronounced below a temperature of 10°C. The coefficient of consolidation is unaffected by temperature within the range of 20. to 27°C but is changed by a drop in temperature to 10°C or 4.5°C. In shown fig. 2.10, the family of pressure-void ratio curves obtained from the test plotted with temperature as a parameter.

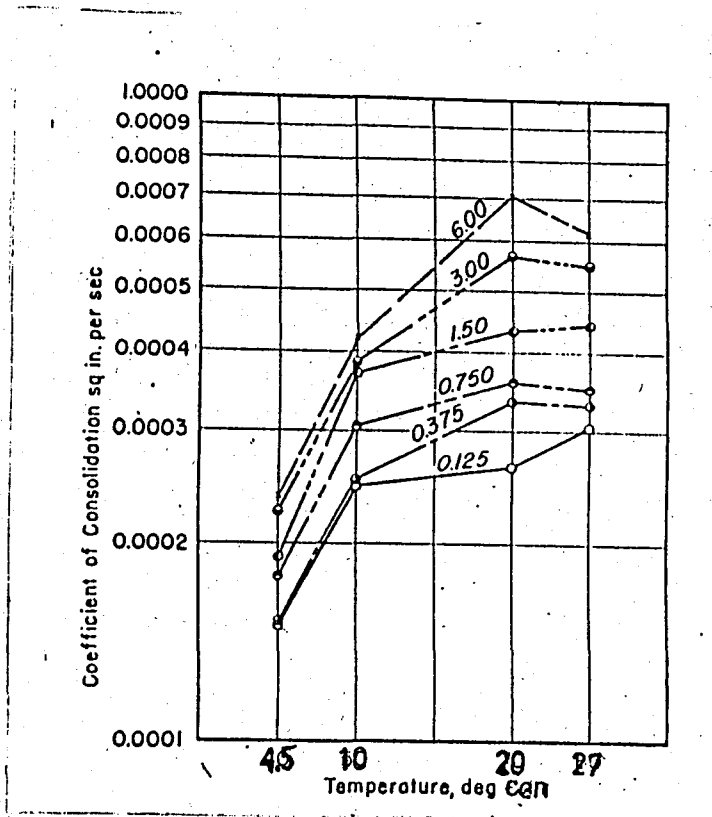


Fig. 2.9 - Effect of Temperature on Coefficient of Consolidation. Average Applied Pressure in Tons per sq ft as a Parameter.

It is apparent that these curves are of the same general shape along a considerable part of their length. A general interpretation of this relationship would mean that for any specific pressure increment the amount of compression is the same regardless of temperature. Hence it can be concluded that none of the factors in Eq.23. is effected by temperature.

$$S = H \cdot \Delta P \cdot m_v$$

(23)

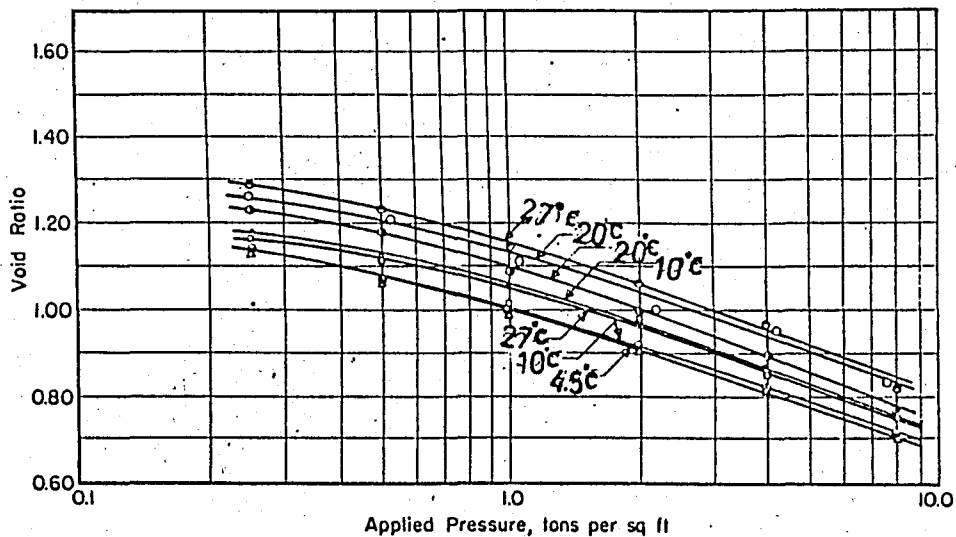


Fig. 2.10 - Effect of Temperature on the Compression Curve.

Void ratio determinations and determinations relating to the coefficient of volume compressibility are not effected by change in temperature between the range of 27 and 4.5°C.

Paaswell (7) has investigated the temperature effects on clay soil consolidation. The influence of increasing the temperature in a consolidating soil is examined by consideration of the thermal energy input from the temperature change. This energy provides the potential necessary to cause flow through physical changes in the pore water and the soil water interface. A fixed ring consolidometer was designed to accommodate a heating element in the water bath which surrounded the sample in fig. 2.11.

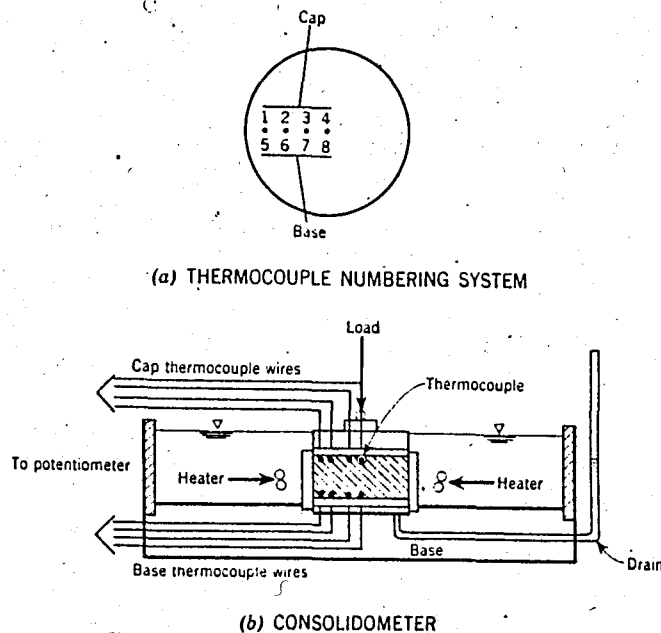


Fig. 2.11 - Schematics of a Temperature Controlled Consolidometer.

This design allow a high degree of control over the magnitude and rate of temperature rise on the surface of the sample. Temperature is measured by calibrated copper-contantan thermocouples. These fine wire thermocouples are positioned at the top and bottom drainage surfaces of the soil sample. The soil chosen is penn soil, compacted to the given density. The procedure used for the tests consist of loading the soil, at a fixed temperature (25°C), in increments, until the desired stress level is obtained .

At this level the strain rate is observed, and when consolidation is considered complete, a temperature rise is established at the surfaces of the sample. These temperature rises are of three types: Low temperature-long time, high temperature-long time, and high temperature-rapid time.

Long time - low temperature rise:

This test series have been investigated the effects of a small temperature rise ($T=10^{\circ}\text{C}$, from 20°C to 30°C) over a period of 2 hr to 2-1/2 hr (4°C per hr - 5°C per hr) by Paaswell. In figs. 2.12(a) - 2.12 (d) it can be seen that the change in the percentage of strain vary from 0.1 % under a stress of 0.2 kg. per. cm^2 to 0.225 % under a stress of 1.55 kg. per. cm^2 . This indicates that the effect of temperature rise becomes more marked as the stress level increases. The slope of the strain-time curve closely approximates in shape the slope of the temperature-time curves. The slope of the temperature-time curve indicates a relatively slow initial temperature increase (from $t= 0$ min to 20 min), followed by a more rapid temperature increase during a period from 20 min, to 90 min, then followed by a decreasing approach to the final temperature at a period of 2 hr to 2-1/2 hr after inception of the change. The increase in consolidation is caused by a constantly increasing heat energy level within the entire system.

Long time - high temperature rise:

When there is a large temperature increase in the soil ($\Delta T= 30^{\circ}\text{C}$), the strain effects become more pronounced. Changes in the specimen become marked both with respect to time and space.

The evidence of this is illustrated in figs. 2.13(a) to 2.13(d), which plot both the percentage of strain and of temperature as a function of time, for various load levels. ($P = 0.39$ kg per cm^2 to $P = 3.12$ kg per cm^2).

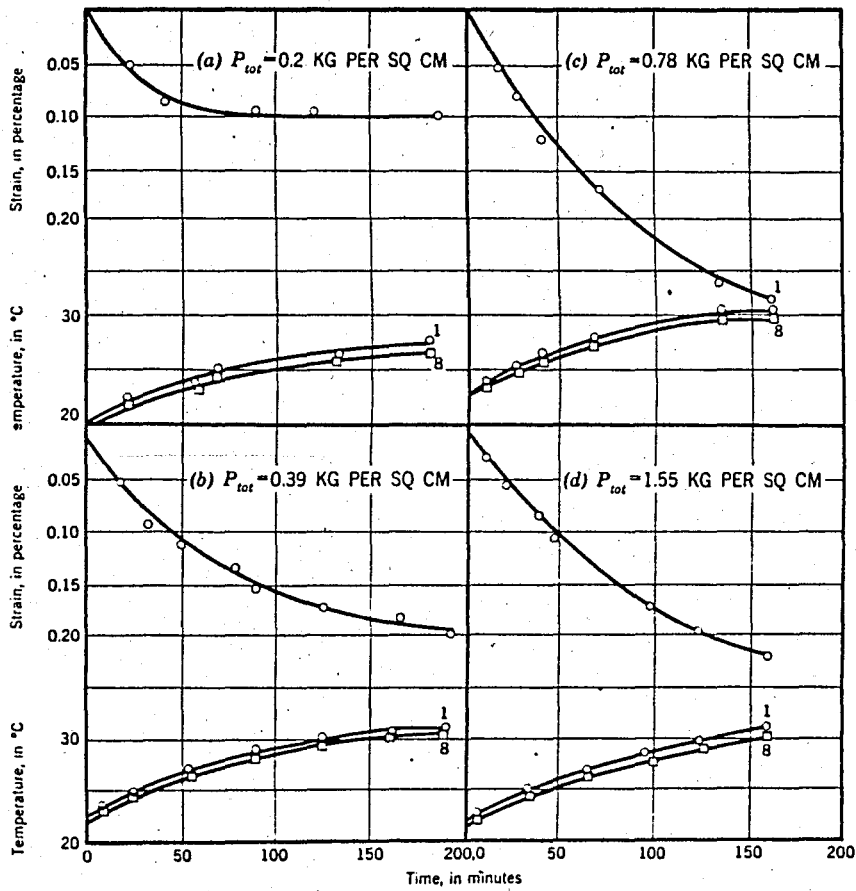


Fig. 2.12 Strain Versus Time: Long Time, Low Temperature Rise.

The temperature rise vary from 25 - 30°C to 55 - 60°C, and occur over a period of 4 hr to 5 hr. Whereas in each case the temperature have reached 95 % of more of its final value after 3 hr, the strain do not reach 95 % of its final value until 4 hr to 4 - 1/2 hr have passed. The total amount of strain in the high temperature rise tests vary from 0.9 % to 1.15 %. As the expected amount of strain for a constant temperature test ($T = 30^{\circ}\text{C}$) for this same time period 4 hr is less than 0.02 %, it is evident that the temperature has caused a marked change in strain in the consolidation process. Over the surface of the sample there is a slight temperature lag between surface points 1 and 8. This lag vary from 1°C to 3°C and is most evident through the middle and later stages of the test.

Short time - High temperature rise:

The most pronounced temperature effects are apparent in the short time, high temperature rise tests. In a period of approximately 15 min, the boundary temperature is raised by approximately 55°C (3.7°C per min), because of the design of the system. The amount of strain is large, varying from 1.8 % under a stress increment of 0.2 kg per cm² to 2.2 % under a stress increment of 3.12 kg per cm². From $t = 3$ min to $t = 13$ min, the temperature rise is nearly linear. During this time the temperature difference vary from 5°C to 20-25°C between the points 1 and 8. The strain reach a limit as the soil sample temperature become constant. This limit is well illustrated in fig.2.14.(a) through 2.14(b), for after 14 min the temperature at the outside of the sample becomes constant and at the inside approaches a constant limit, and the strain approaches a constant limit.

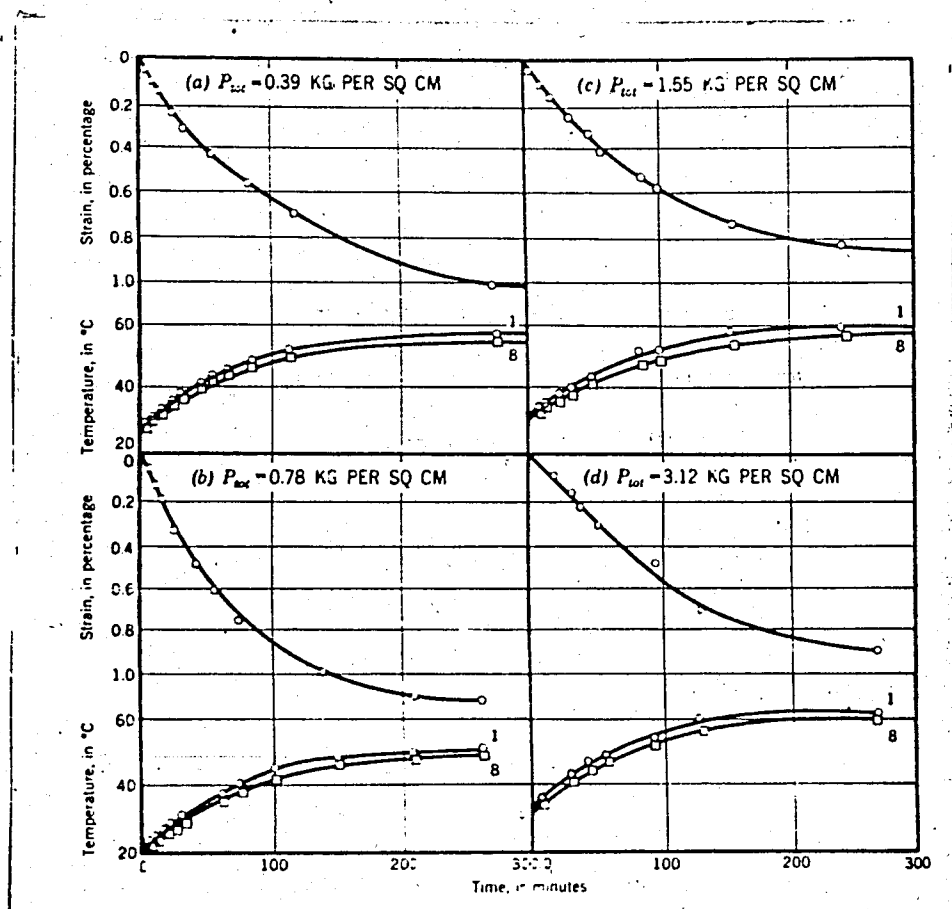


Fig. 2.13. Strain Versus - Time Long Time - High Temperature Rise.

The following conclusions can be drawn:

1 - Noticeable strain effects are produced in the soil when temperature differences are applied at given stress levels.

2 - The strain-time relationship for small temperature difference is similar to the temperature-time relationship.

3 - Large temperature changes simulate thermal loads in that a definite noticeable strain-time relationship results in which the strain increases as the temperature increases.

This relationship evident in both long-time and short-time temperature gradients, indicating that this phenomenon affects the primary type of consolidation more than the secondary type of consolidation, with a rapid flow of water out of rapidly changing voids.

4 - Temperature increases create a decrease in the viscosity of the system as a whole, thus leading to a decrease in shear resistance of the system.

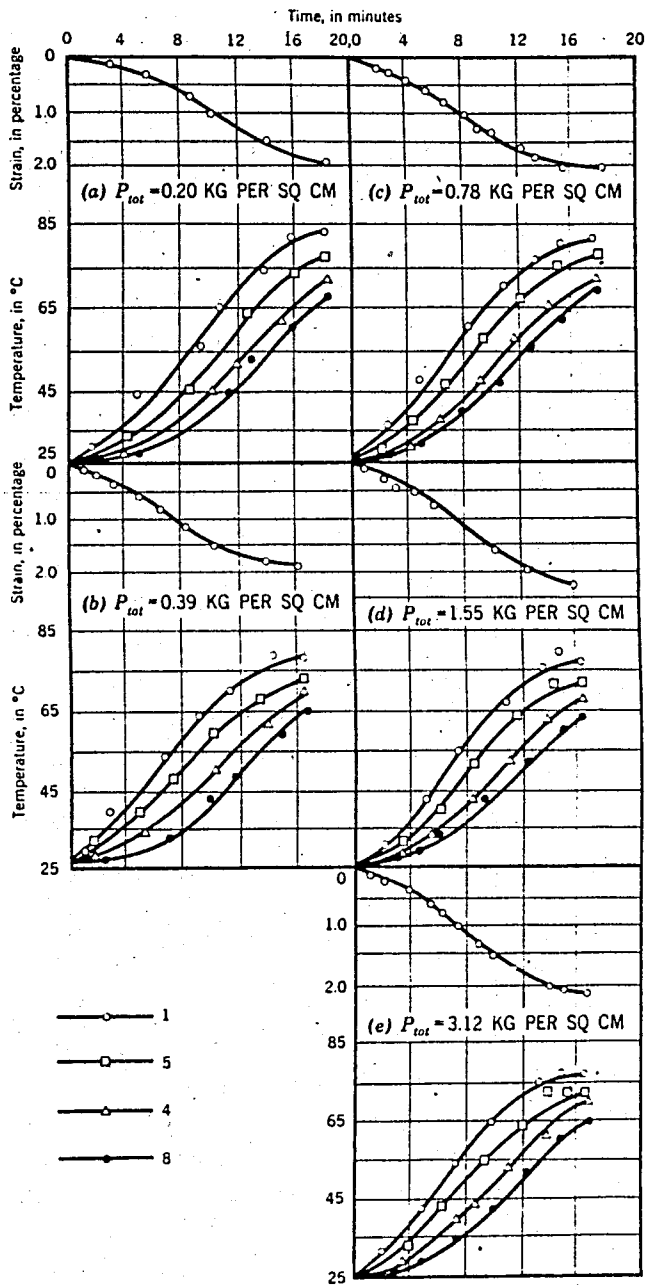


Fig. 2.14. Strain Versus Time: High, Rapid Temperature Rise.

CHAPTER 3 TESTING PROCEDURE

A. MATERIALS

1. Clay with Low Plastisity (Topser-Yellow) :

Generally, it contains silt and fine sand. This clay has low plastisity. Index properties were obtained from laboratory experiments as follows:

$$L.L = 50.0 \%$$

$$P.L = 24.8 \%$$

$$P.I = 25.2 \%$$

$$G_s = 2.70 \text{ t/m}^3$$

2. Clay with High Plasticity (Boğazköy-Grey) :

Generally, it contains silt and fine sand. This clay is highly plastic and some of the index properties are :

$$L.L = 70.0 \%$$

$$P.L = 35.2 \%$$

$$P.I = 34.8 \%$$

$$G_s = 2.57 \text{ t/m}^3$$

B. MINEROLOGICAL PROPERTIES OF CLAY USED

Minerology can be considered fundamental to the understanding of geotechnical properties, even though mineralogical determinations are not made for many geotechnical investigations. The properties of clay soils can not be explained without consideration of mineralogy. X-ray diffraction is the most widely used method for identification of fine-grained soil minerals and the study of their crystal structure. The results of x-ray analysis on these clay that have been done in İ.T.Ü. Maçka Maden Faculty. Show that;

a- Clay with low plasticity has as main mineral kaolinite with a little amount of quartz and illite. The soil consists of 40-45 % clay, 50-55 % silt, and 5 % fine sand.

b- Clay with high plasticity, has as main mineral kaolinite with a little amount of quartz and illite. The soil consists of 45-55% clay, 40-50 % silt, and 5 % fine Sand.

The following involves general information on kaolinite, illite, and quartz minerals.

The lattice of kaolinite is made of repeating layers of silica and alumina sharing oxygen atoms between them. The layers are held together by hydrogen bonds having hydroxyl ions, $(OH)^-$, from the alumina sheet and oxygens from the silica sheet. A typical kaolinite crystal may be 70-100 layers thick. kaolinites are found in soils that have undergone considerable weathering in warm and moist climates. they have low liquid limit and low activity, (1,2)

The three-layer primary element with the potassium ions occupy positions between the adjacent O^{-2} base planes. Formed is a clay mineral is known as illite. The potassium ion bonds the two sheets to gather firmly. Illite does not swell so much in the presence of water. although it expands more than kaolinite. (1.2)

Quartz (silica) is a clear transparent mineral formed from the slow cooling of liquid magma. Its high resistance to chemical weathering enables it to be broken into small particles by mechanical weathering without change in composition. It is the principal mineral in sand and silts. (1.2)

C. EQUIPMENT

The apparatus used during the tests is shown in fig. (3.1.). In addition to the unit shown, and a photograph of a complete assembly is shown in fig (3.2). The compressive properties of a soil are studied by means of an oedometer. An oedometer consists of a brass ring (1) into which a soil sample (2) is placed. Here the soil sample is in a laterally confined state. On top and at the bottom of the soil sample there are porous filter stones (3), one on each side of the sample, to permit a two way drainage of water expelled out of the voids from the soil sample under a vertical load, p . The axial, vertical load is applied on the soil sample by means of a loading yoke through a steel ball bearing (5) which rests on a circular loading plate (6), providing a uniform pressure distribution on the soil sample. The soil sample is subjected to predetermined load increments. The load externally applied on the soil sample compresses the soil, squeezes some water out from the voids of the soil, and the soil sample thus decreases in thickness. This volume change is measured by an Ames dial gage (7). The volume change readings are made at definite time intervals for each load increment. The diameter of the ring (1) is 6.00 cm. Its height is 2.54 cm. (10)

To evaluate the effect of temperature on a consolidating soil, it was necessary to develop an oedometer which could provide heating of the soil sample. A container was made of sheet-iron to accommodate a heating element, a thermostat, and a floater in the water bath. It was illustrated in fig. 3.3.

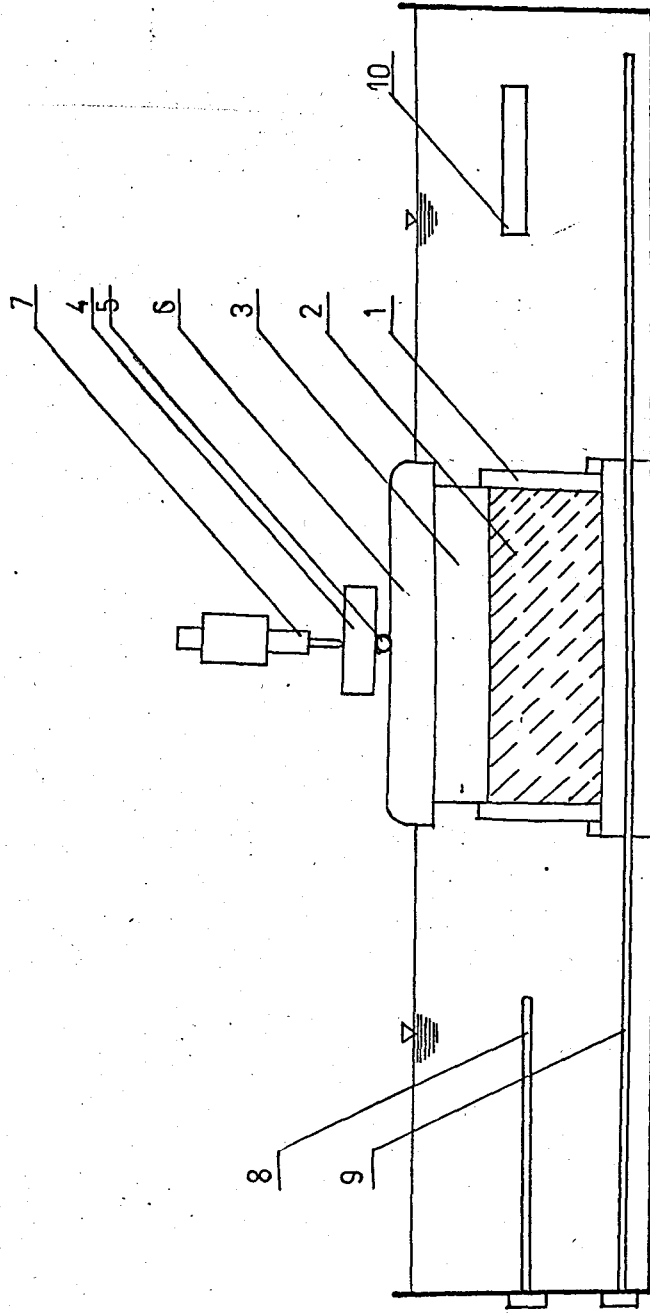


Fig-3.1. Schematic of a Temperature Controlled Consolidameter.

A container has a height of 6.00 cm, a length of 50 cm, and a width of 18 cm. The water in the container was heated by heating element which was made of copper. (8). The temperature of water at specific degrees was measured by thermostat (9). When the water level in the container was gradually decreasing because of evaporation, we made a floater to replace the evaporated water. This design allowed a high degree of control over the rate of temperature rise on the soil-water system. All of them was illustrated in fig.3.4. and fig. 3.3.

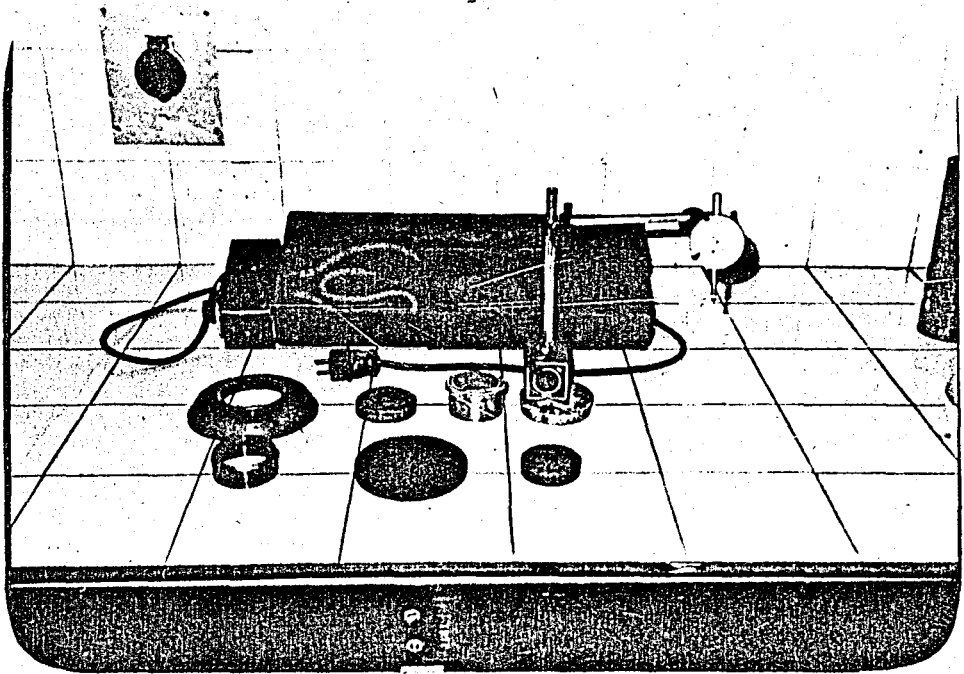


Fig. 3.2. Consolidometer.

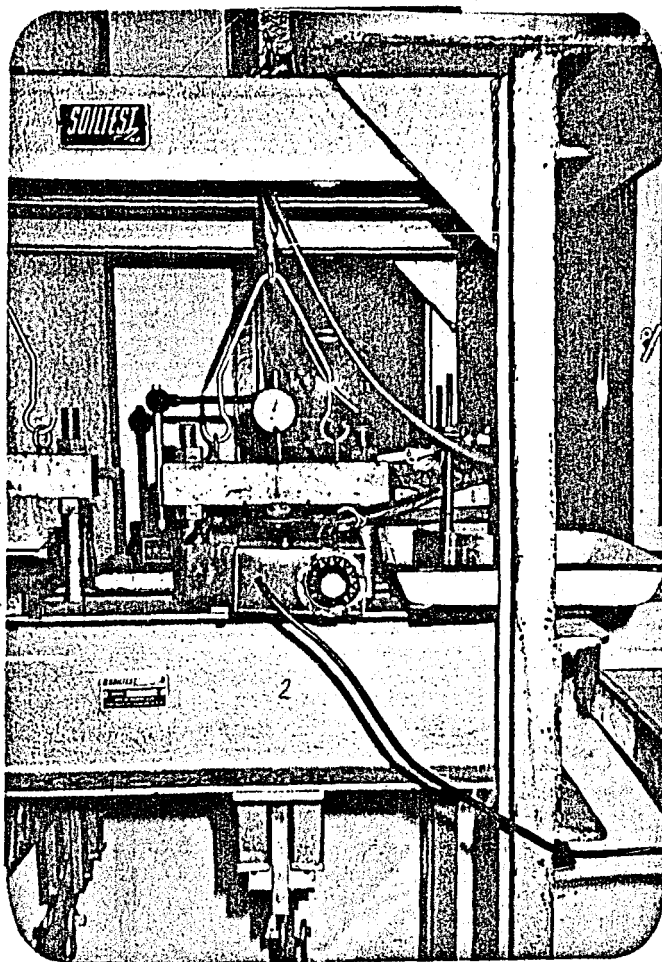


Fig. 3.3. Consolidometer and Loading Device.

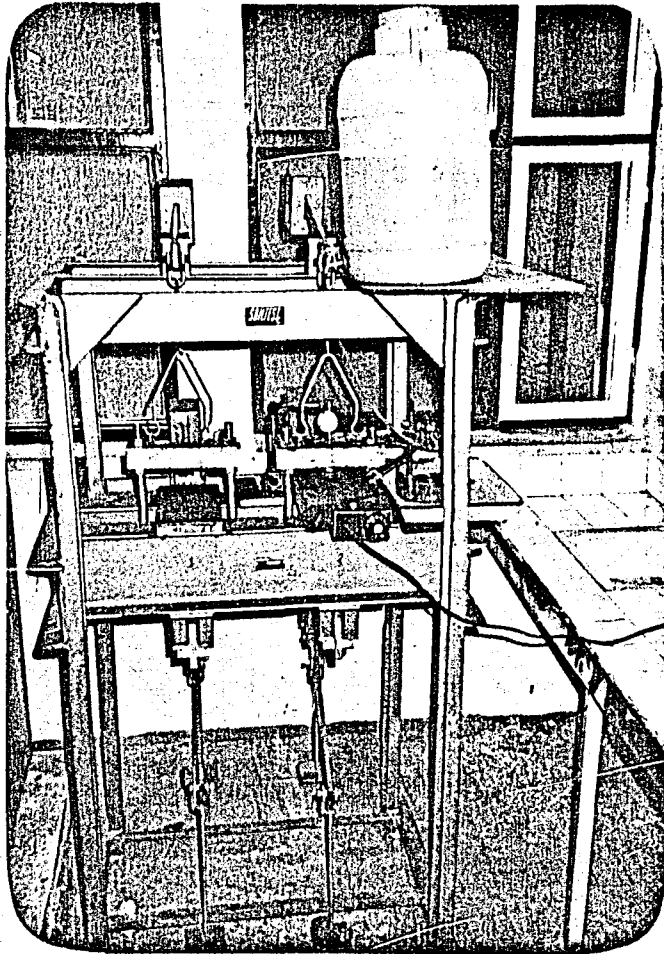


Fig. 3.4. Consolidometer and Loading Device.

D. MATERIAL AND SAMPLE PREPARATION

The materials used in the tests are first dried in the oven and then sieved from a No: 40 sieve. To get the material in a condition suitable for testing it was first necessary to thoroughly mix the clay with sufficient water to bring the sample to a water content slightly below the liquid limit. The initial moisture content of the samples for lean clay varied from 42 % to 48 % with the average value 45 %, for the fat clay the water content varied from 67 % to 70 % with the average value being 68.5 % .

1 - Grain Size Analysis Diagrams.

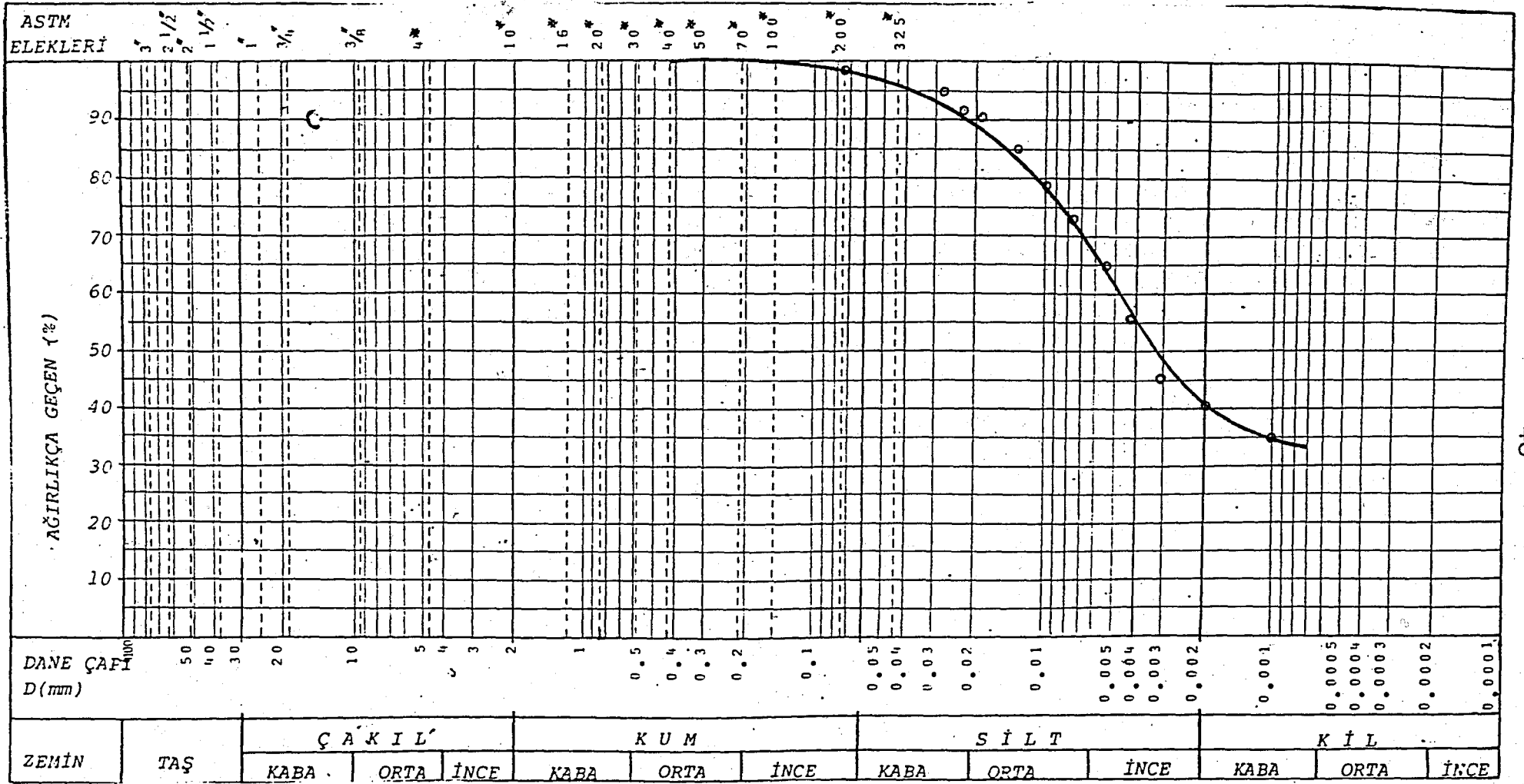


Fig.3.5. Grain Size Distribution Diagram For Topser-Yellow

ASTM
ELEKLERİ

3 2 1 3/8 4 10 16 20 30 40 50 70 100 200 325

AĞIRLIĞA GEÇEN (%)

90
80
70
60
50
40
30
20
10

DANE ÇAPFI
D(mm)

50 40 30 20 10 5 4 3 2 1 0.5 0.4 0.3 0.2 0.1 0.05 0.04 0.03 0.02 0.01 0.005 0.004 0.003 0.002 0.001 0.0005 0.0004 0.0003 0.0002 0.0001

ZEMİN	TAŞ	ÇAKIL			KUM			SİLT			KİL		
		KABA	ORTA	İNCE	KABA	ORTA	İNCE	KABA	ORTA	İNCE	KABA	ORTA	İNCE

47

Fig.3.6. Grain Size Distribution Diagram For Boğazköy - Grey.

E. TESTING

To study the effect of temperature on the consolidation characteristics of clay, six consolidation tests were performed: three tests were made with a clay of low plasticity and the others made with a clay of relatively high plasticity. After material preparation, molding the material was accomplished by pressing thin layers of material into the consolidometer ring with the spatula. Taking care not to leave among voids. Before assembling the consolidometer care was taken to ensure that the porous stones were saturated.

Tests were performed under constant loads which are 1.00, 2.00, 4.00 kg. per. sq. cm. Each load increment, until we reached the constant load, is allowed to remain on the soil sample for a period of 24 hours. During the application of constant load, the temperature of the soil-water was 20°C. After we reached to the desired load on each specimen, the temperature rise was established at the soil-water system. These temperature rises were:

- a - From 20°C to 40°C,
- b - From 40°C to 60°C,
- c - From 60°C to 80°C.

Each temperature step was allowed to remain on the specimen for 24 hours.

F. EVALUATION OF TEST RESULTS

1 - Calculation of Void Ratios:

Consolidation-test datas are obtained from a test and used as follows. (9)

Weight, dimensions (height and diameter), and water content of the original consolidation test specimen are obtained so that the initial void ratio e_i and cross-sectional area A can be computed and the initial height of the sample can be established. The dry weight of soil, w_d , can be determined from the weight of the wet soil and water content if known at the beginning of the test as,

$$W_d = \frac{W w_i}{1 + w_i}$$

The volume of the solids, V_s , can be computed using

$$V_s = \frac{W_d}{\gamma_s}$$

Where: γ_s is the unit weight of soil grains.

The height of soil solids, H_s , can be readily computed using

$$H_s = \frac{V_s}{A}$$

Where: A is the area of oedometer ring.

The initial height of voids can be computed using,

$$H_v = H_{\text{initial}} - H_s$$

And the initial void ratio, e_i , is

$$e_i = \frac{H_v}{H_s}$$

After completed the test, the clay sample is removed from the apparatus and its water content is determined by weighing, drying, and weighing again. Final void ratio can be computed using,

$$\Delta e = \frac{\Delta H}{H_i} (1 + e_i)$$

$$e_i - e_f = \frac{\Delta H}{H_i} (1 + e_i)$$

$$e_f = e_i - \frac{1 + e_i}{H_i} \Delta H$$

From an arithmetic plot of e versus pressure one can obtain the "coefficient of compressibility a_v " as

$$a_v = \frac{\Delta e}{\Delta P} = \frac{e_i - e_f}{p_f - p_i} \text{ cm}^2/\text{kg}$$

and the "coefficient of volume compressibility M_v " as

$$M_v = \frac{a_v}{1 + e_j} \text{ cm}^2/\text{kg}$$

2. Computation of coefficient of consolidation:

A semilog plot:

Usually one plots the settlement versus logarithm time, as illustrated in figure. 3.7, for the purpose of obtaining the time at a given percent of consolidation. (6,9) The use

of settlement versus log time curve. requires finding the initial dial reading D_0 . To obtain D_0 on the semilogarithmic plot, if the early part of the curve is parabolic, select a time t_1 and a time $t_2 = 4t_1$. Measure the ordinate y from t_1 to t_2 on the curve and lay this same value of y of vertical above t_1 . Draw a horizontal line through this point and call the intercept of this line on the DR. ordinate D_0 . If the early part of the curve is not parabolic, use the actual dial reading at $t = 0$ for D_0 . To obtain D_{100} from the DR versus log time curve, draw tangents to the middle and end parts of the curve as shown in fig. 3.7. At the intersection of the tangents, project horizontally to the curve ordinate to read D_{100} . To obtain t_{100} project horizontally from the tangent intersection to the curve, then vertically down to the abscissa for the time value. With D_0 and D_{100} established, one may obtain the dial reading corresponding to 50 percent consolidation D_{50} as

$$D_{50} = \frac{D_0 + D_{100}}{2}$$

Average drainage length, H_d , can be calculated as

$$H = \frac{(H_0 - \Delta H_{\text{initial}}) + (H_0 - \Delta H_{\text{final}})}{2}$$

$$H_d = \frac{H}{2} \quad (24)$$

The time at 50 percent consolidation t_{50} was used to find the coefficient of consolidation C_v :

$$C_v = \frac{T_v \times H_d^2}{t} \quad \text{cm}^2/\text{sn.}$$

Where: T_v = Time factor (0.197 for $U = 50$ percent)

From table 2.1.

t = time for the corresponding time factor T .

H = Average length of the longest drainage path during the given load increment. Use Eq. 2.4.

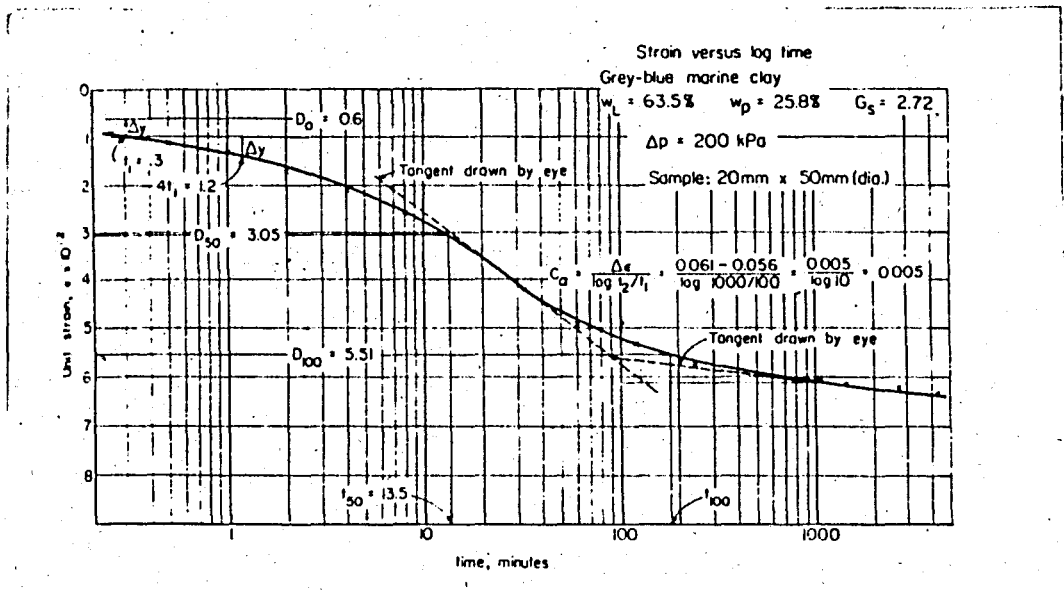


Fig. 3.7 Plot of strain vs. log time and data obtained from plot.

3. Expansion of Brass Ring:

Dimensions of brass ring increase as the temperature of the brass ring is increased. Fig. 3.8 shows a ring whose diameter is D_0 at some reference temperature t_0 , and whose diameter is D at some higher temperature t . The difference $D - D_0 = \Delta D$ is the amount of the ring has expanded on heating where $\Delta D = \Delta d_1 + \Delta d_2$. The increase in diameter, Δd is proportional to the original length D_0 , and very nearly proportional to the increase in temperature, $t - t_0$ or Δt . That is, (10)

$$\Delta D \propto D_0 \Delta t,$$

or

$$\Delta D = \alpha \times D_0 \times \Delta t$$

Where: α is a proportionality constant.

Another relation is obtained by replacing ΔD by $D - D_0$ and solving for D .

$$D = D_0(1 + \alpha \Delta t) \quad (25)$$

Since D_0 , D , and ΔD are all expressed in the same unit, the units of α are "reciprocal degrees" (centigrade). The coefficient of linear expansion of brass is given as

$$\alpha = 2 \times 10^{-5} (^\circ\text{C}^{-1}) \quad \text{Ref. (10)}$$

This means that a brass ring one centimeter long at 0°C , increases in length by 0.00005 cm when heated to 1°C .

Initial diameter of the ring at 20°C , D_0 , is 6.00 cm.

Final diameter of the ring, D , for various temperatures can be calculated as follows: Using Eq. 25 we obtain,

For 40°C $D = 6.0024$ cm,

For 60°C $D = 6.0048$ cm,

For 80°C $D = 6.0072$ cm.

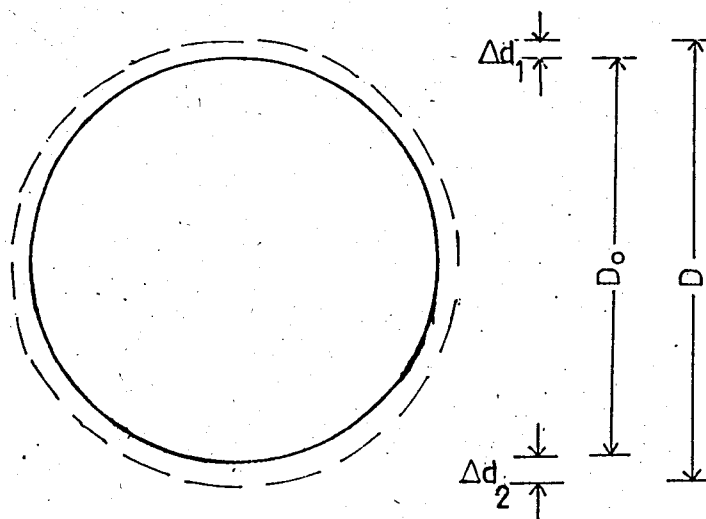


Fig. 3.8 Expansion of the Ring.

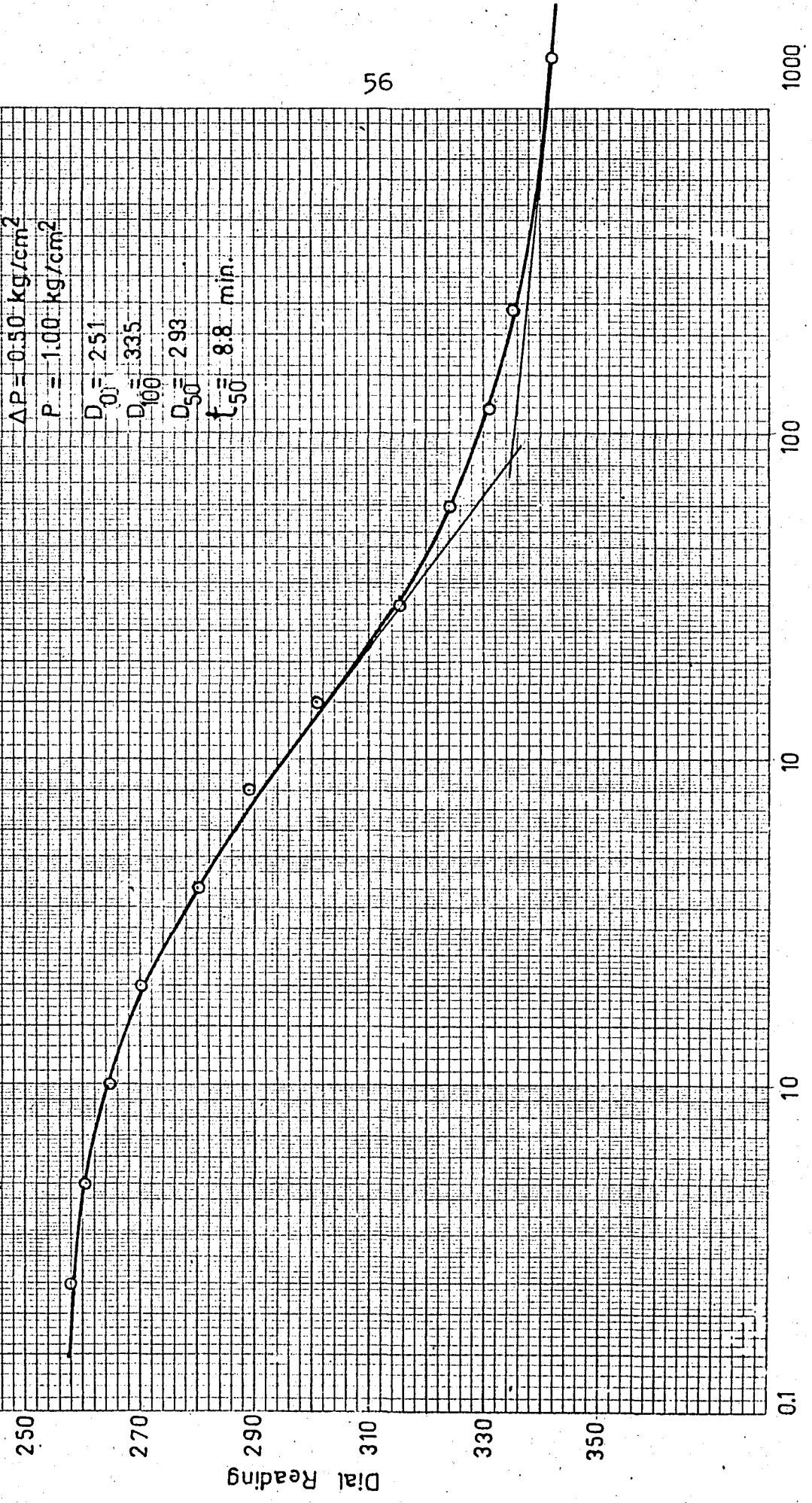
CHAPTER 4 TEST RESULTS

A. CLAY WITH LOW PLASTICITY (Topser-~~Yellow~~)TEST - 1:(Topser-~~Yellow~~)

P = 1.00 kg. per. sq. cm.

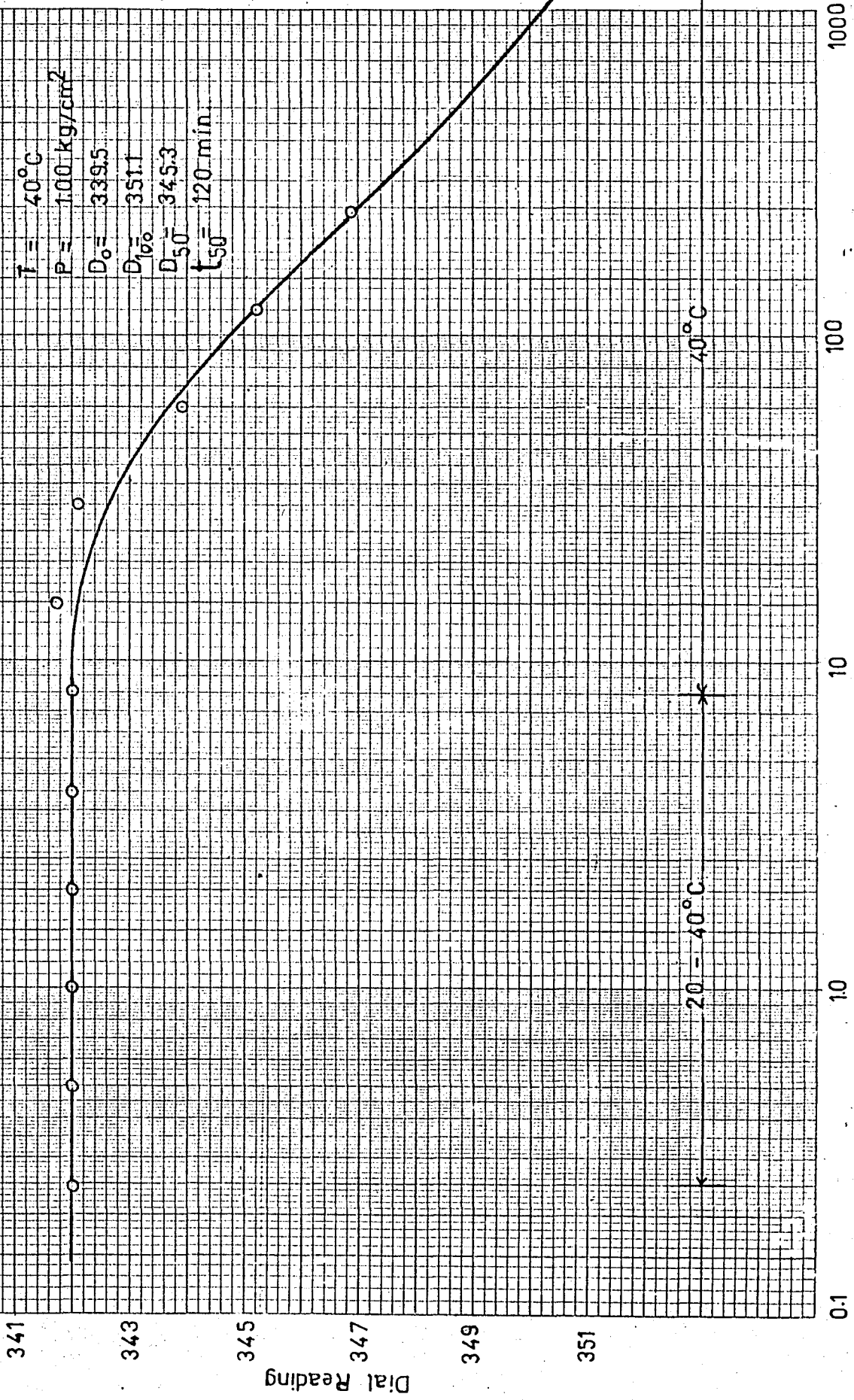
 $W_i = 42.70 \%$ $W_f = 33.75 \%$

$T = 20^{\circ}\text{C}$
 $\Delta P = 0.50 \text{ kg/cm}^2$
 $P = 1.00 \text{ kg/cm}^2$
 $D_{0.1} = 251$
 $D_{100} = 335$
 $D_{50} = 293$
 $t_{50} = 8.8 \text{ min.}$

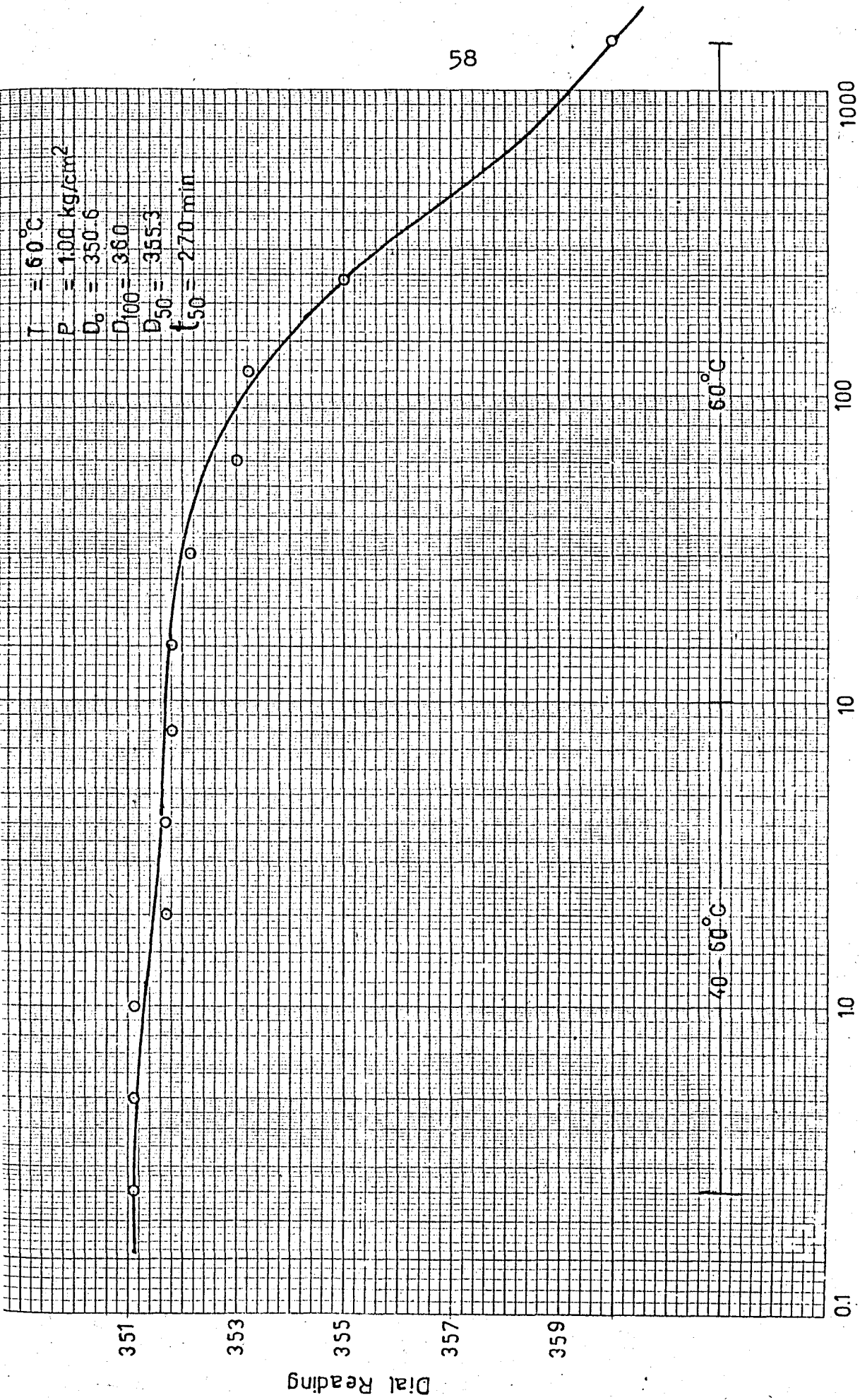


Log Time. min.
Fig. 4.12. Plot of DR. vs. Log time.(min).

$T = 40^{\circ}\text{C}$
 $P = 1.00 \text{ kg/cm}^2$
 $D_0 = 339.5$
 $D_{100} = 351.1$
 $D_{50} = 345.3$
 $t_{50} = 120 \text{ min.}$



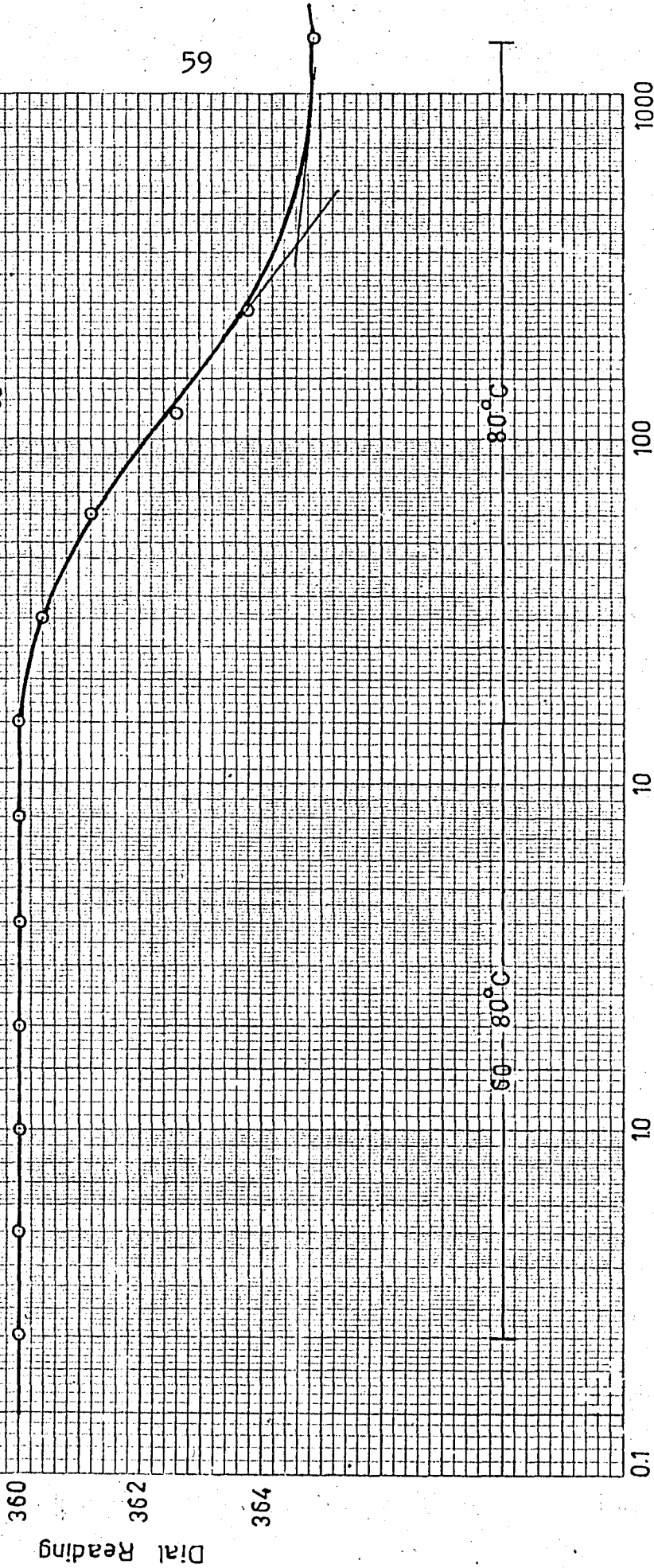
Log Time .min.
Fig: 4.1.2. Plot of DR. vs. Log time(min).



Log Time.min

Fig:4.1.3 Plot of DR. vs. Log time(min)

$T = 80^{\circ}\text{C}$
 $P = 1.00 \text{ kg/cm}^2$
 $D_0 = 358.8$
 $D_{100} = 364.6$
 $D_{50} = 361.7$
 $t_{50} = 80 \text{ min}$



Log Time.min.

Fig: 4.4. Plot of DR. vs. Log time(min)

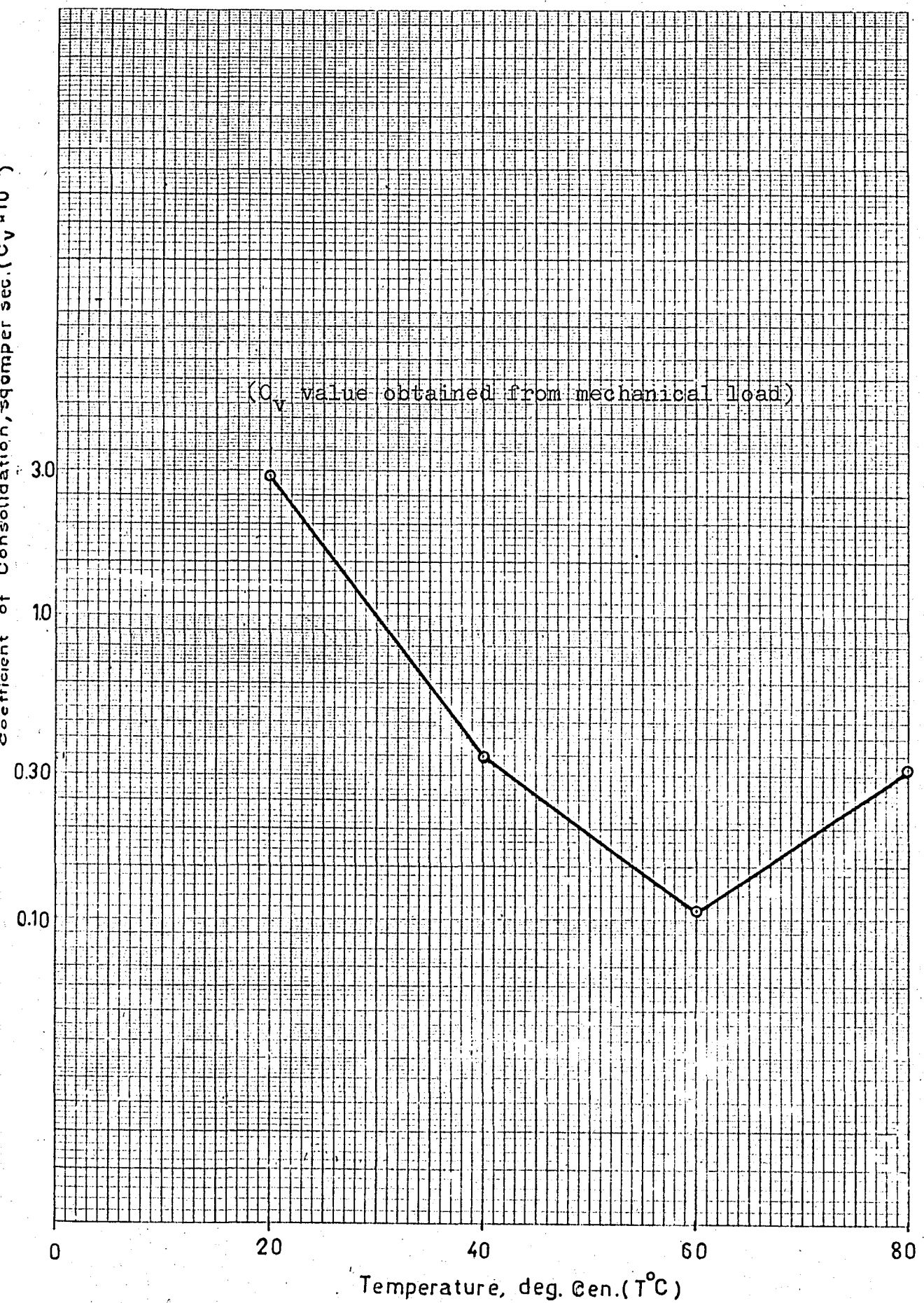


Fig. 4. 5. Effect of Temperature on Coefficient of Consolidation ($P=100$ kg)

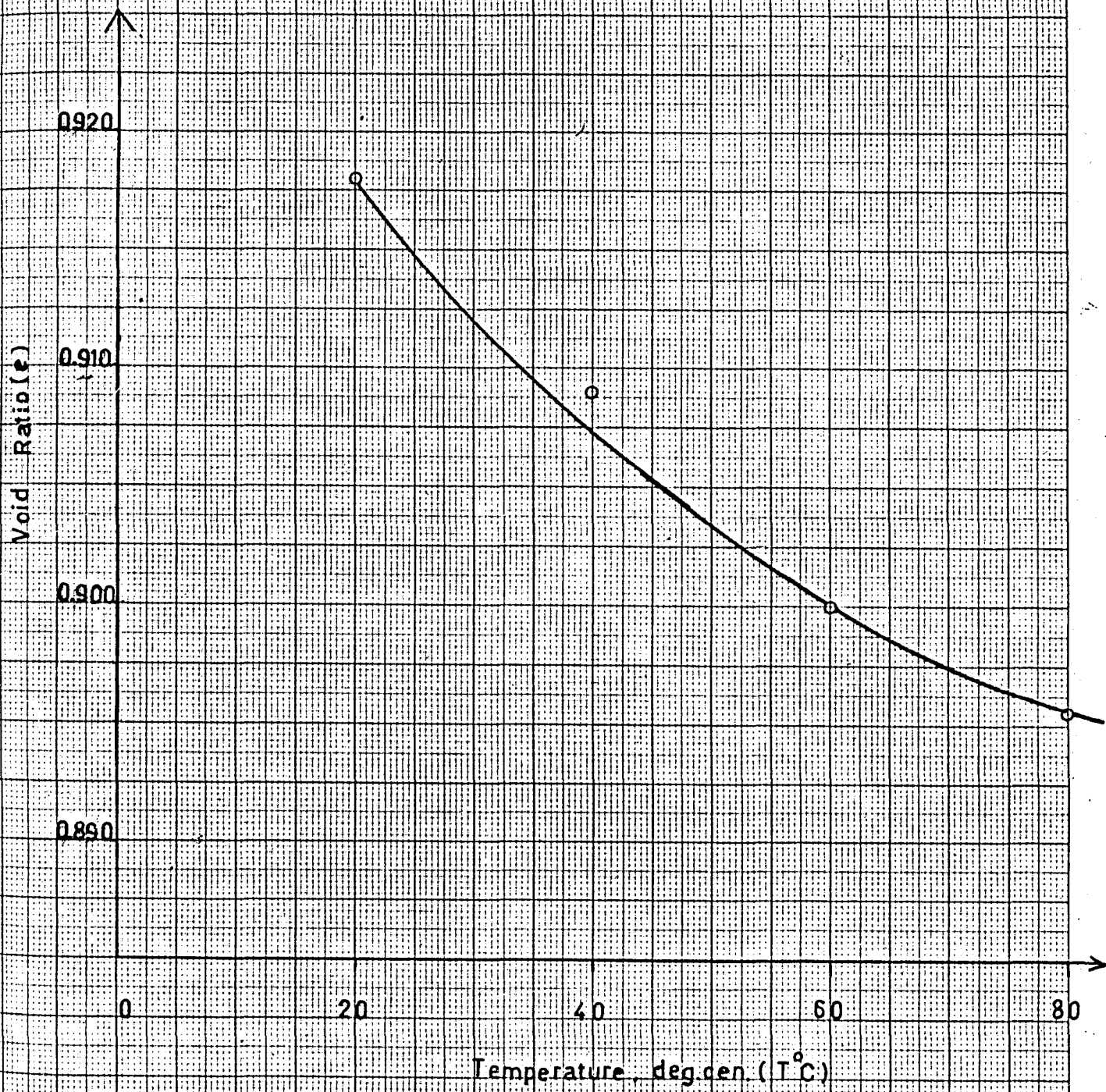


Fig: 4. 6. Effect of Temperature on Void Ratio, for $P=100 \text{ kg/cm}^2$

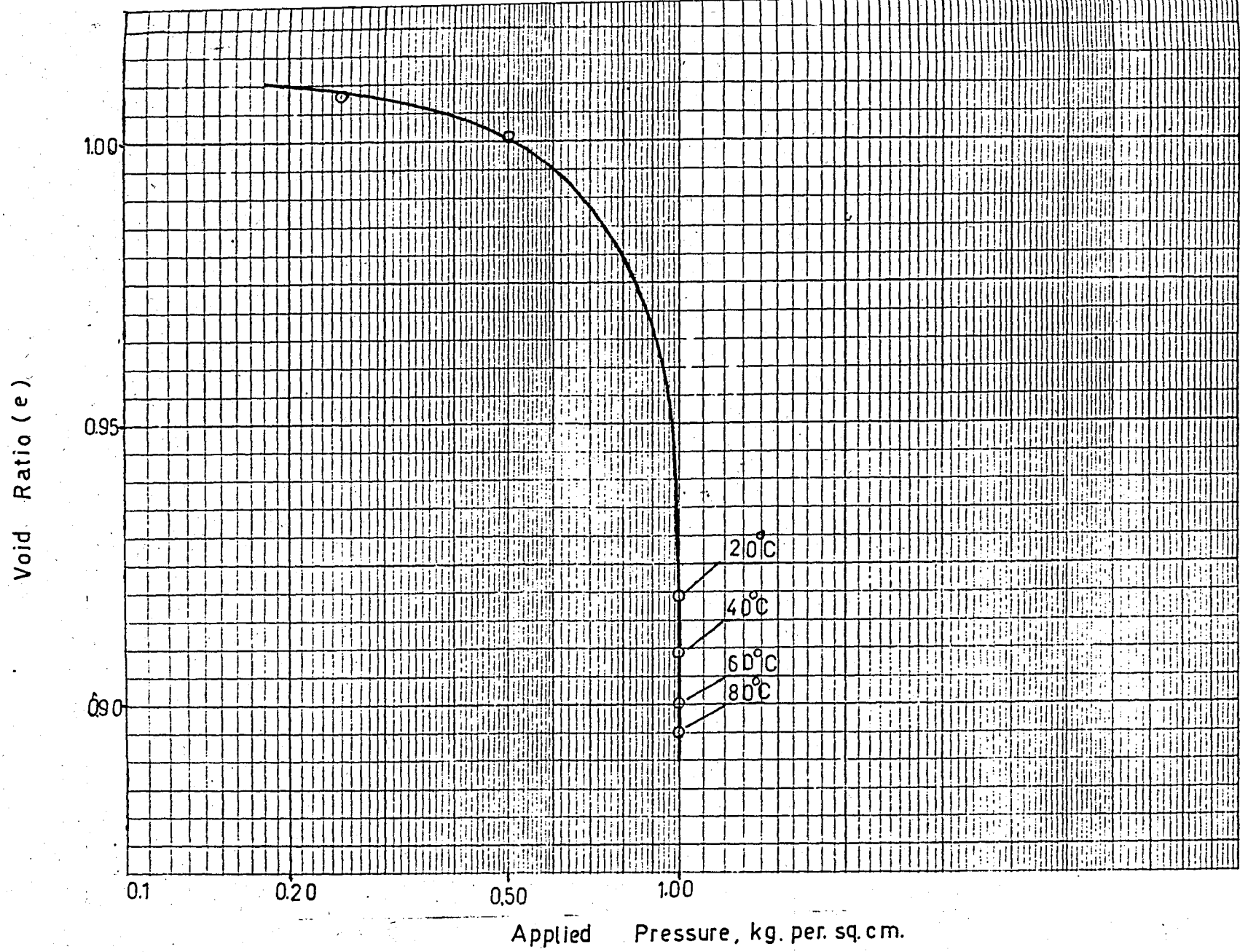


Fig. 4.7. Effect of Temperature on the Compression Curve, For $P=1\text{ kg/cm}^2$.

TEST - 2 (Topser-Yellow)

P = 2.00 kg.per.sq.cm.

$W_i = 45.13 \%$

$W_f = 29.34 \%$

$T = 20^{\circ}\text{C}$
 $\Delta P = 100 \text{ kg/cm}^2$
 $P = 200 \text{ kg/cm}^2$
 $D_0 = 3.35$
 $D_{100} = 4.60.2$
 $D_{50} = 4.07.6$
 $t_{50} = 11 \text{ min}$

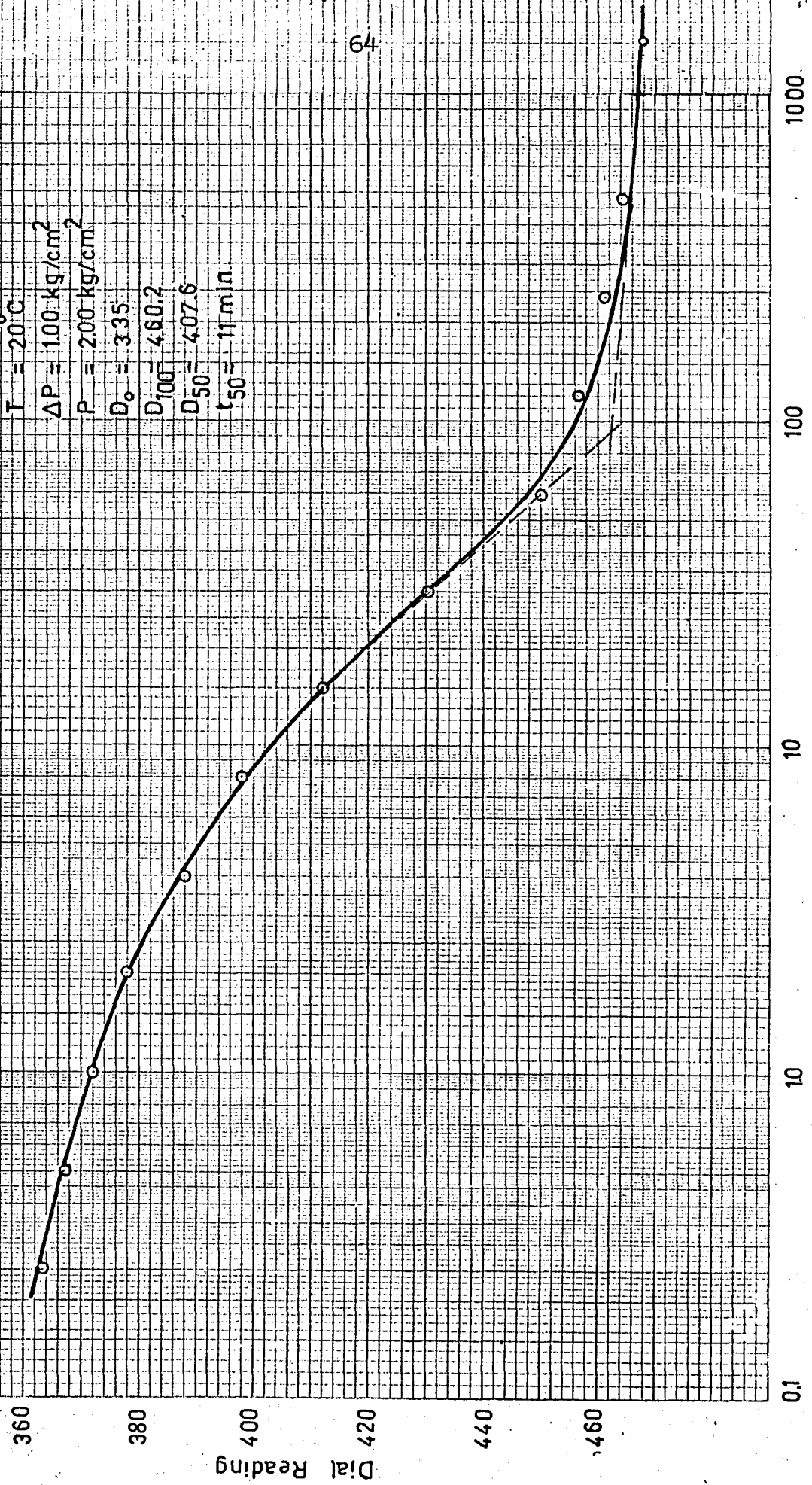


Fig:4.8. Plot of Dial Reading vs Log time(min)

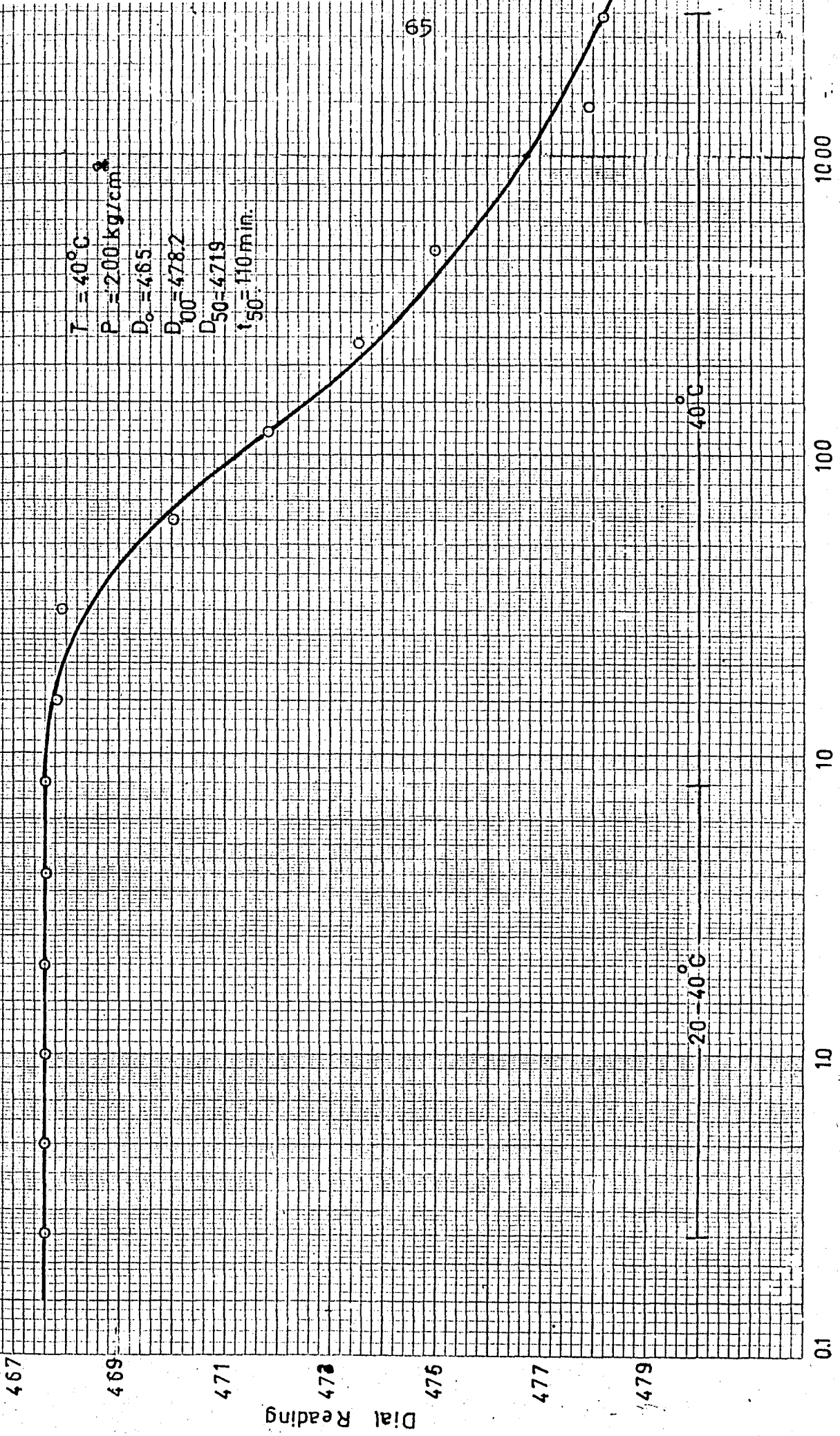


Fig: 4.9. Plot of DR. vs. Log time(min)

$T = 60^{\circ}\text{C}$
 $P = 2.00 \text{ kg/cm}^2$
 $D_0 = 477$
 $D_{100} = 483$
 $D_{50} = 480$
 $t_{50} = 100 \text{ min.}$

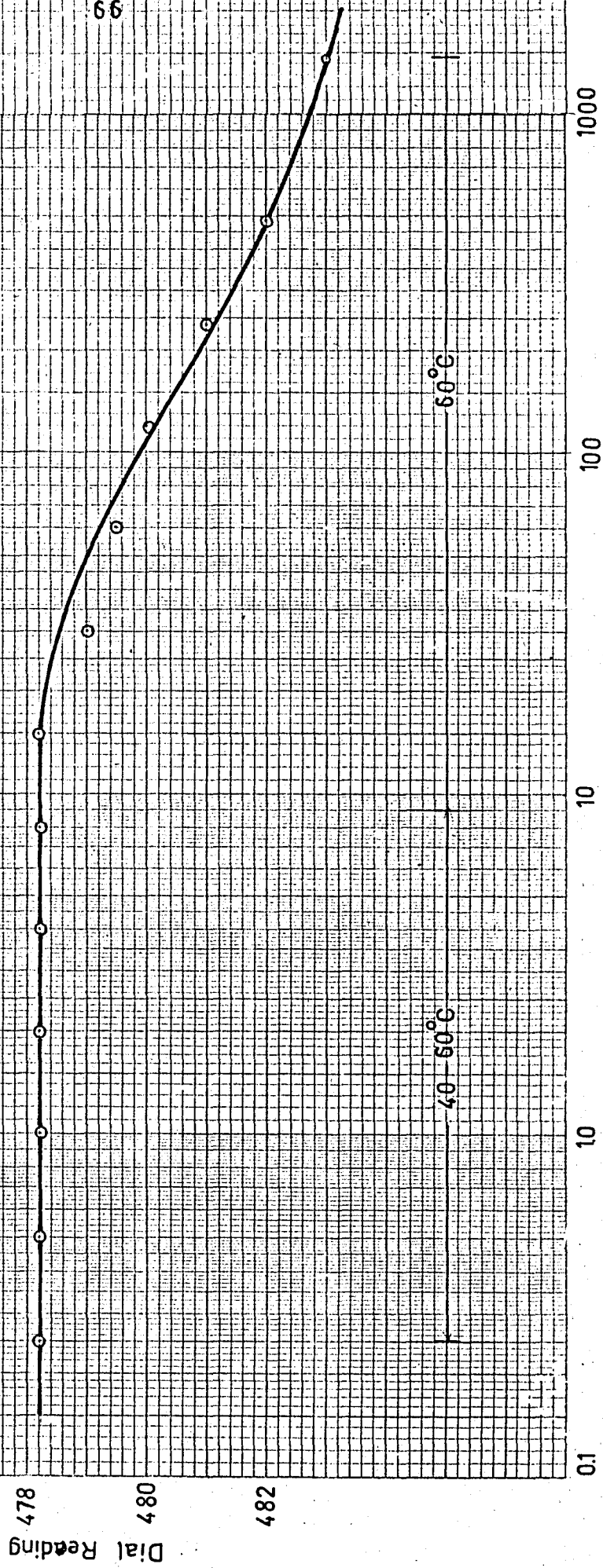
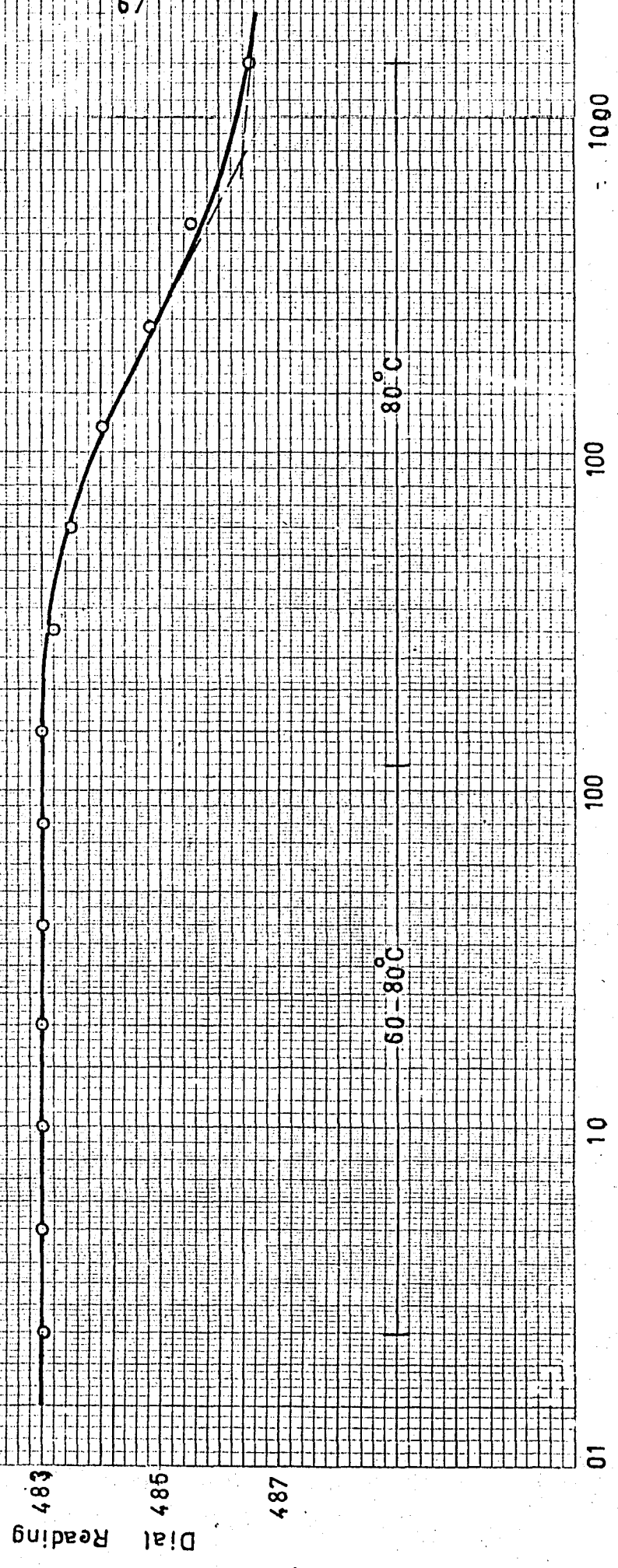


Fig: 4. 10. Plot of DR. vs. Log time (min)

$T = 80^{\circ}\text{C}$
 $P = 2.00 \text{ kg/cm}^2$
 $D_0 = 482$
 $D_{100} = 486.4$
 $D_{50} = 484.2$
 $t_{50} = 130 \text{ min}$



Coefficient of Consolidation, sq. cm. per. sec. ($C_v \times 10^4$)

5.0

 $(C_v$ value obtained from mechanical load)

1.0

0.5

0.1

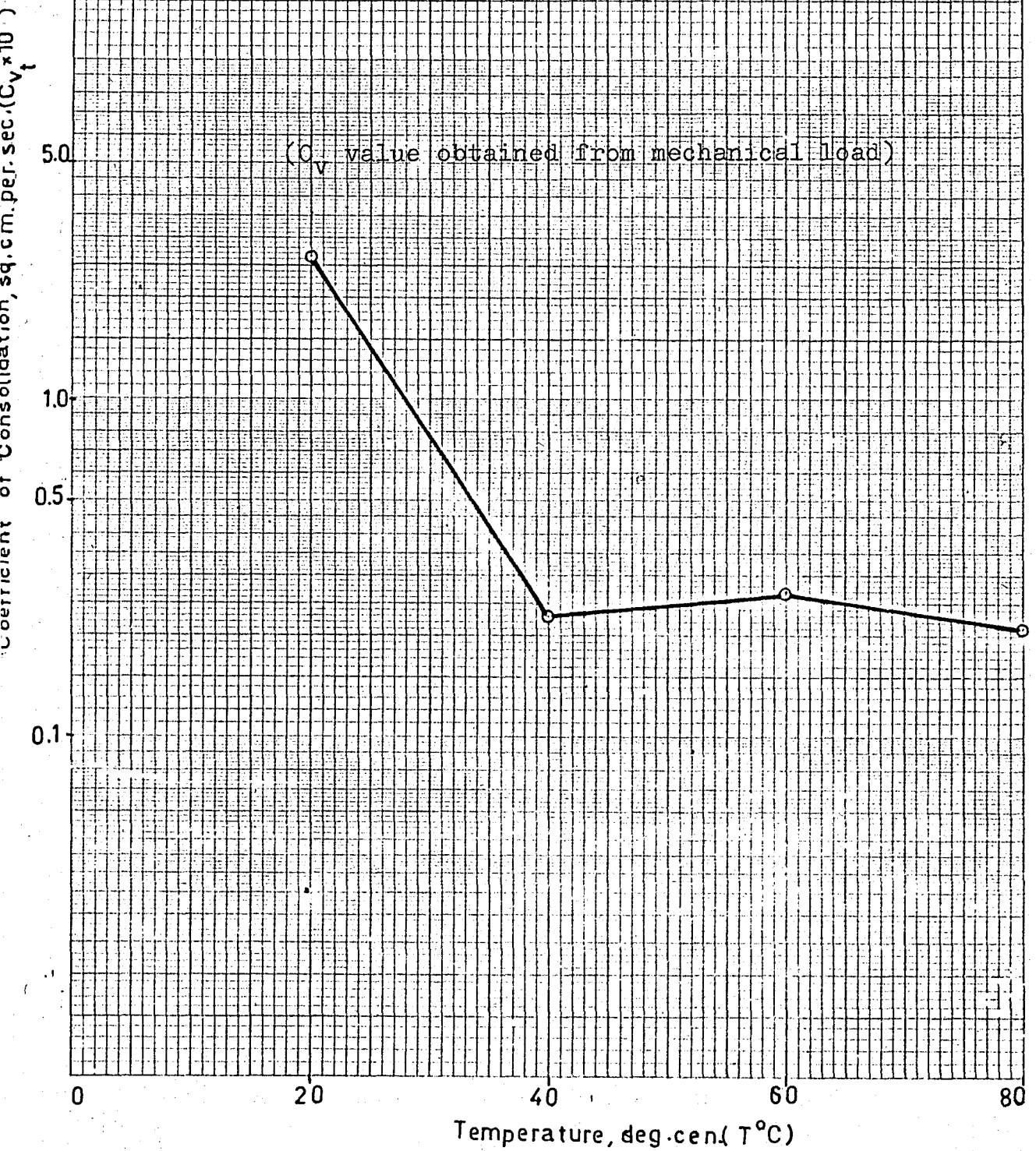
0

20

40

60

80

Temperature, deg. cen. ($T^{\circ}C$)Fig. 4. 12. Effect of Temperature on Coefficient of Consolidation, ($P = 2.00 \text{ kg/cm}^2$)

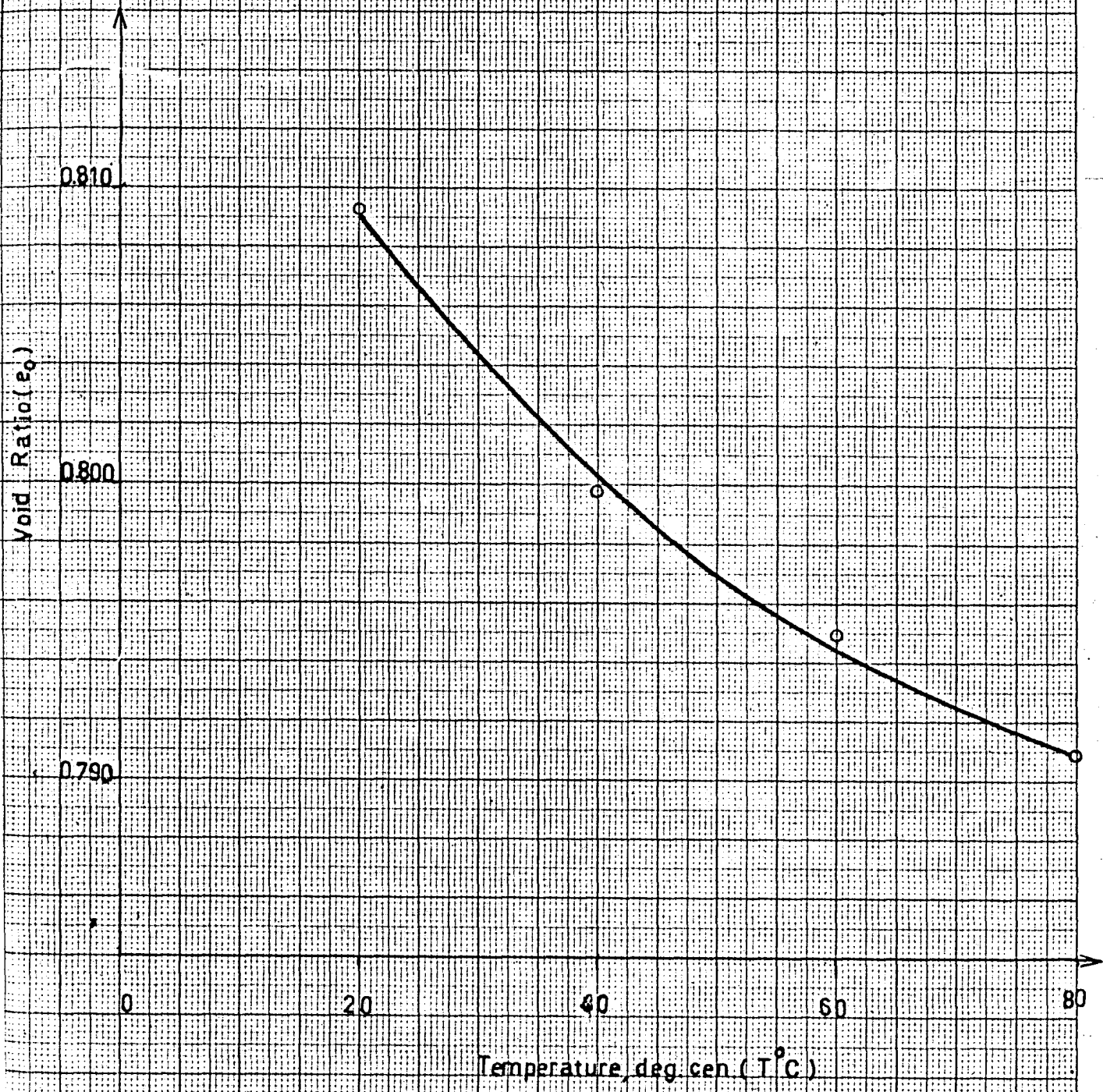


Fig. 4. 13. Effect of Temperature on Void Ratio, for $P=2.00 \text{ kg/cm}^2$

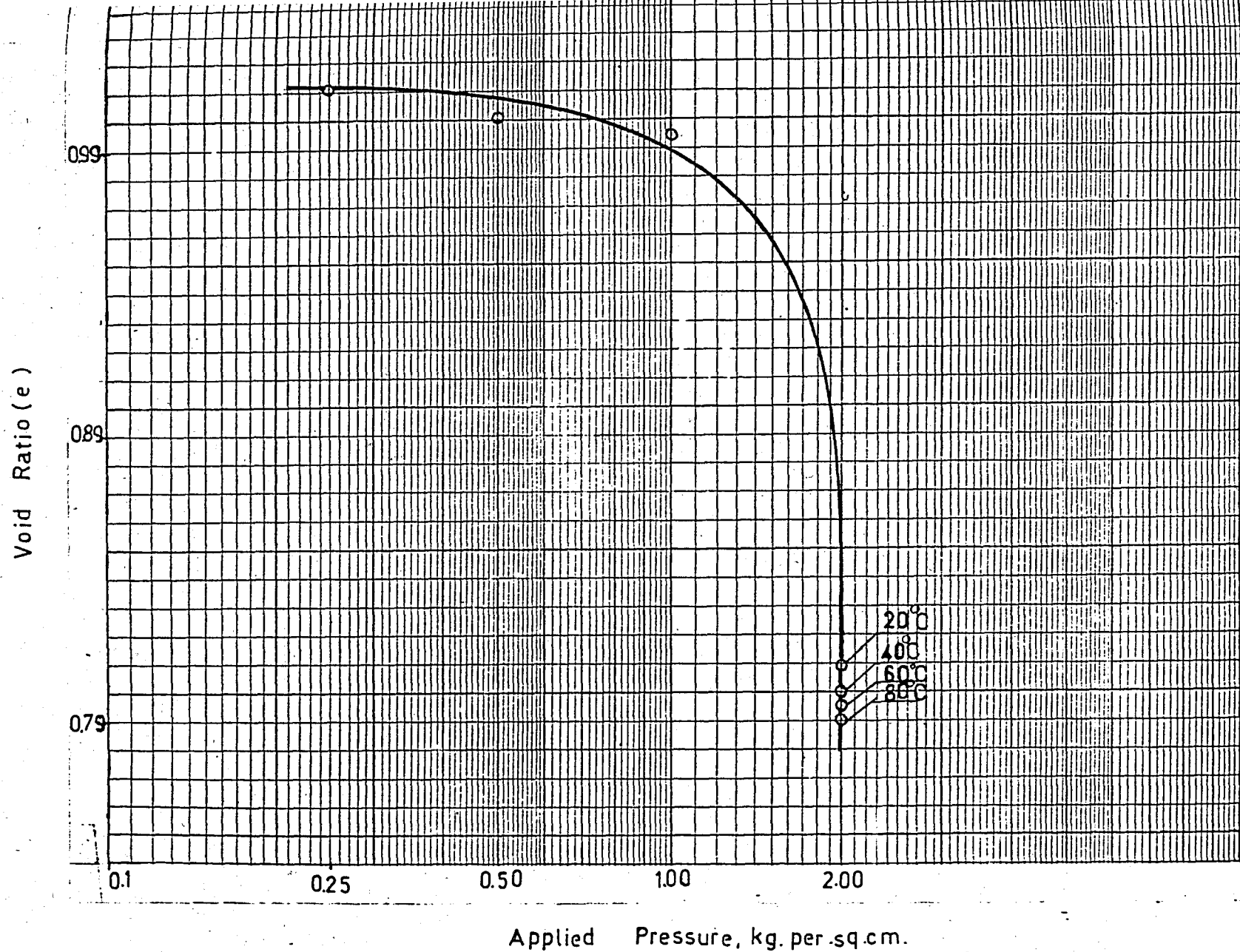


Fig: 4. 14. Effect of Temperature on the Compression Curve, For $P=2.00 \text{ kg/cm}^2$.

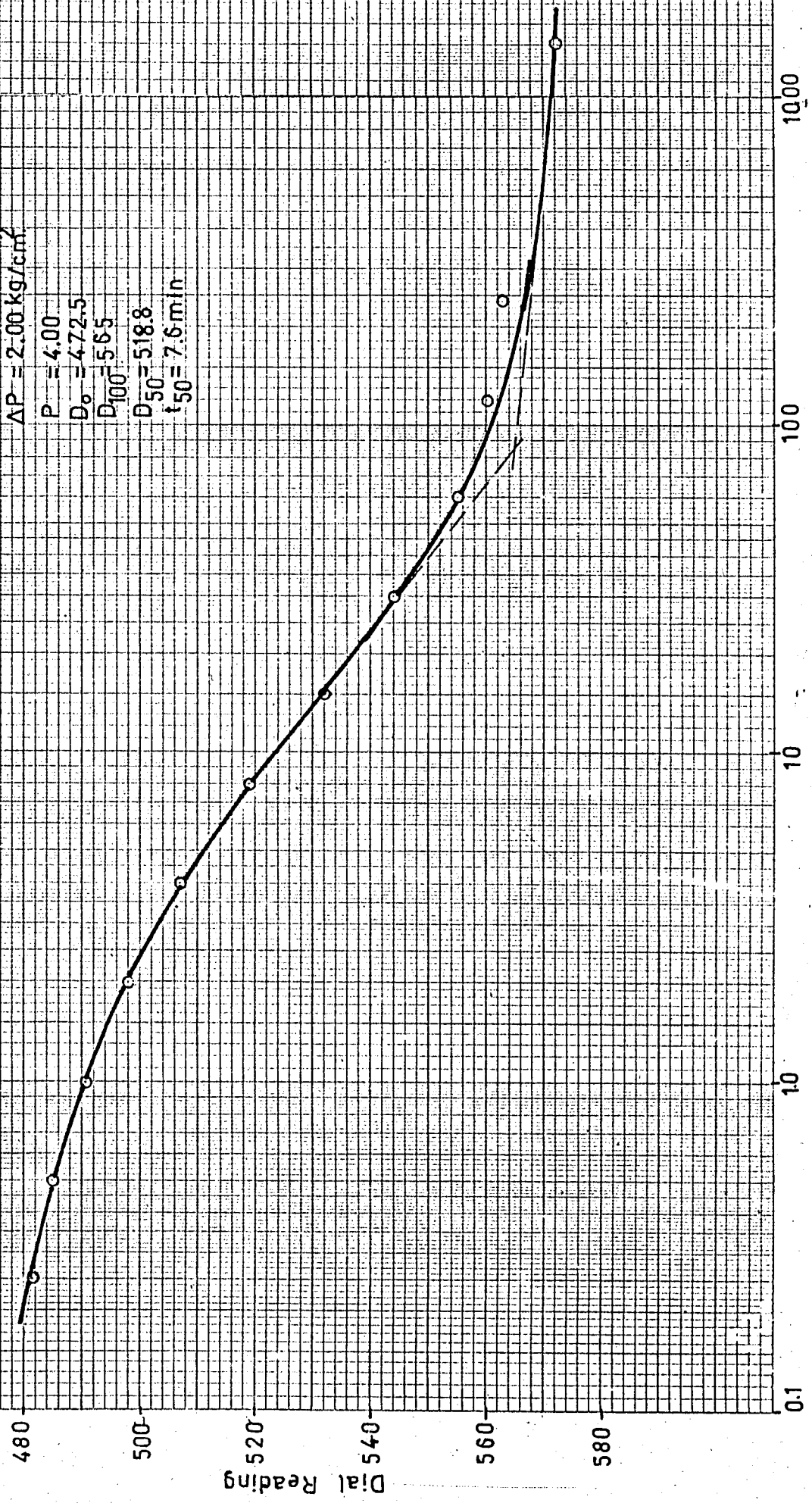
TEST - 3:(Topser-Yellow)

P = 4.00 kg.per.sq.cm.

$W_i = 48.50 \%$

$W_f = 27.27 \%$

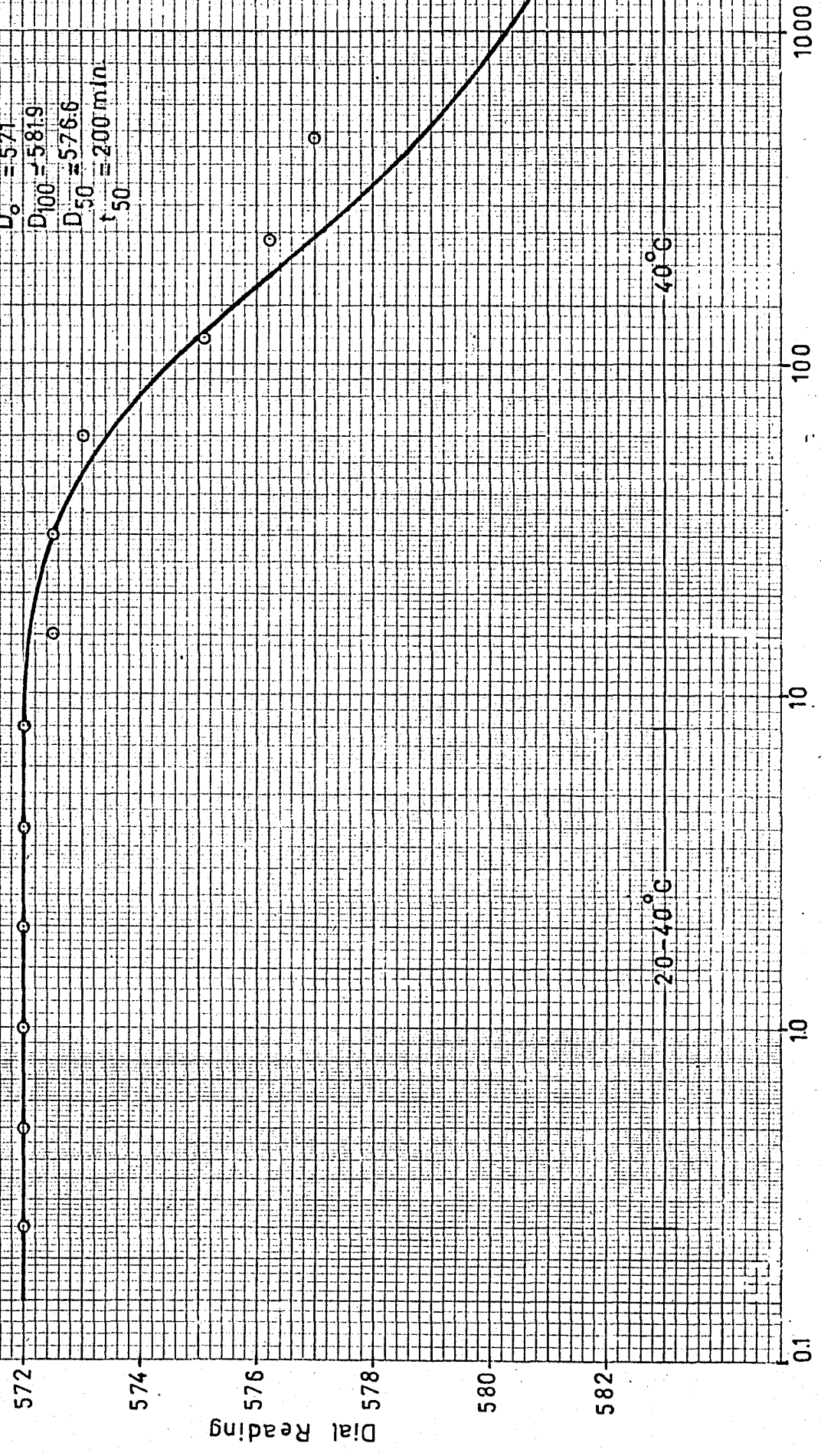
$T = 20^{\circ}\text{C}$
 $\Delta P = 2.00 \text{ kg/cm}^2$
 $P = 4.00$
 $D_0 = 472.5$
 $D_{100} = 565$
 $D_{50} = 518.8$
 $t_{50} = 7.6 \text{ min}$



Log Time (min)

Fig:4. 15. Plot of DR. vs. Log time (min)

$T = 40^{\circ}\text{C}$
 $P = 4.00 \text{ kg/cm}^2$
 $D_0 = 5.71$
 $D_{100} = 581.9$
 $D_{50} = 576.6$
 $t_{50} = 200 \text{ min}$



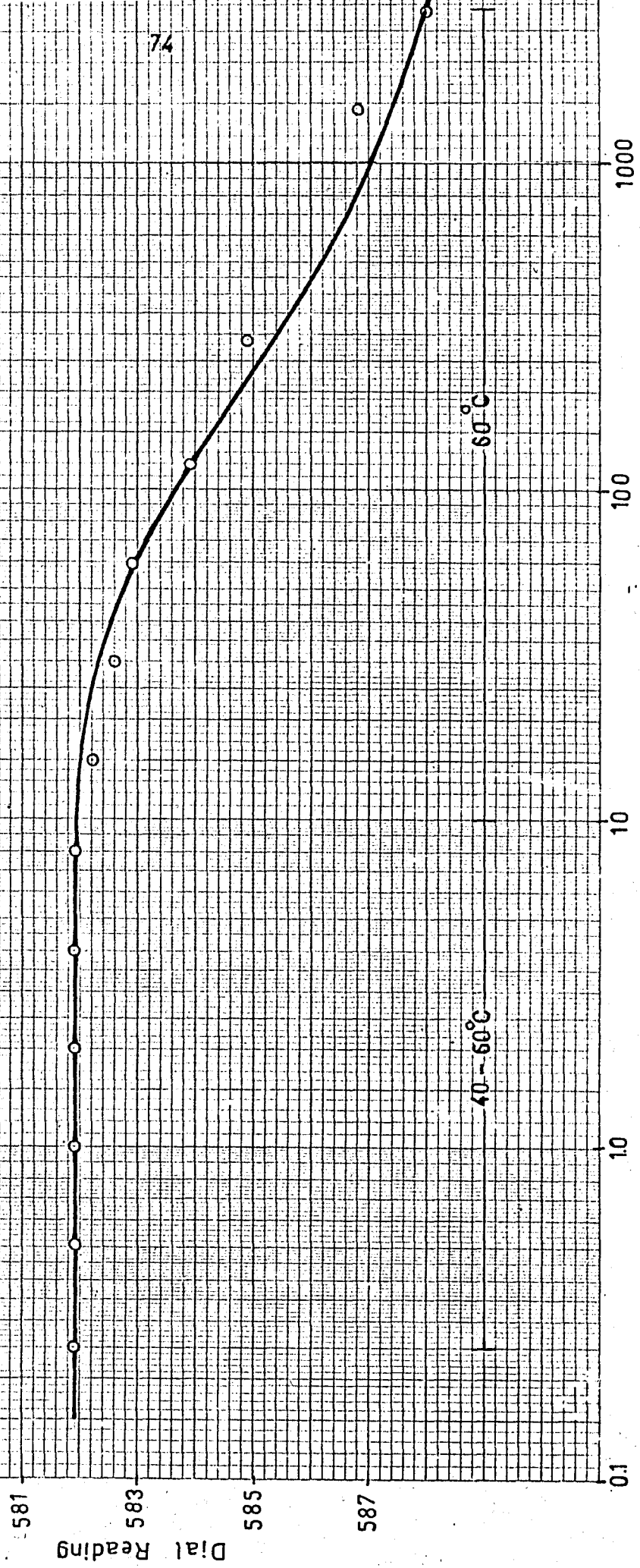
20-40°C

40°C

Log Time (min)

Fig. 4. 16. Plot of DR. vs. Log time.

$T = 60^{\circ}\text{C}$
 $P = 400 \text{ kg/cm}^2$
 $D_0 = 581$
 $D_{100} = 588$
 $D_{50} = 584.5$
 $t_{50} = 200 \text{ min.}$



Log Time(min)

Fig:4. 17. Plot of DR. vs. Log time.

$T = 80^{\circ}\text{C}$
 $P = 4.00 \text{ kg/cm}^2$
 $D_0 = 587.1$
 $D_{100} = 590.8$
 $D_{50} = 588.95$
 $t_{50} = 70 \text{ min.}$

Dial Reading

588

590

592

60-80°C

80°C

01

10

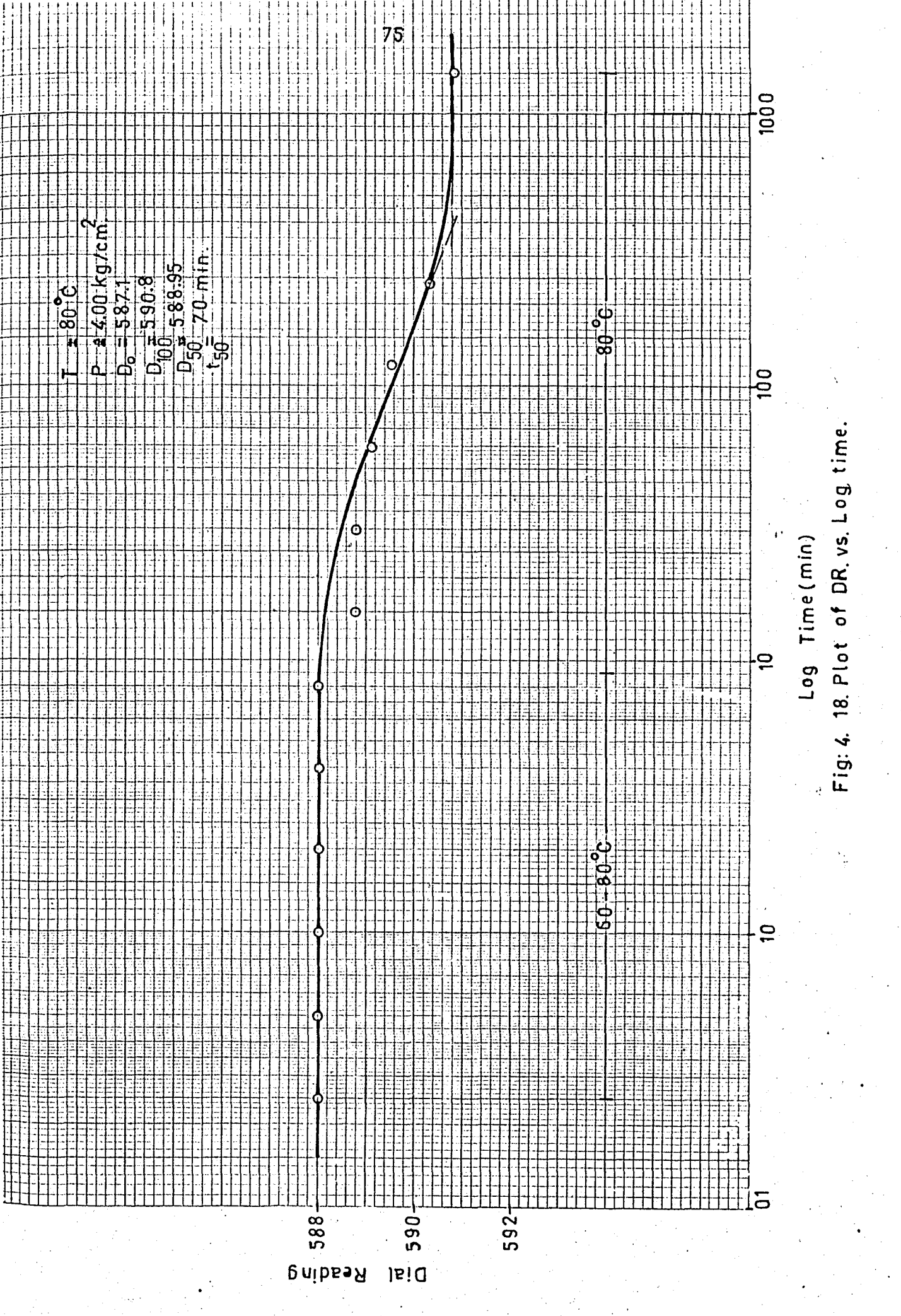
10

100

1000

Log Time (min)

Fig: 4. 18. Plot of DR. vs. Log time.



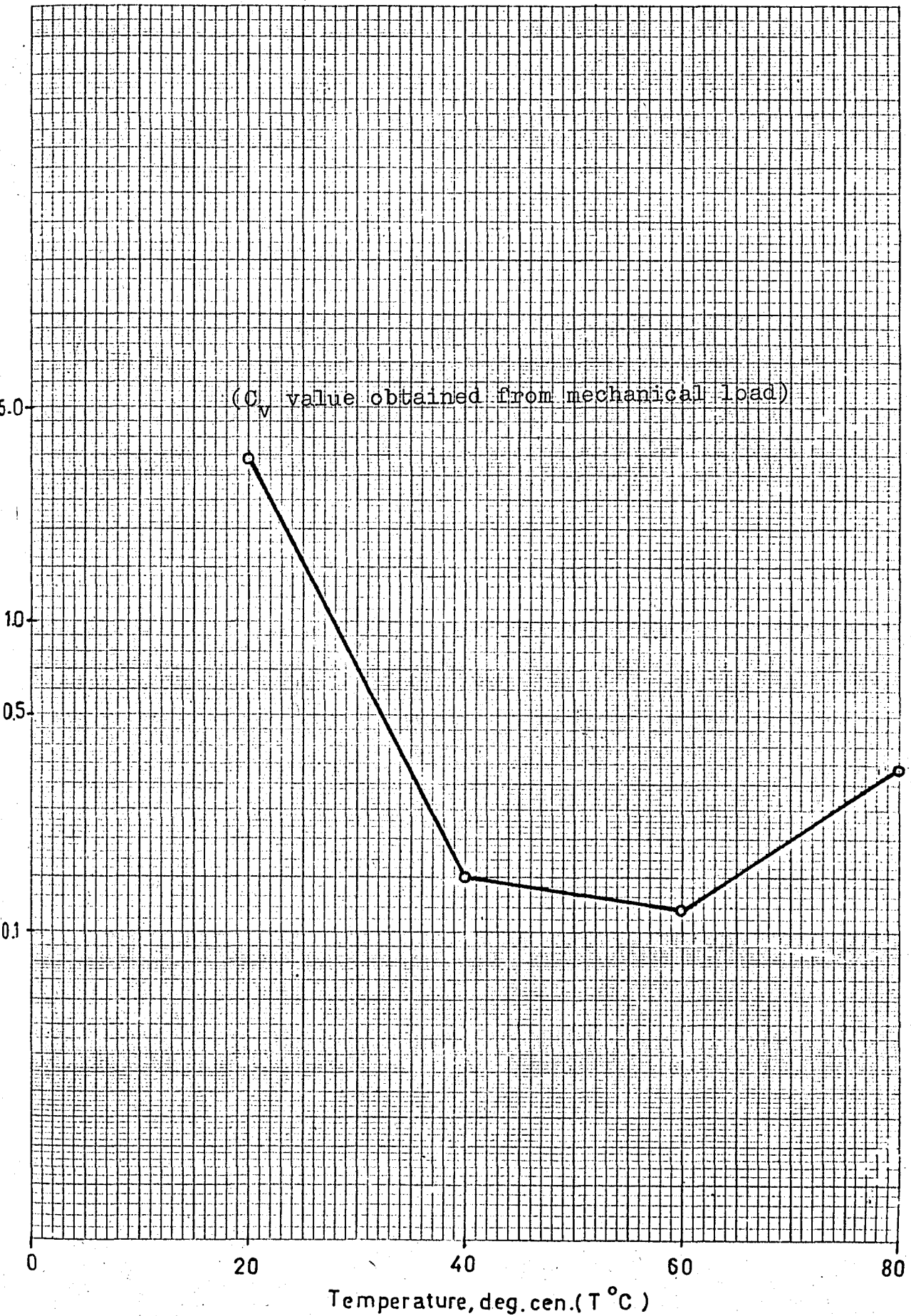


Fig:4. 19. Effect of Temperature on Coefficient of Consolidation, $P = 4.00 \text{ kg/cm}^2$

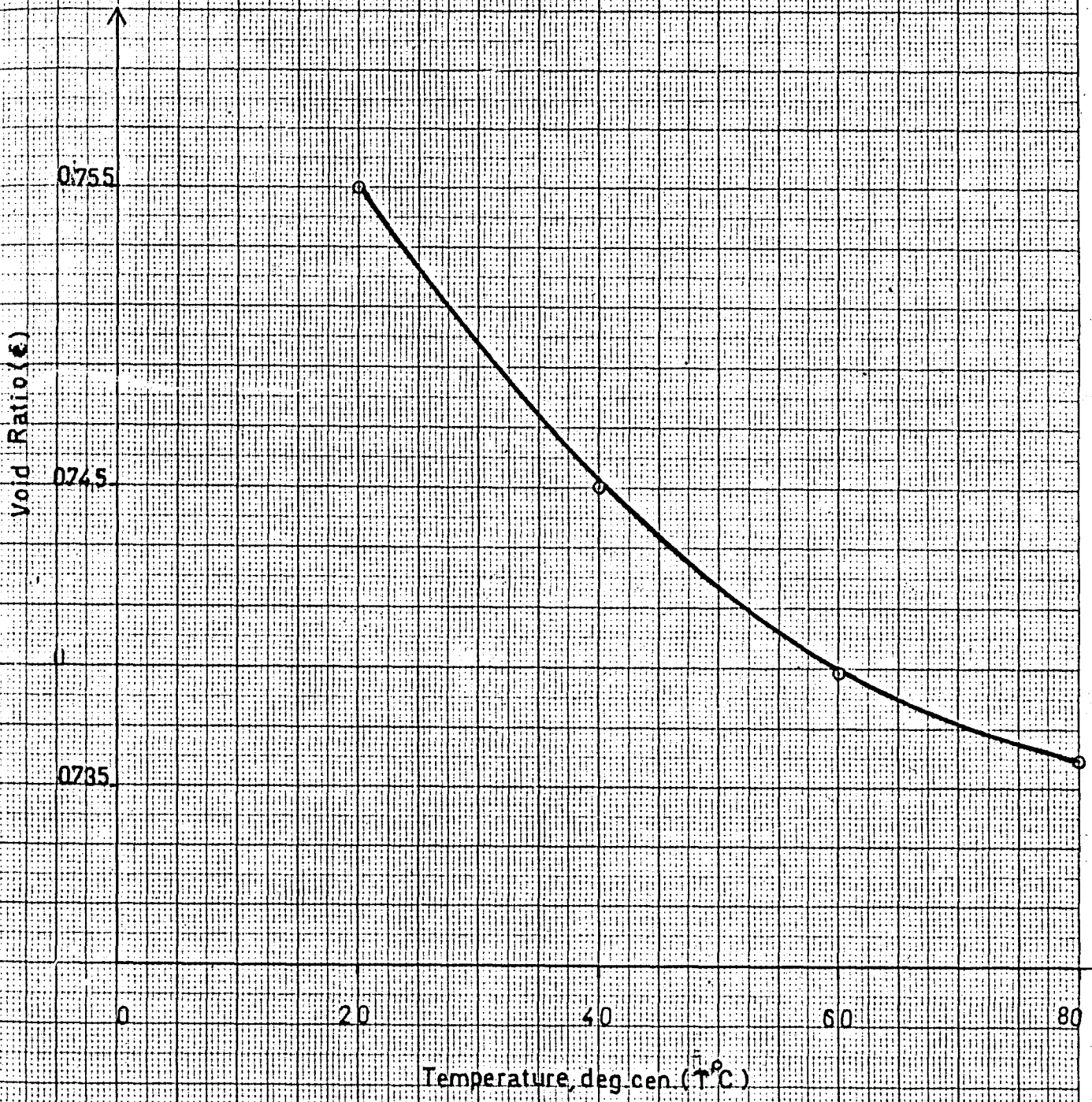


Fig. 4. 20. Effect of Temperature on Void Ratio, for $P=4.00 \text{ kg/cm}^2$

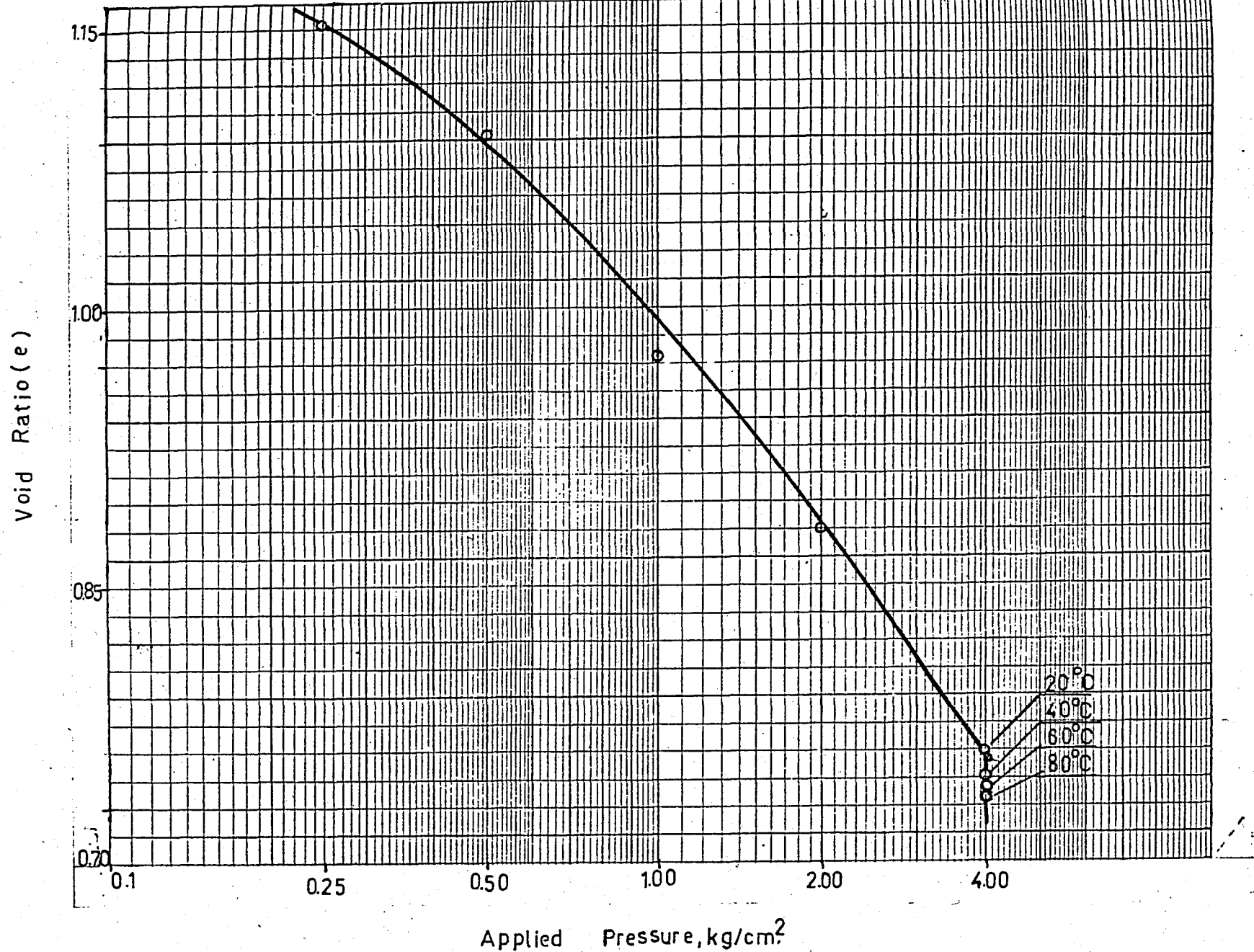


Fig:4. 21. Effect of Temperature on the Compression Curve, for $P = 4.00 \text{ kg/cm}^2$

B. CLAY WITH HIGH PLASTICITY (Boğazköy-Grey)

TEST - 1: (Boğazköy-Grey)

$P = 1.00$ kg.per.sq.cm.

$W_i = 70.63$ %

$W_f = 48.63$ %

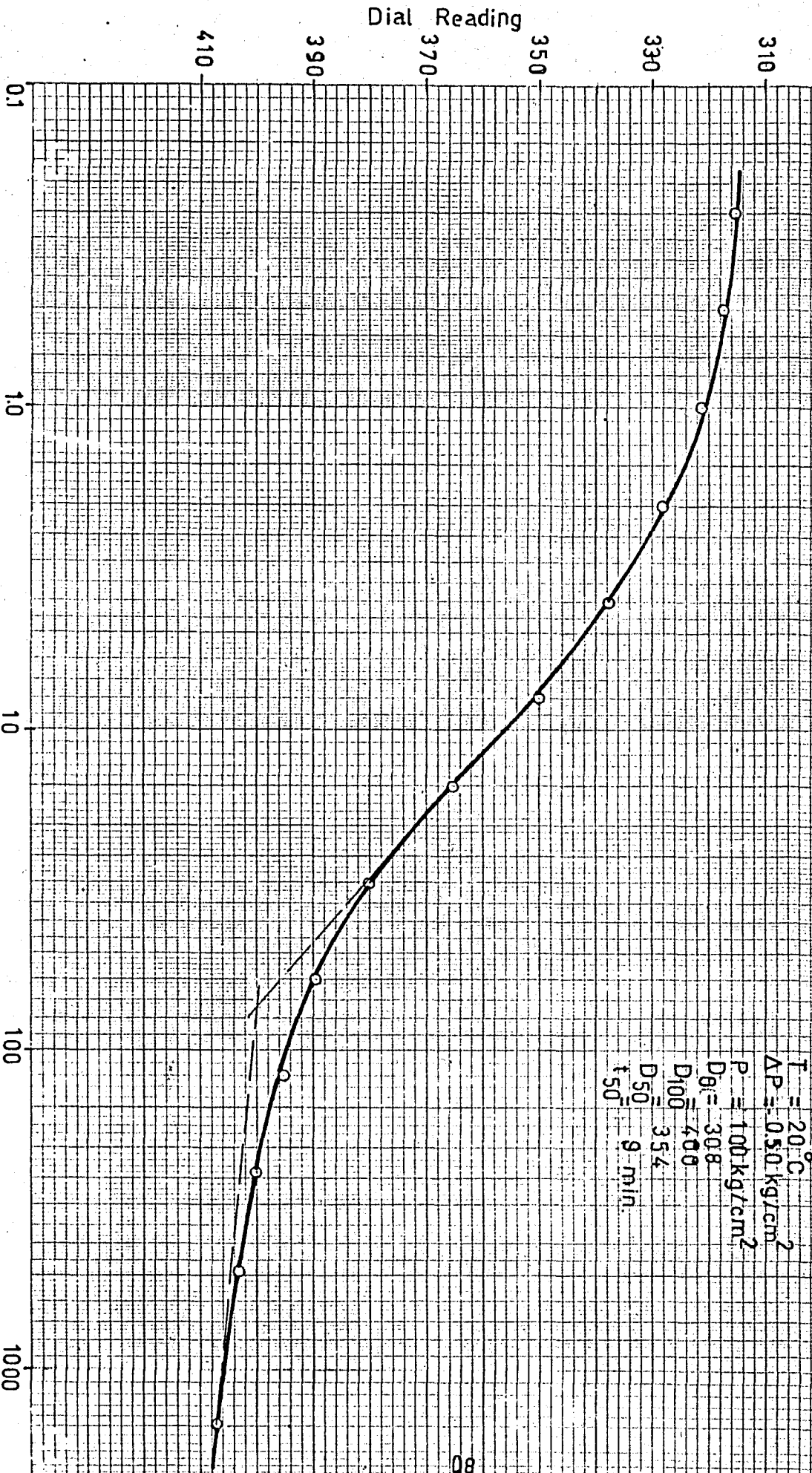


Fig. 4. 22. Plot of DR. vs. Log time.

$T = 40^{\circ}\text{C}$
 $P = 100 \text{ kg/cm}^2$
 $D_0 = 404.8$
 $D_{100} = 418$
 $D_{50} = 411.4$
 $t_{50} = 100 \text{ min.}$

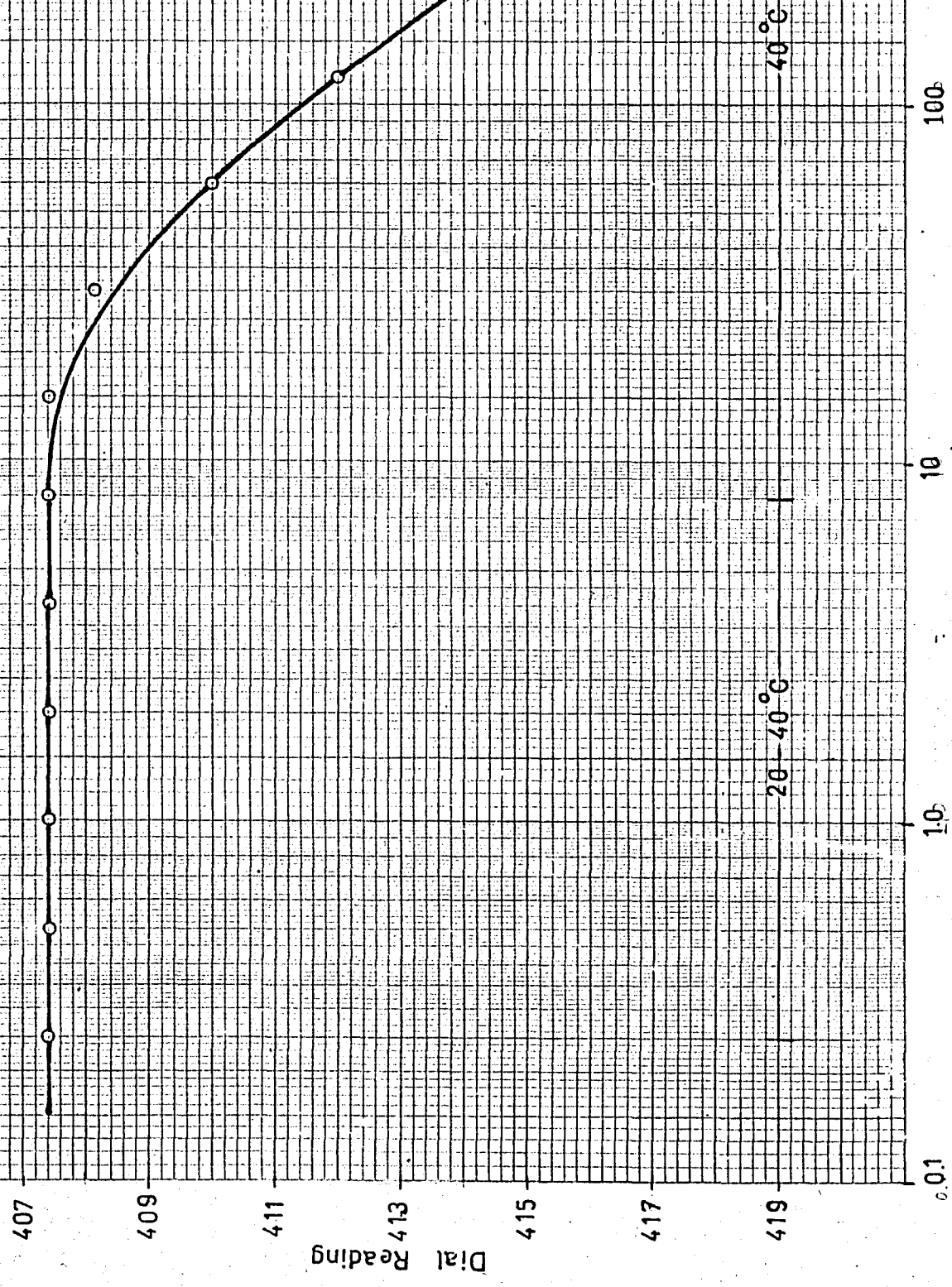


Fig: 4. 23. Plot of DR. vs. Log time.

$T = 60^{\circ}\text{C}$
 $P = 1.00 \text{ kg/cm}^2$
 $D_0 = 417.8$
 $D_{100} = 428.4$
 $D_{50} = 423.1$
 $t_{50} = 150 \text{ min}$

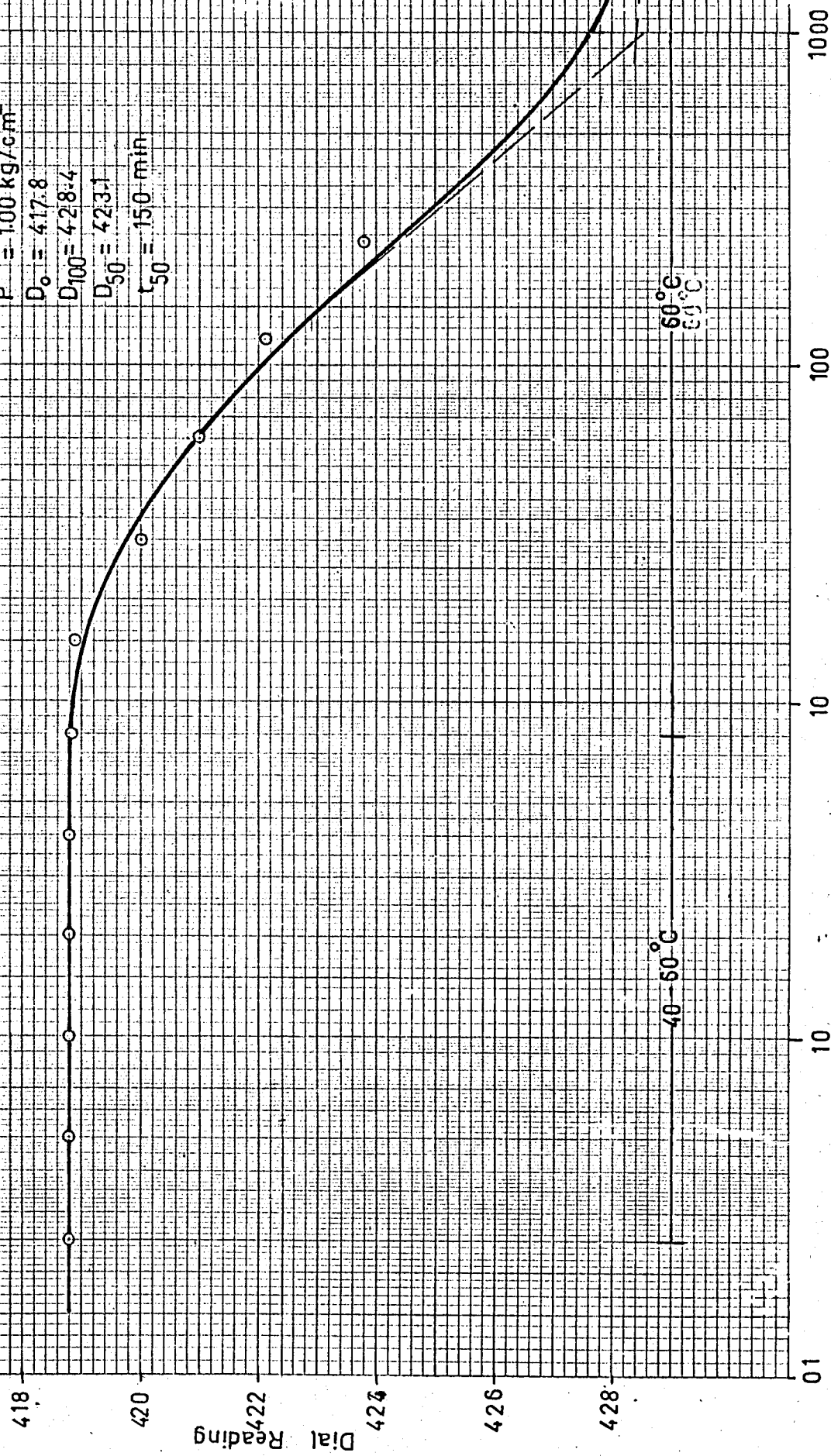


Fig: 4. 24. Plot of DR. vs. Log time.

$T = 80^{\circ}\text{C}$
 $P = 100 \text{ kg/cm}^2$
 $D_0 = 427.8$
 $D_{100} = 432.6$
 $D_{50} = 430.1$
 $t_{50} = 140 \text{ min}$

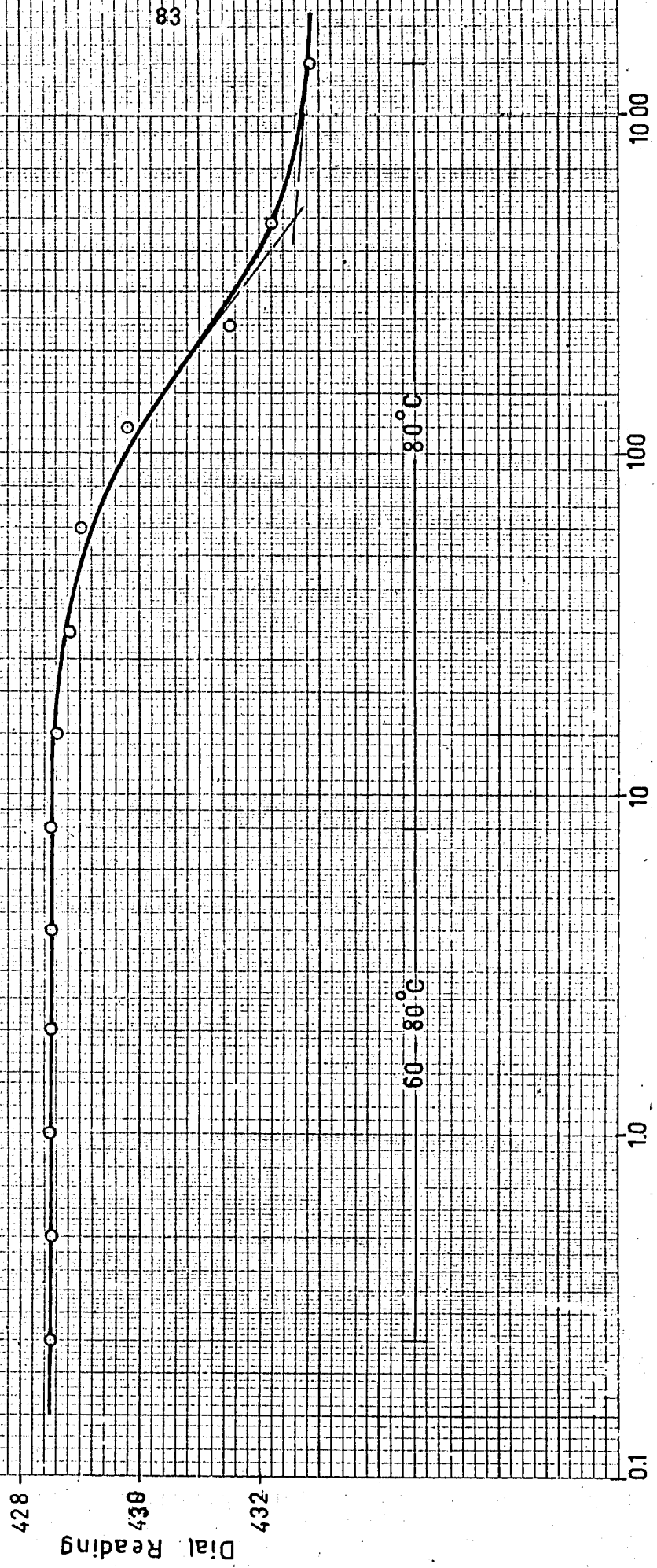


Fig: 4. 25. Plot of DR. vs. Log time.

Coefficient of Consolidation, sq. cm. per. sec. ($C_v \times 10$) $(C_v$ value obtained from mechanical load)

50

10

0.5

0.1

0

20

40

60

80

Temperature, deg. cen. ($T^{\circ}C$)Fig:4. 26. Effect of Temperature on Coefficient of Consolidation, $P = 1.00 \text{ kg/cm}^2$

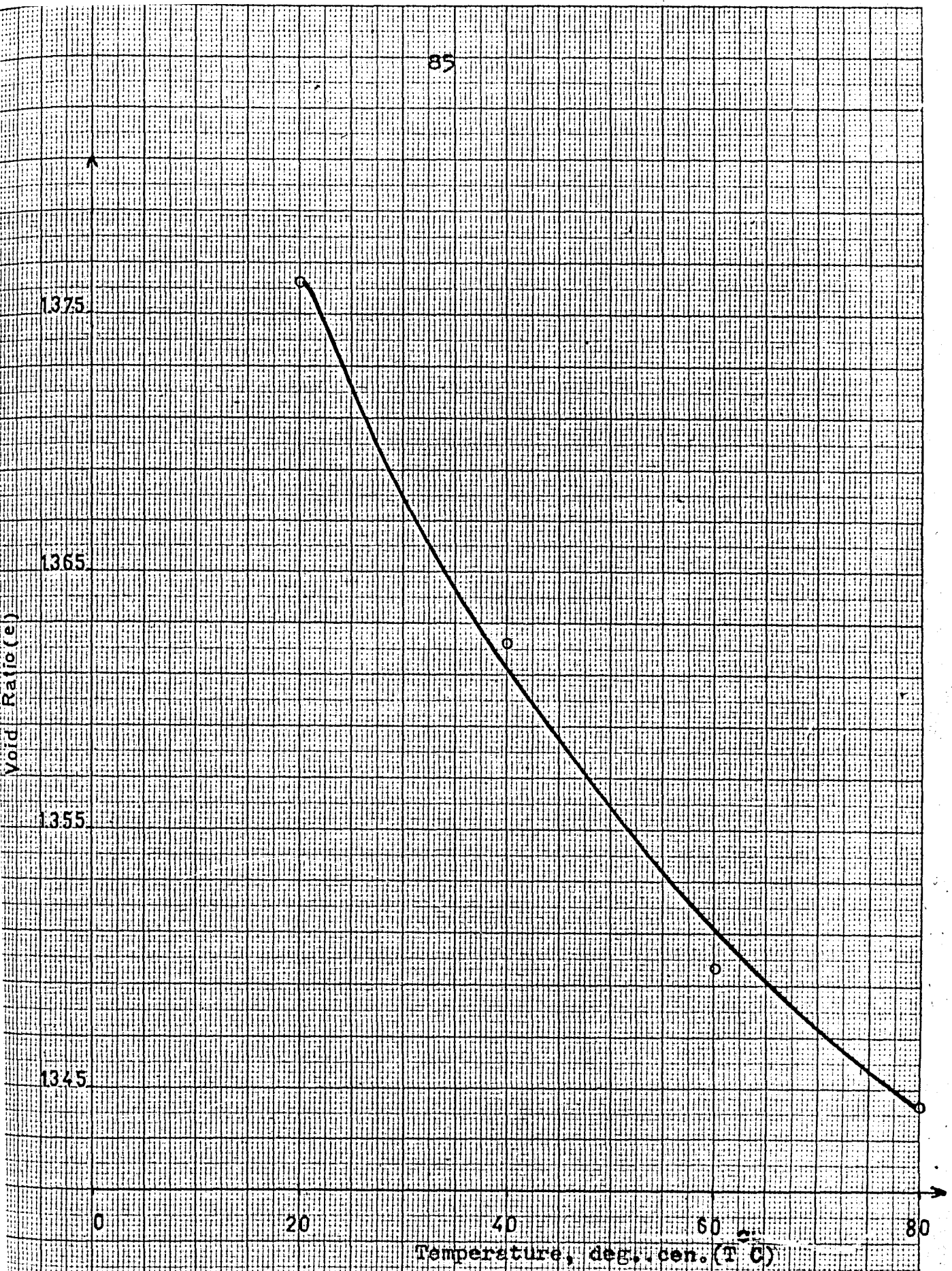


Fig. 4. 27. Effect of Temperature on Void Ratio, $P=100\text{kg}/2\text{cm}$

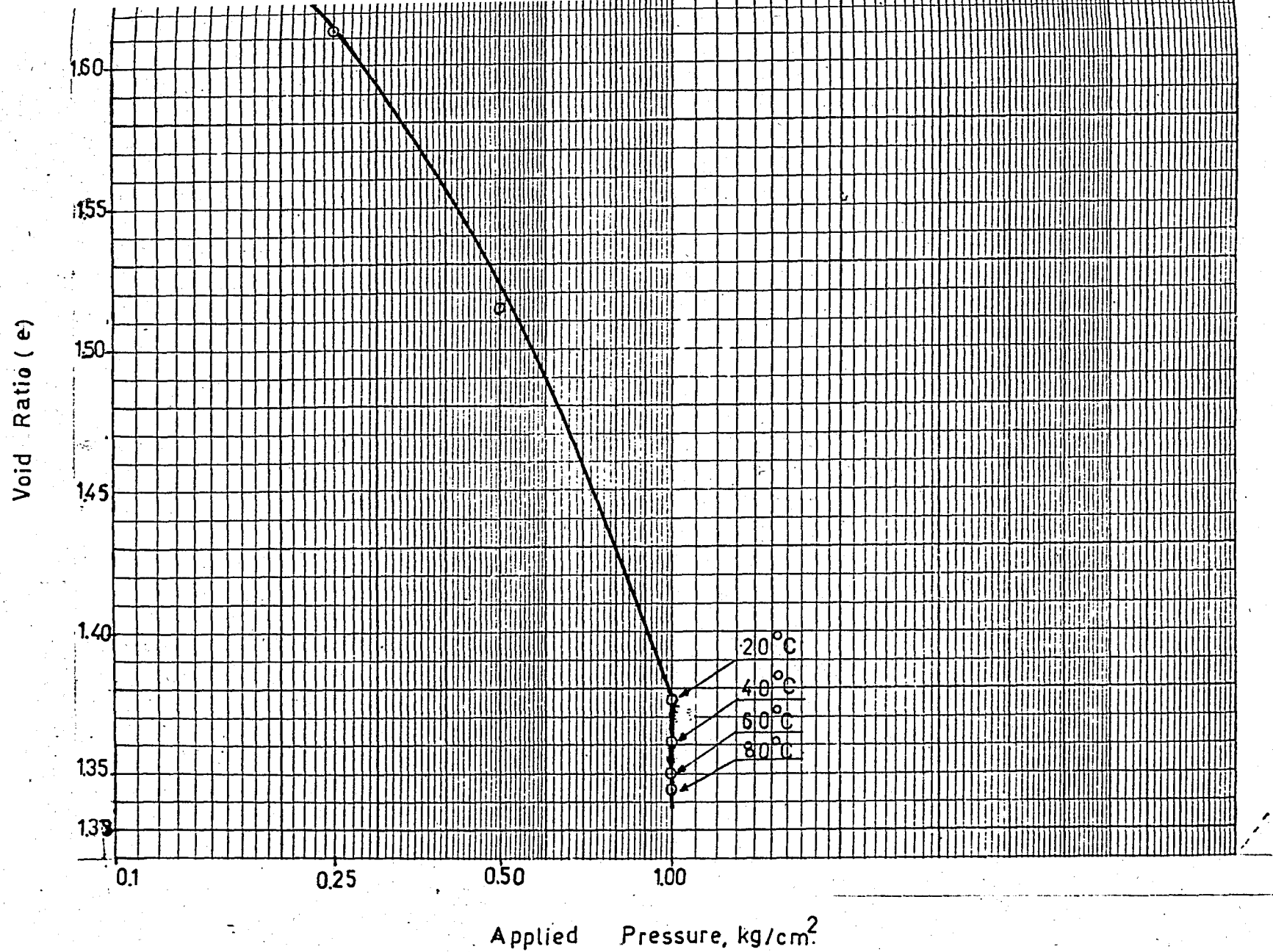


Fig: 4. 28. Effect of Temperature on the Compression Curve, for $P = 100 \text{ kg/cm}^2$.

TEST - 2:(Bogazköy-Grey)

$P = 2.00 \text{ kg.per.sq.cm.}$

$W_i = 67.00 \%$

$W_f = 45.28 \%$

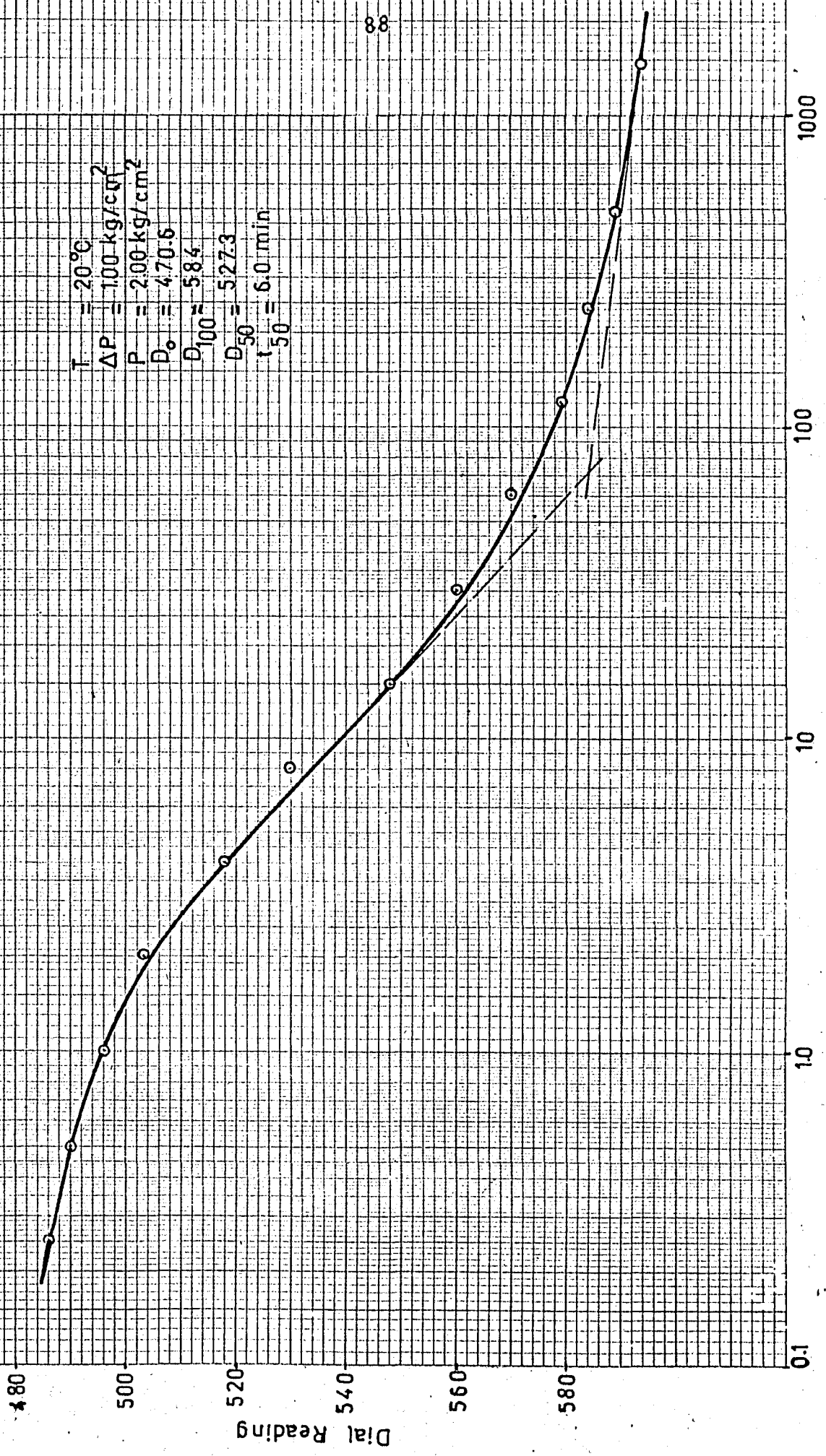
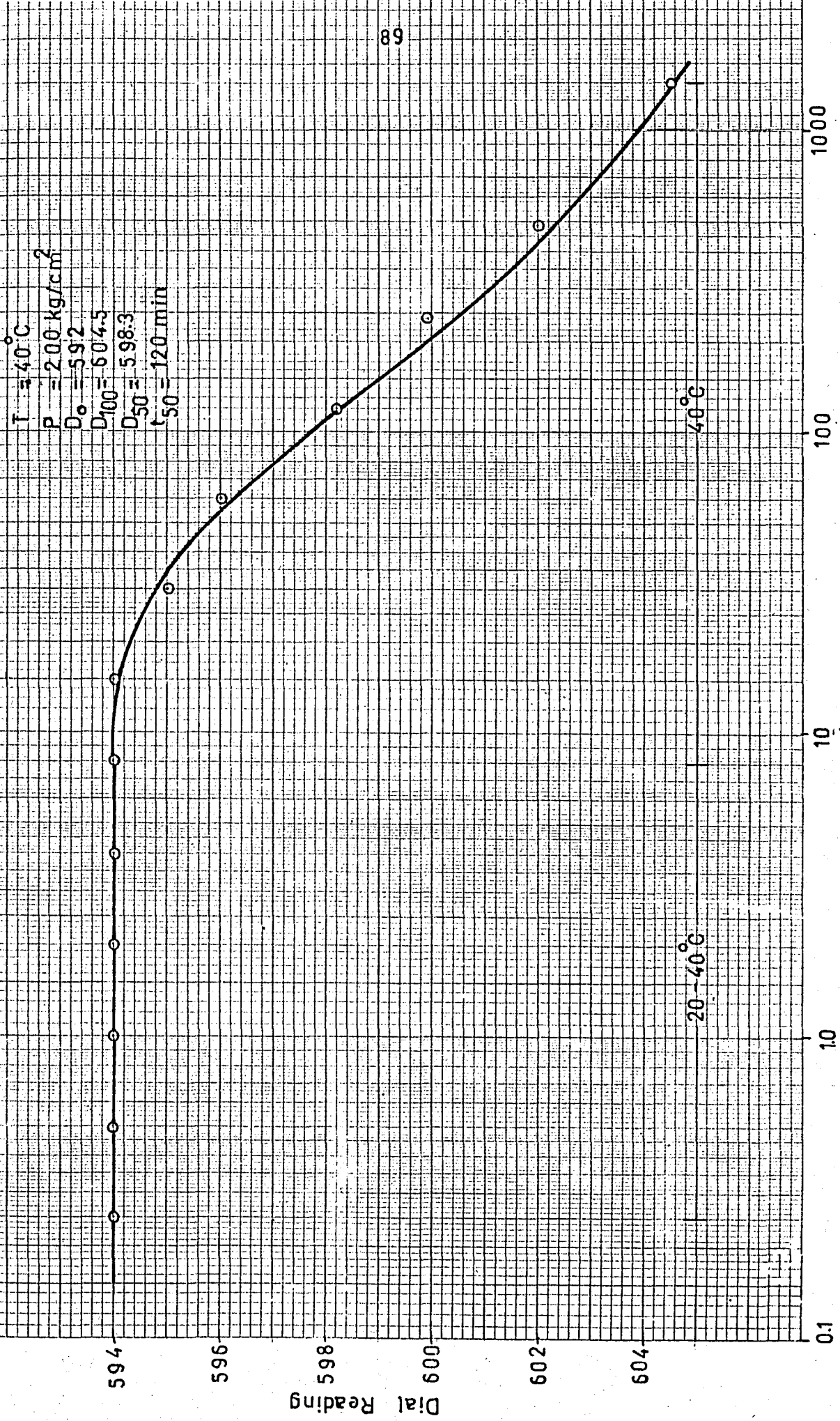


Fig: 4. 29. Plot of DR. vs. Log time.

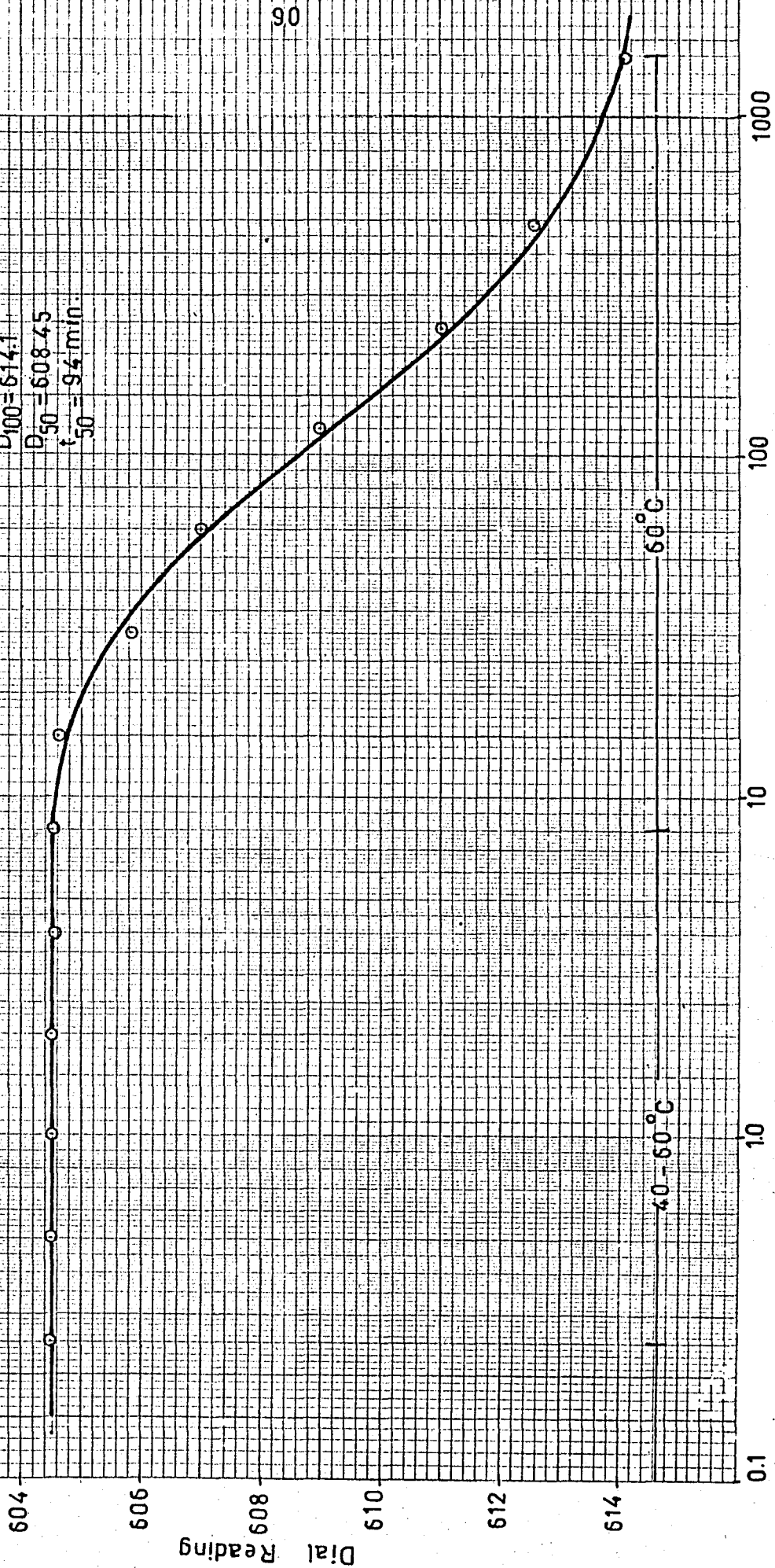
$T = 40^{\circ}\text{C}$
 $P = 2.00 \text{ kg/cm}^2$
 $D_0 = 59.2$
 $D_{100} = 604.5$
 $D_{50} = 598.3$
 $t_{50} = 120 \text{ min}$



Log Time (min).

Fig. 4. 30. Plot of DR. vs. Log time.

$T = 60^{\circ}\text{C}$
 $R = 200 \text{ kg/cm}^2$
 $D_0 = 602.8$
 $D_{100} = 614.1$
 $D_{50} = 608.45$
 $t_{50} = 94 \text{ min.}$



Log Time (min)
 Fig: 4. 31. Plot of DR. vs. Log time.

$T = 80^{\circ}\text{C}$
 $P = 200 \text{ kg/cm}^2$
 $D_0 = 6122$
 $D_{100} = 6215$
 $D_{50} = 616.85$
 $t_{50} = 155 \text{ min.}$

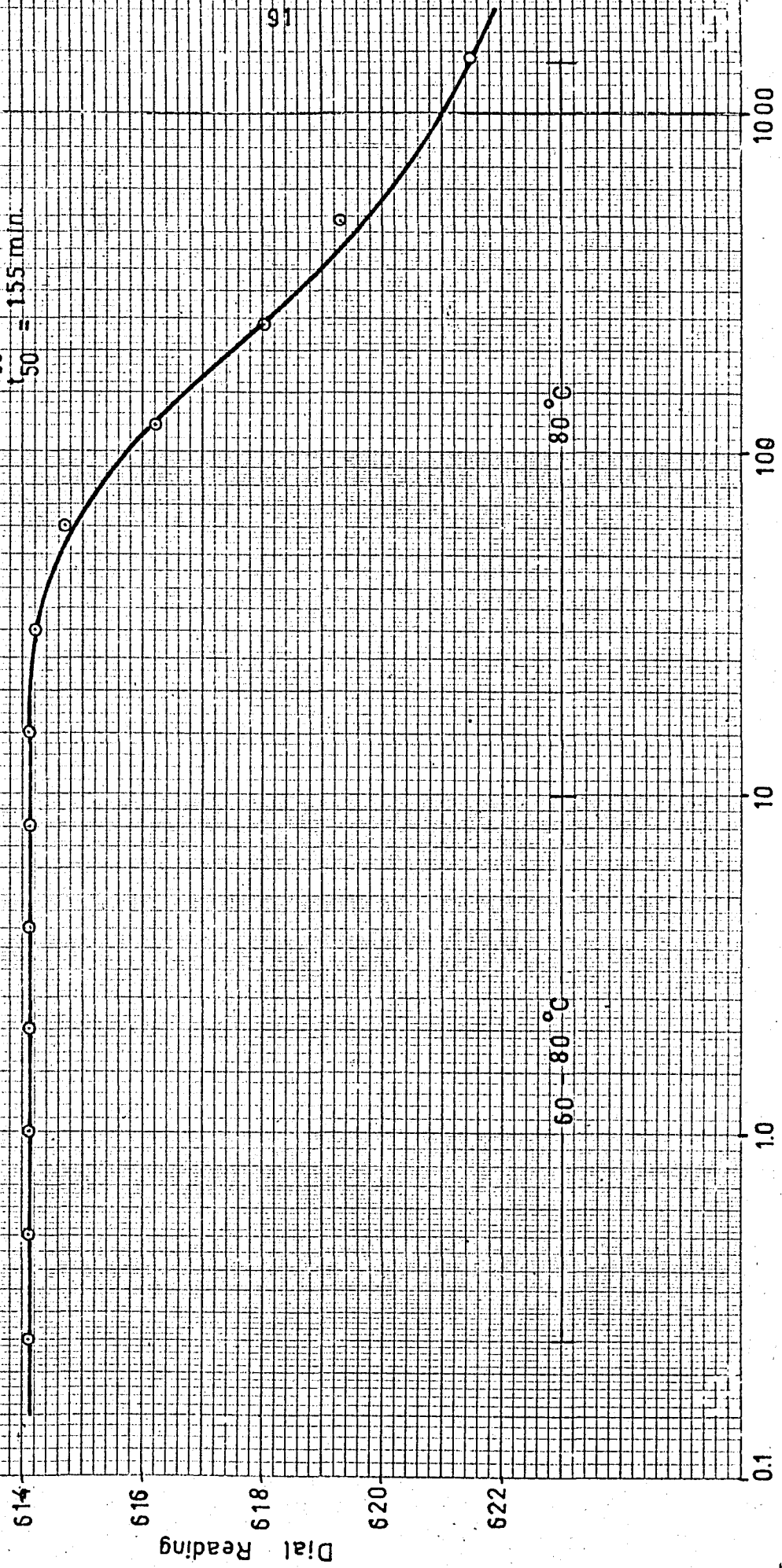


Fig. 4. 32. Plot of DR vs. Log time.

Coefficient of Consolidation sq.cm.per. sec. ($C_v \times 10^{-4}$)

DATA SHEET No. 40. LOGARITHMIC $\times 2$ M.M (4 CYCLE)

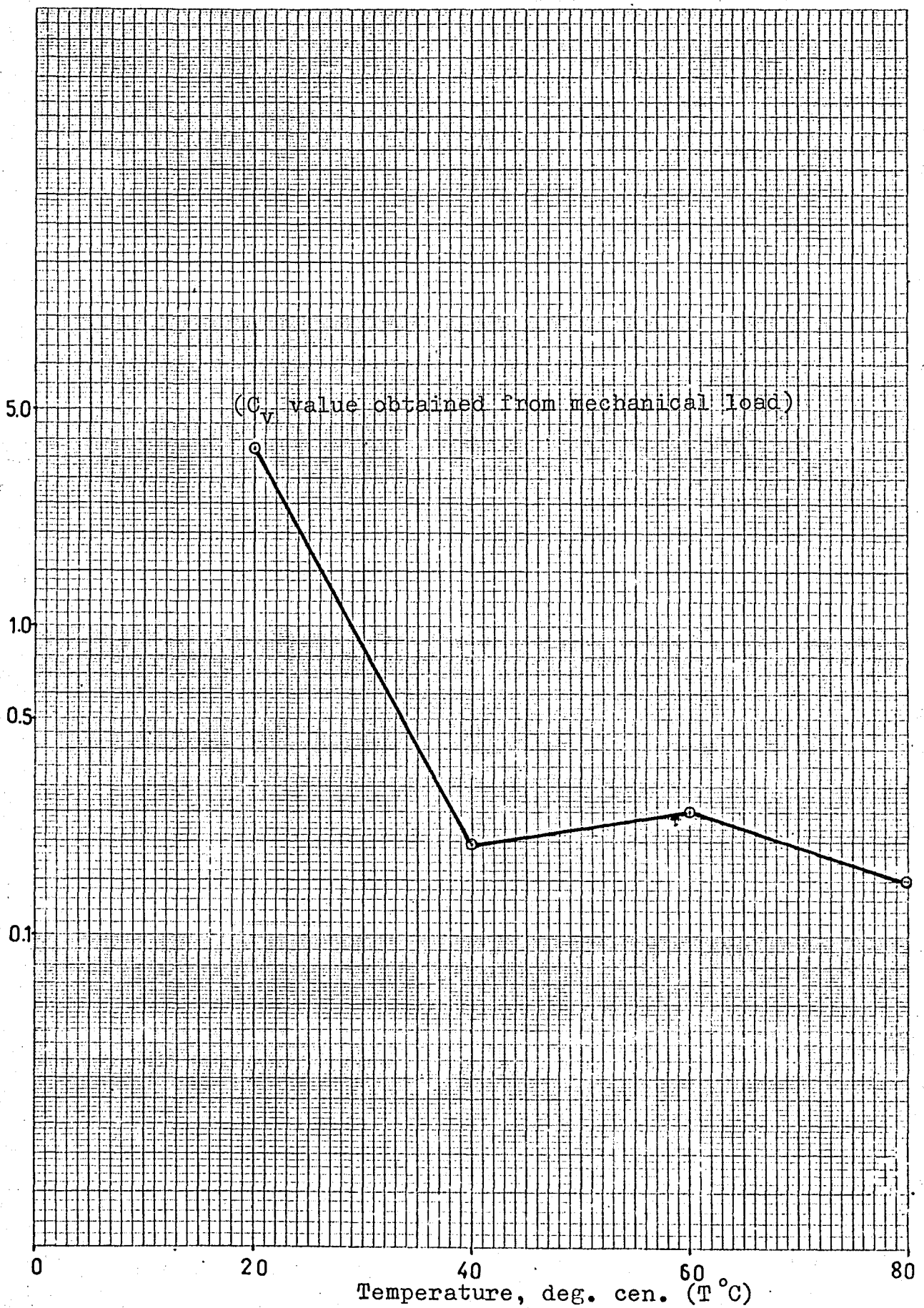


Fig:4. 33. Effect of Temperature on Coefficient of Consolidation for $P = 2.00 \text{ kg/cm}^2$.

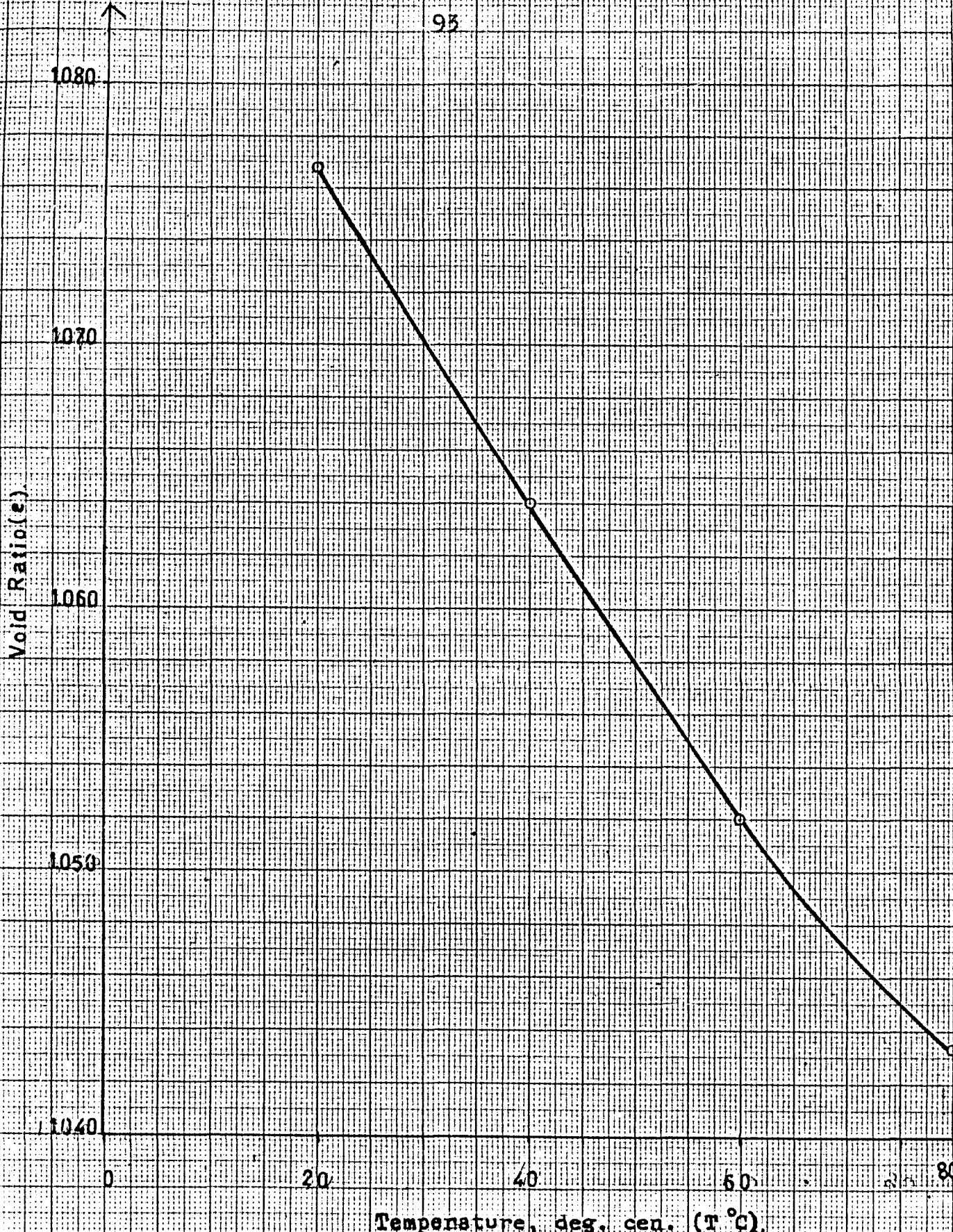


Fig:4. 34. Effect of Temperature on Void Ratio, for P 2.00 kg/cm².

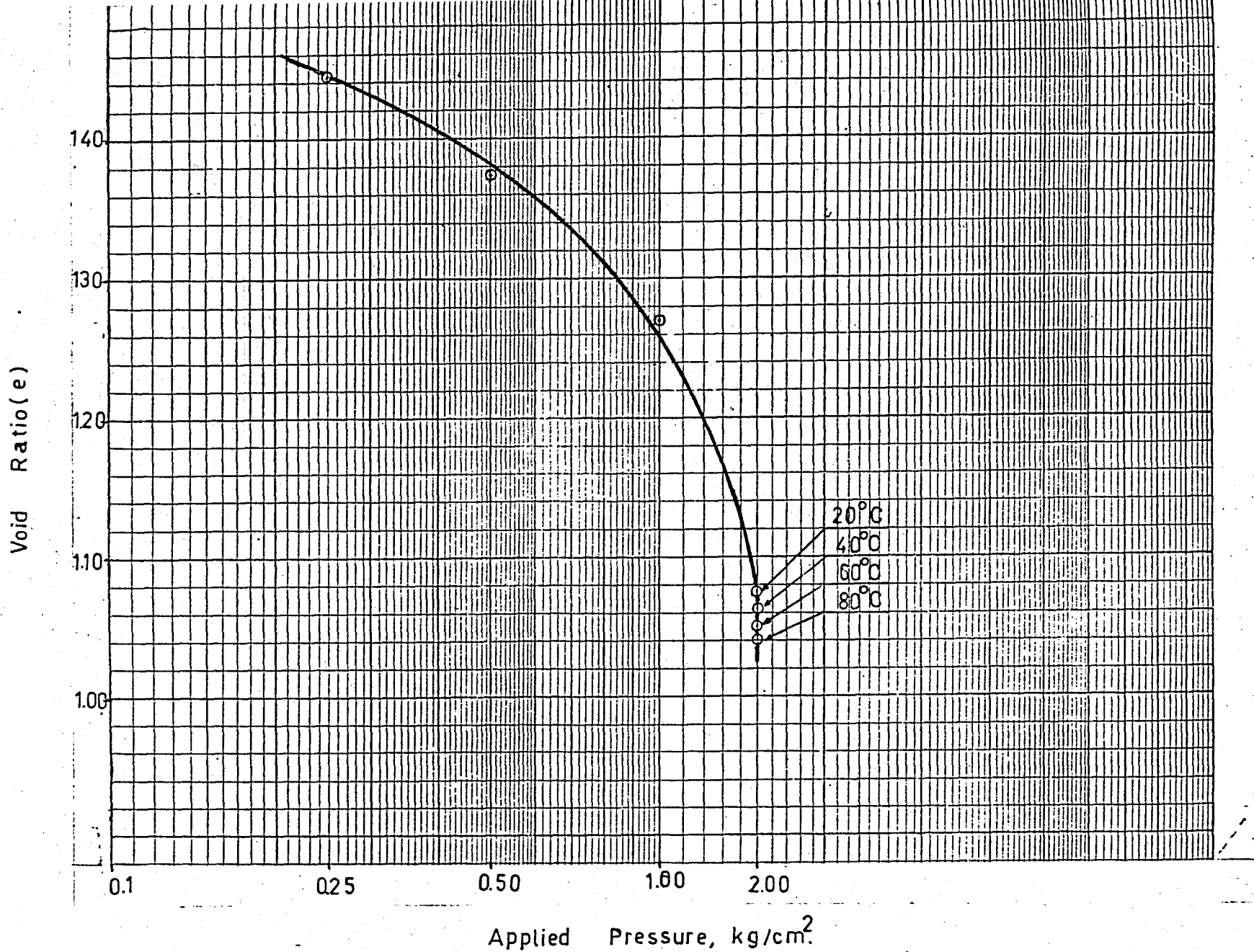


Fig: 4. 35. Effect of Temperature on the Compression Curve, for $P=2.00 \text{ kg/cm}^2$.

TEST -3: (Boğazköy-Grey)

P 4.00 kg.per.sq.cm.

W_i 68.40 %

W_f 39.35 %

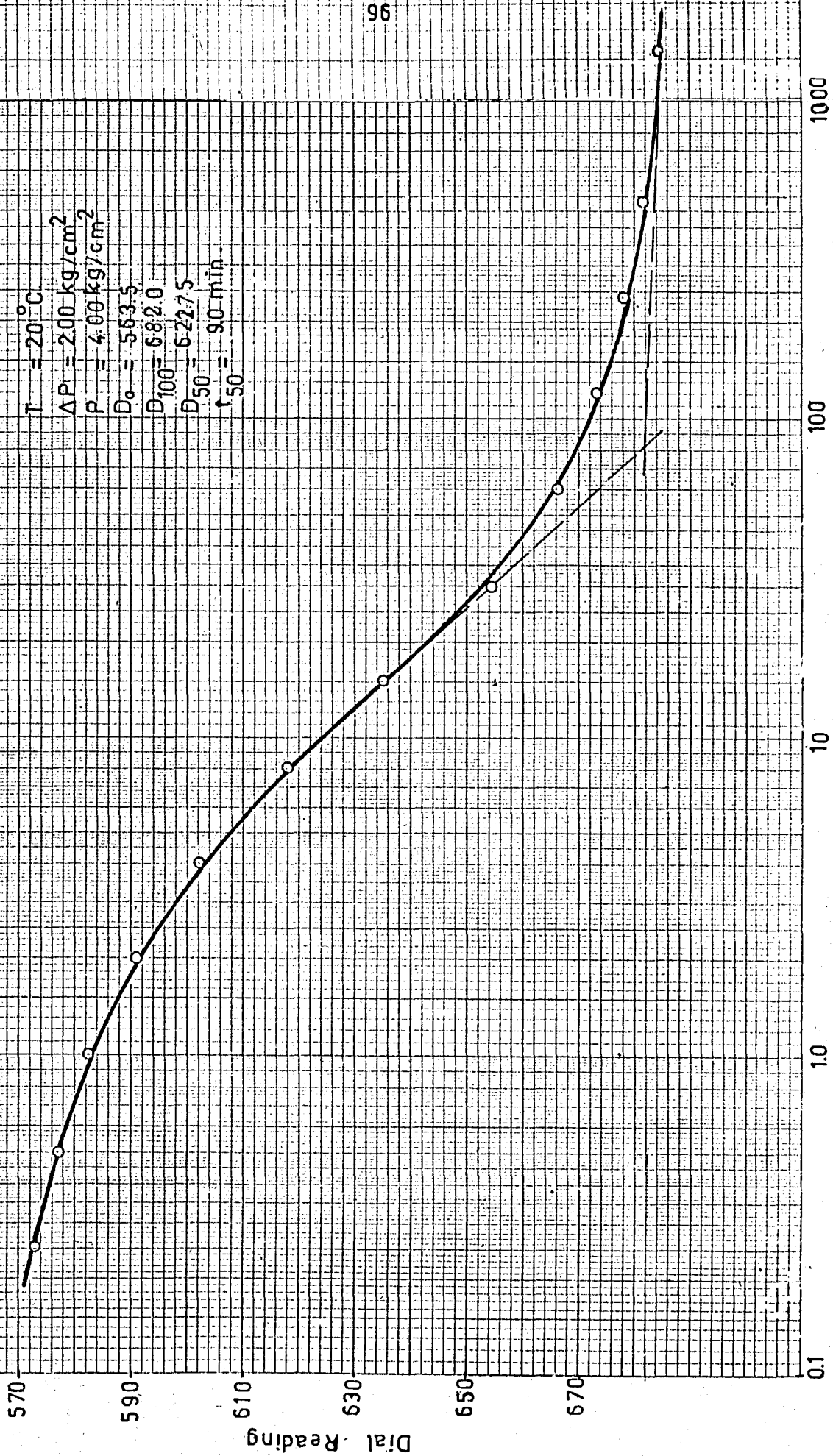


Fig: 4. 36. Plot of DR. vs. Log time.

$T = 40^{\circ}\text{C}$
 $P = 4.00 \text{ kg/cm}^2$
 $D_0 = 6.81$
 $D_{100} = 6.99$
 $D_{50} = 6.90$
 $t_{50} = 110 \text{ min.}$

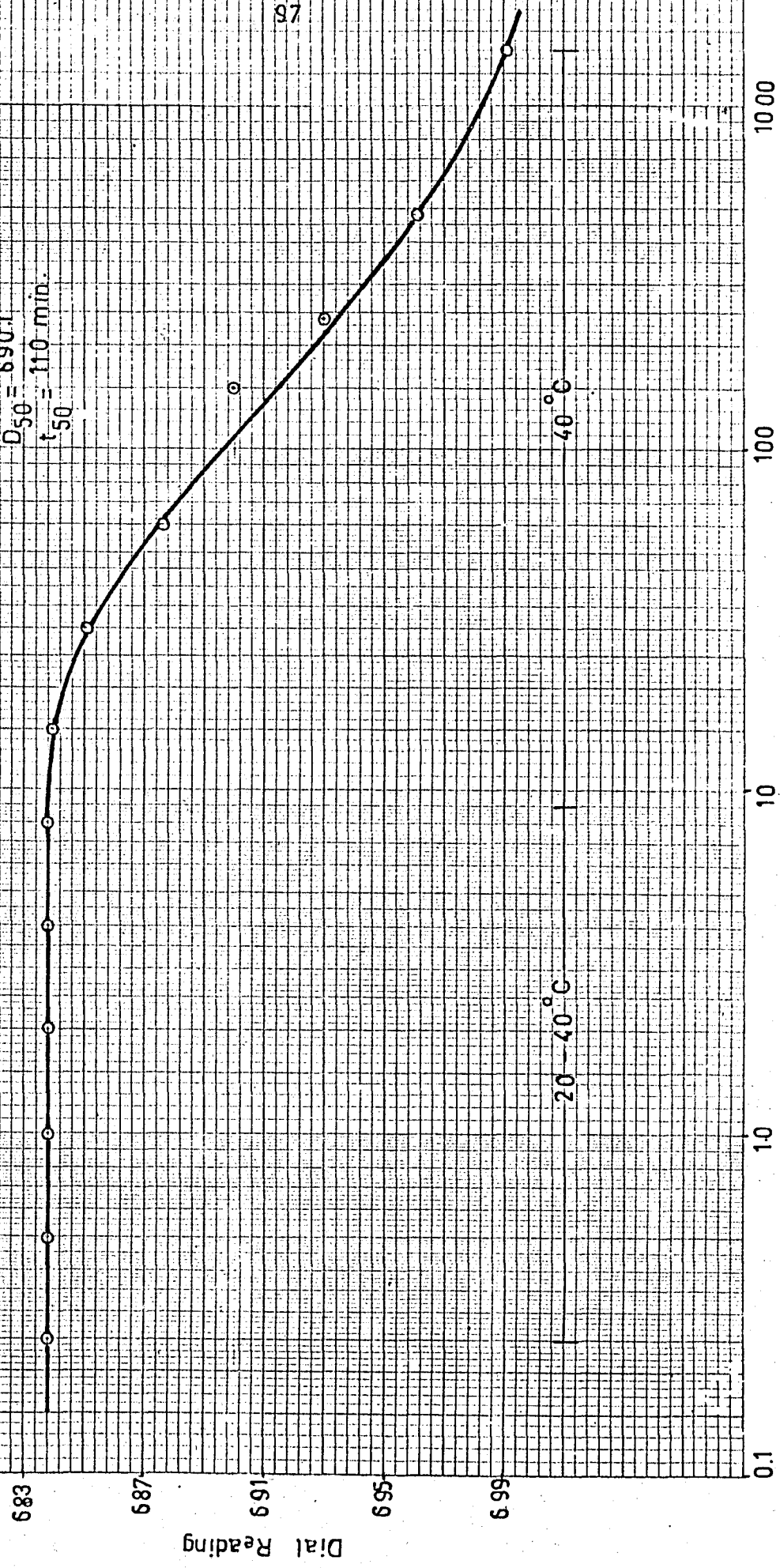


Fig. 4. 37. Plot of DR. vs. Log time.

$T = 60^{\circ}\text{C}$
 $P = 400 \text{ kg/cm}^2$
 $D_0 = 697$
 $D_{100} = 709.1$
 $D_{50} = 703$
 $t_{50} = 135 \text{ min}$

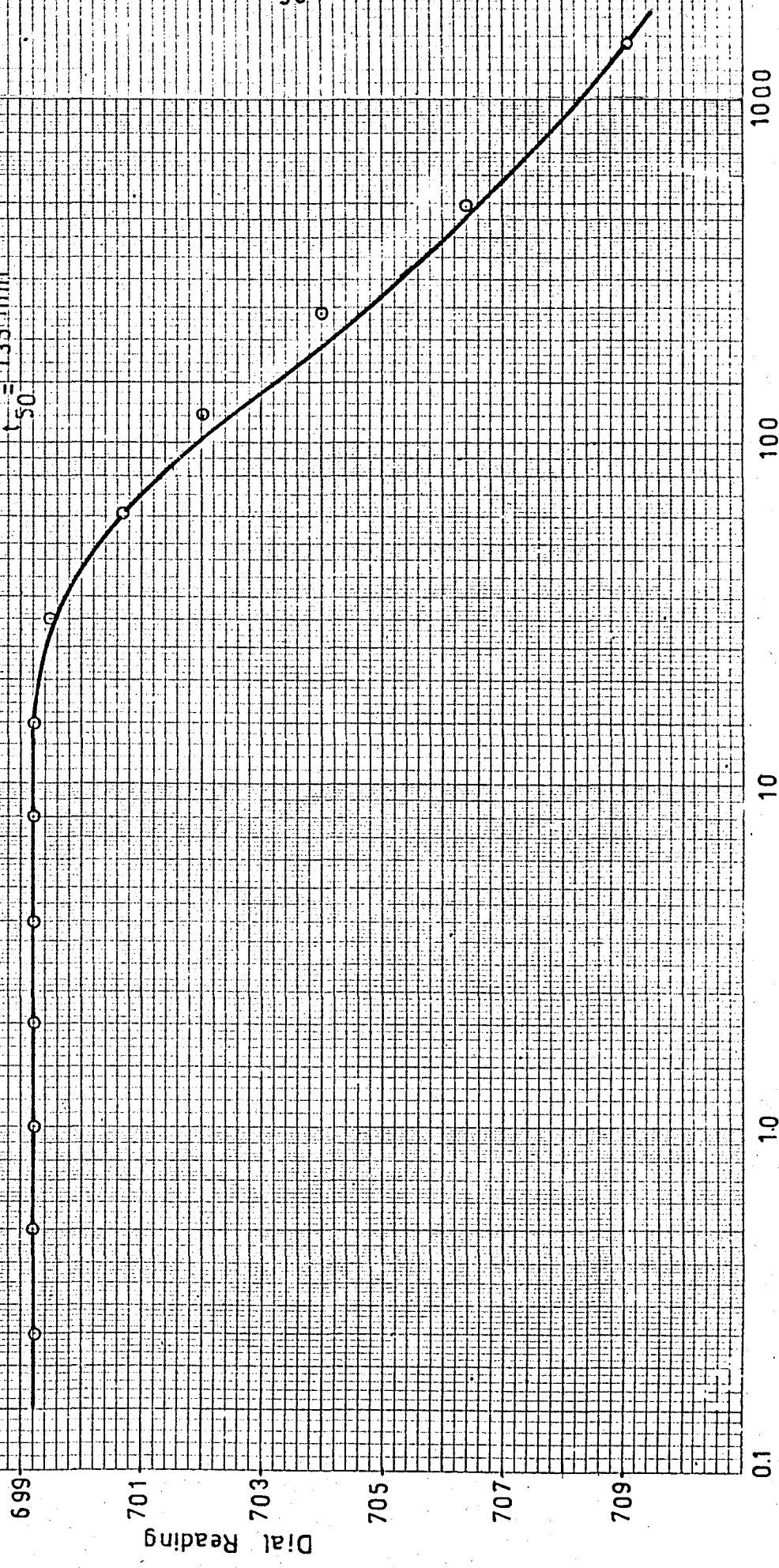


Fig: 4.38. Plot of DR. vs. Log time,

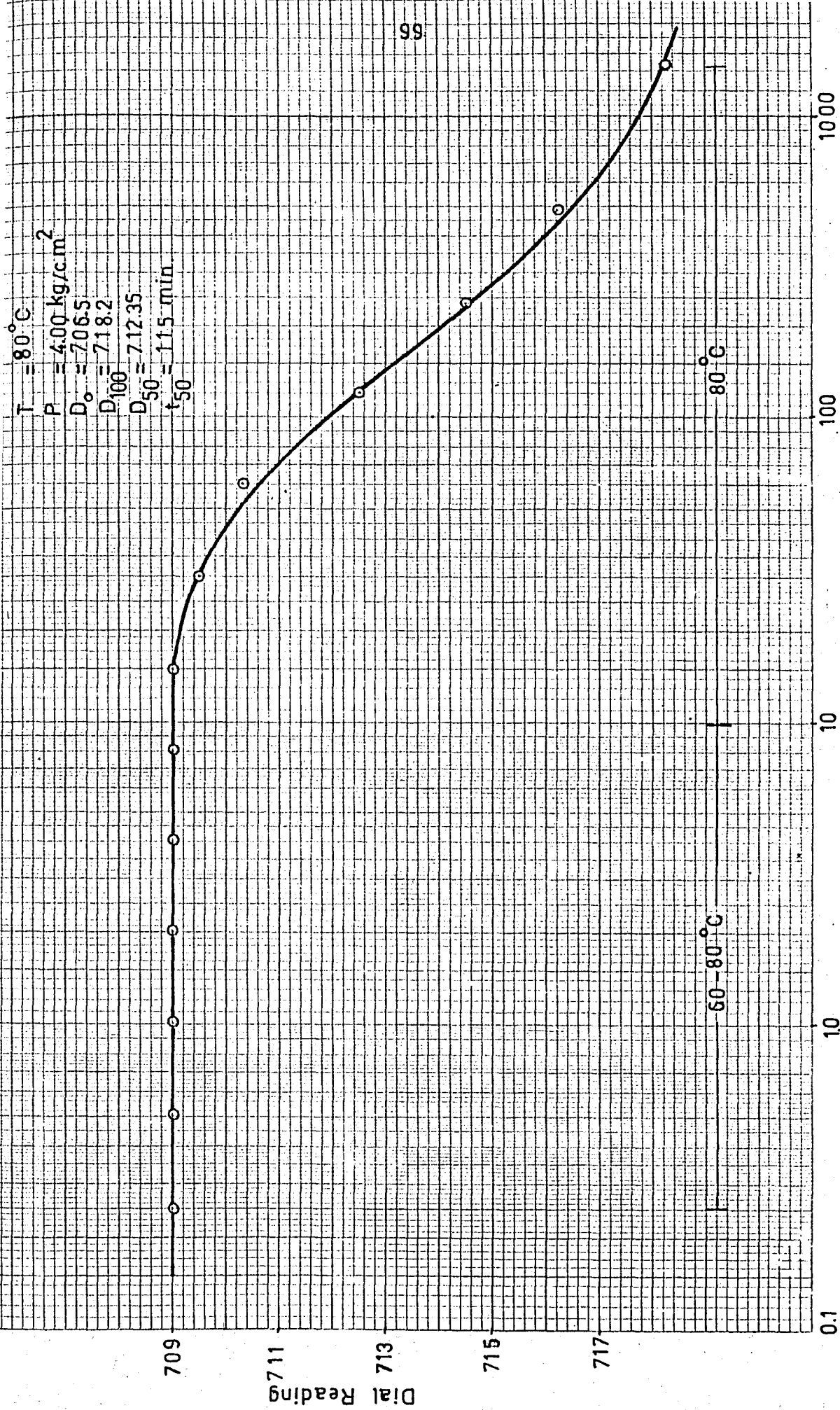


Fig: 4.39. Plot of DR. vs. Log time.

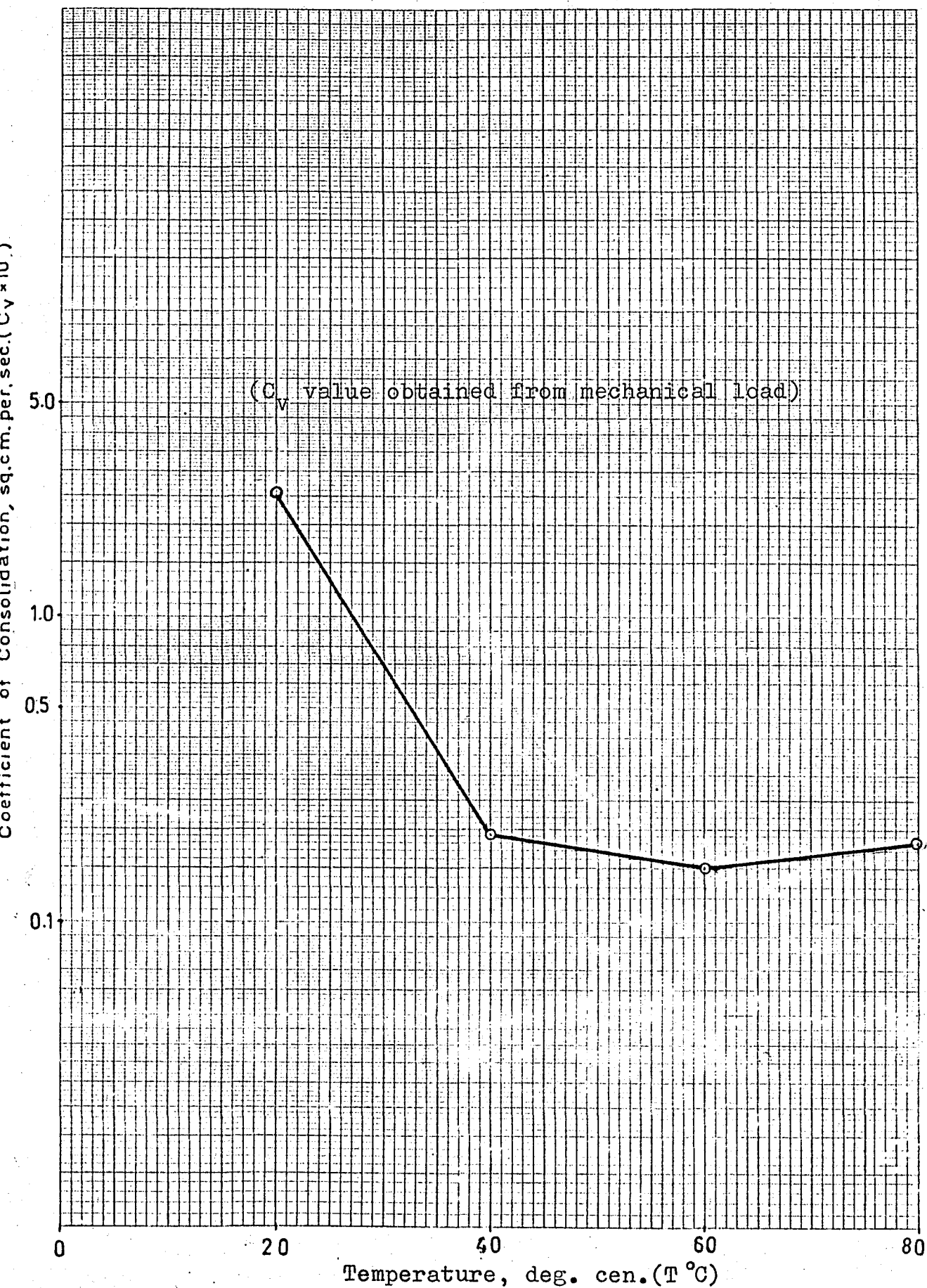


Fig:4. 40. Effect of Temperature on Coefficient of Consolidation, for $P = 4.00 \text{ kg/cm}^2$.

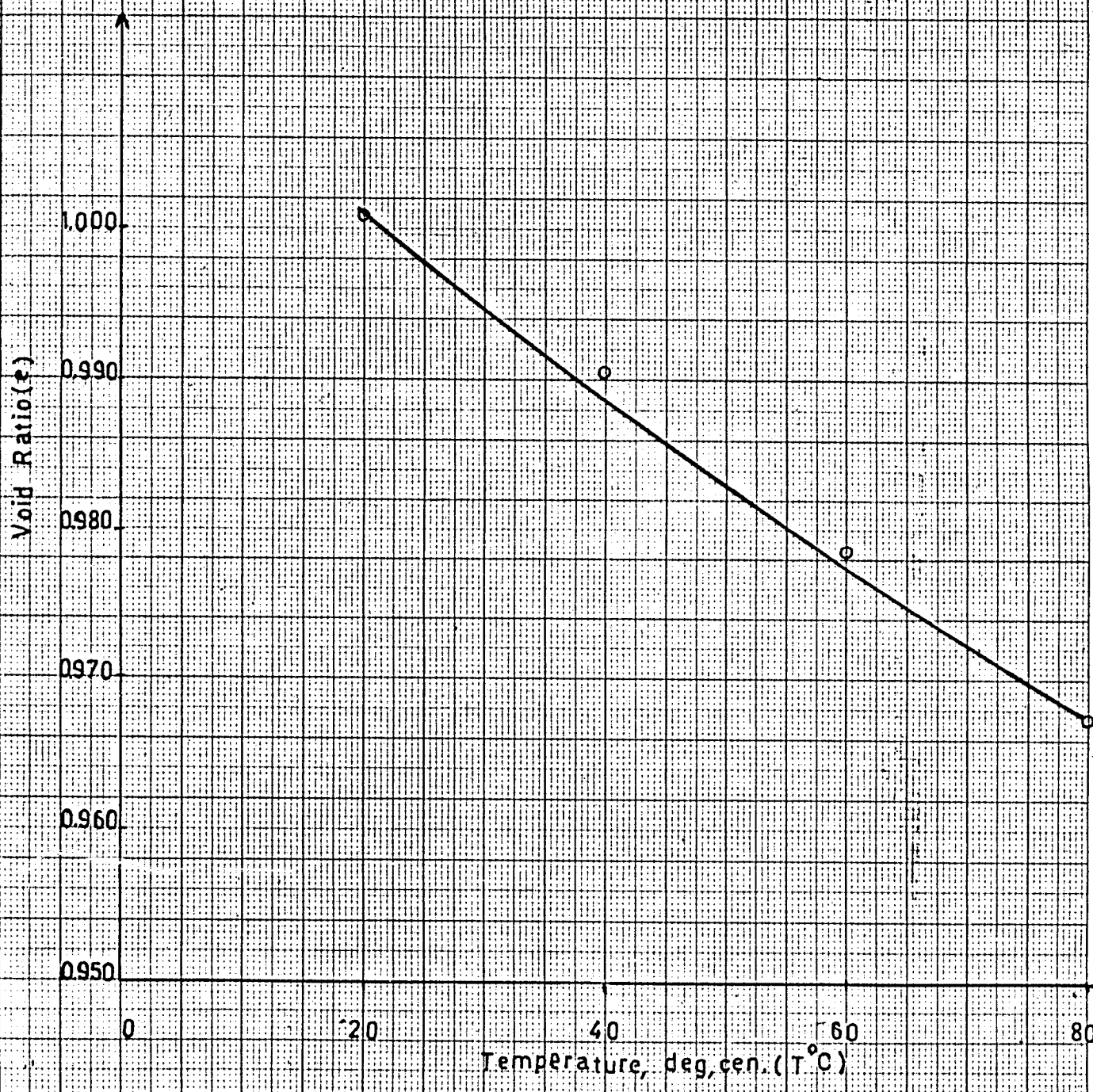


Fig: 4. 41 Effect of Temperature on Void Ratio, for P= 400kN/m²

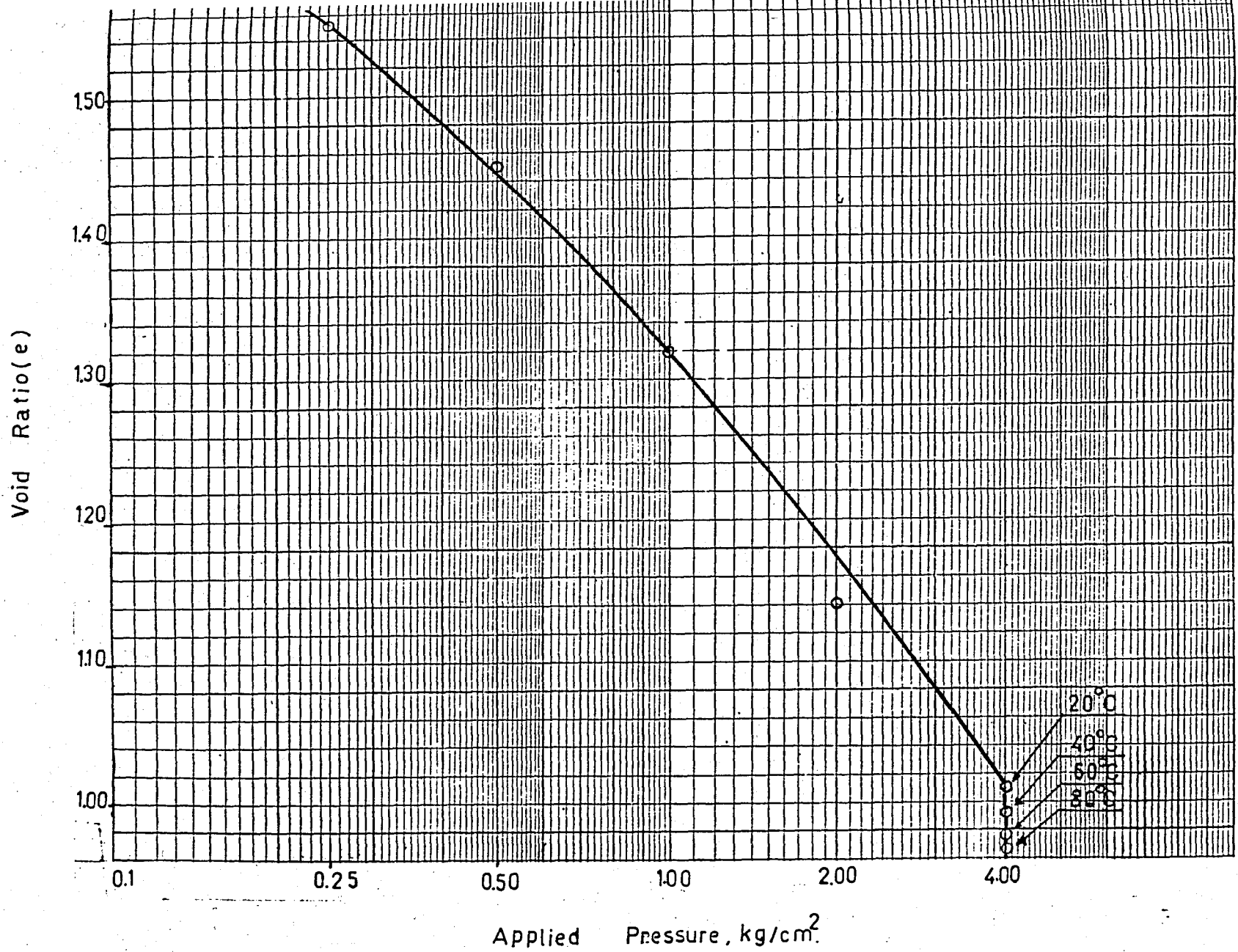


Fig: 4. 42 Effect of Temperature on the Compression Curve, for $P = 4.00 \text{ kg/cm}^2$

C - INTERPRATATION OF TEST RESULTS

After the experiments done on the various samples within nearly identical void ratio and different constant stress levels the following results can be obtained.

† - For clay with low plasticity and for high plasticity noticeable change in sample height and change in void ratio are produced in the sample when temperature differences are applied at given stress levels. The temperature of 40°C affects the void ratio and change in sample height the most. The temperature of 60°C and 80°C have lesser effects respectively. It is evident that at constant stress level, the increase in temperature would create a decrease in the viscosity of the system as a whole. An applied temperature gradient causes a flow of water out of the system. Temperature causes an increase in ionic movement at the soil particle-water interface, thus establishing the necessary potential for film flow, for here the increase in energy would be most perceptible. For clay with low plasticity, from table 4.1. it is obvious that at constant stress levels of 1.00, 2.00, and 4.00 kg per sq cm, the total effect of temperature on change in sample height was 0.229mm, 0.189mm, and 0.188mm respectively. Fig. 4.43 shows that an increase in temperature causes a decrease in void ratio for fully drained samples. The effect of temperature, for this clay, is more pronounced at a constant stress level of 1.00 kg per sq cm as compared to 2.00 and 4.00 kg per sq cm. This indicates that the effect of temperature is decreasing with increasing the stress levels.

The reason of this mechanism is that this clay has low water content and clay particles have small surface area because of the low plasticity. For clay with high plasticity, from table 4.2 it is obvious that at constant stress levels of 1.00, 2.00, and 4.00 kg per sq cm, the total effect of temperature on change in sample height was 0.254 mm, 0.275 mm, and 0.475 mm respectively. Figure 4.45 shows that an increase in temperature causes a decrease in void ratio for a fully drained samples. The effect of temperature, for this clay, is more pronounced at a constant stress level of 4.00 kg per sq cm. as compared to 2.00 and 1.00 kg per sq cm. This indicates that the effect of temperature increases with increasing stress levels. The reason of this mechanism is that this clay has high water content and clay particles have large surface area because of the high plasticity.

Temperature variations can cause significant changes in the volume of saturated soils. As a consequence, there is a partial collapse of the soil structure and a decrease in void ratio until a sufficient number of additional bonds are formed to enable the soil to carry the stress at higher temperatures. This effect is analogous to secondary compression under a stress increase.

2 - Figure 4.44 and 4.46 show the family of curves indicating the effect of temperature on the coefficient of consolidation due to the temperature change calculated using the semi-log method for clay with low plasticity and clay with high plasticity, respectively. From these curves it can be seen that tests made at 1.00, and 4.00 kg per sq cm re-

sults in a decrease of C_{v_t} at temperatures at 40°C and 60°C as compared an increase in C_{v_t} at 80°C . From these curves it can also be seen that at stress level of 2.00 kg per sq cm, temperature of 40°C indicate a definite decrease in C_{v_t} as compared to 60°C value.

From Eq. 5 it can be seen that C_{v_t} is directly proportional to the coefficient of permeability. It is known that permeability is related to viscosity which in turn is related to temperature. Hence, it can be concluded that the coefficient of consolidation will depend on the temperature. Therefore the coefficient of consolidation should be directly proportional to the temperature.

Applied Pressure P (kg/cm ²)	Temperature T (°C)	Change in Sample ht., ΔH (mm)	Void Ratio e	Coeff. of Consol. C _v x 10 ⁻⁴ (cm ² /sec)
1.00	20	1.02	0.9179	3.730
	40	0.091	0.9091	0.261
	60	0.089	0.9003	0.115
	80	0.049	0.8955	0.385
2.00	20	1.306	0.8093	2.650
	40	0.106	0.7993	0.228
	60	0.048	0.7946	0.272
	80	0.035	0.7900	0.208
4.00	20	1.190	0.7551	3.396
	40	0.099	0.7450	0.152
	60	0.061	0.7388	0.120
	80	0.028	0.7360	0.343

TABLE 4.1 Results of Tests Conducted on Topser Yellow Clay.

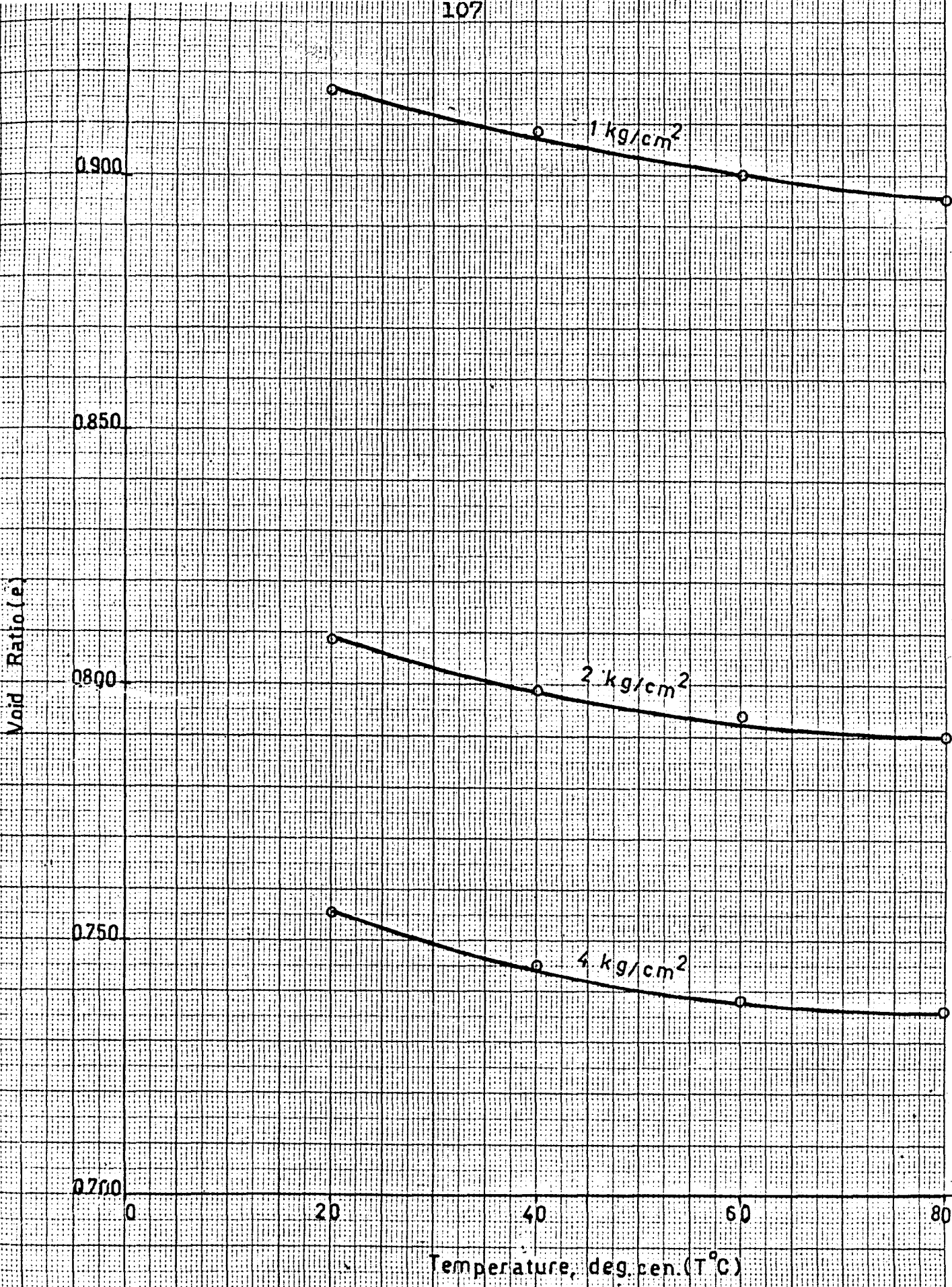


Fig:4. 43. The Family of Temperature - Void Ratio Curves, for Topser-Yellow.

DATA SHEET No. 50. LOGARITHMIC Δ 2 M.M. (4 CYCLE)

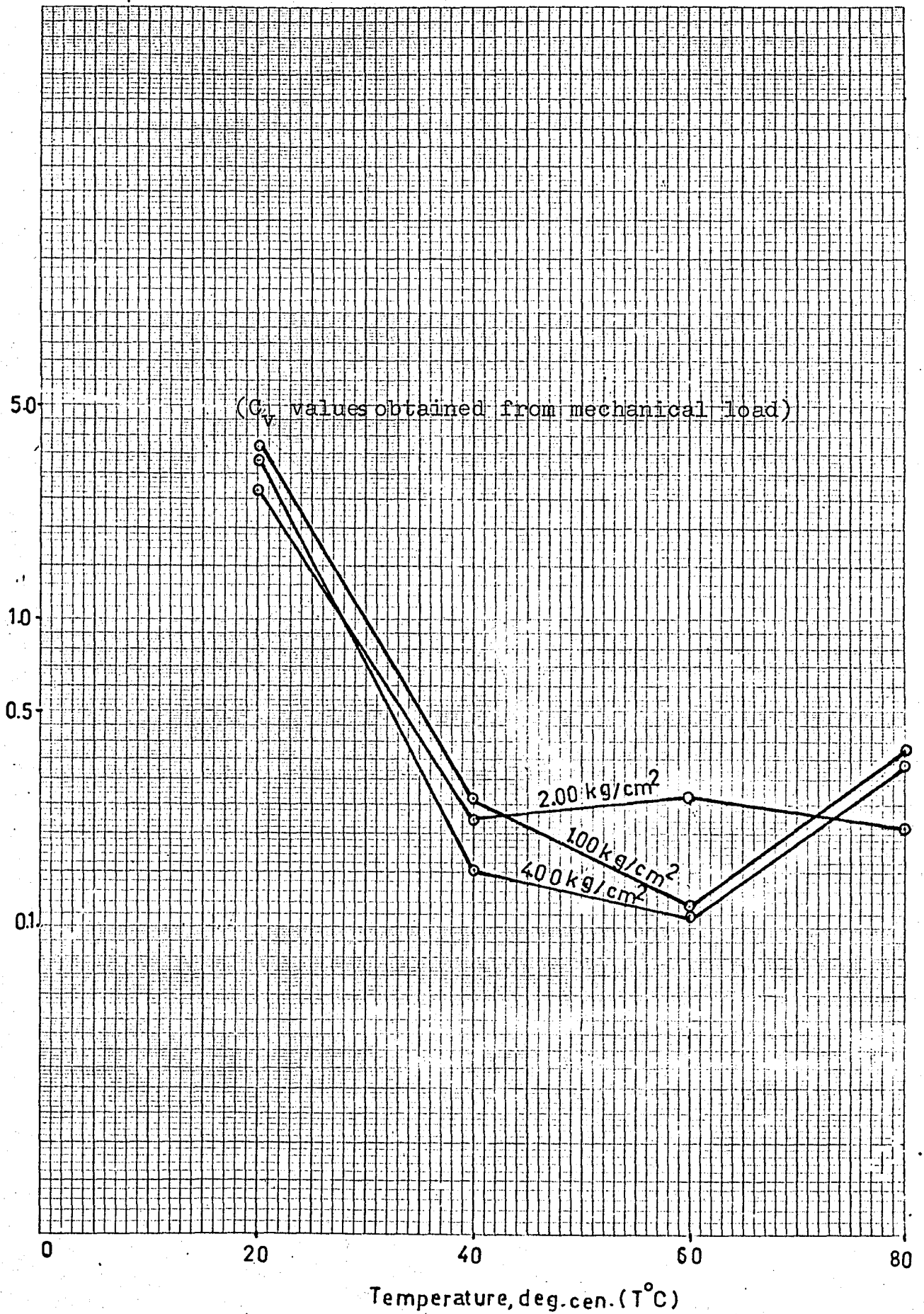


Fig: 4. 42. The Family of Temperature-Coefficient of Consolidation, for Topser Yellow

Applied Pressure P (kg/cm ²)	Temperature T (°C)	Change in sample ht. ΔH (mm)	Void Ratio e	Coeff. of Consol $C_v \times 10^{-4}$ (cm ² /sec.)
1.00	20	1.100	1.3762	3.427
	40	0.112	1.3622	0.292
	60	0.099	1.3497	0.193
	80	0.043	1.3443	0.213
2.00	20	1.590	1.0768	3.852
	40	0.105	1.0640	0.198
	60	0.096	1.0523	0.250
	80	0.074	1.0433	0.150
4.00	20	1.109	1.0100	2.548
	40	0.154	0.9907	0.193
	60	0.099	0.9786	0.155
	80	0.091	0.9674	0.180

TABLE 4.2 Results of Tests Conducted on Boğazköy Grey Clay.

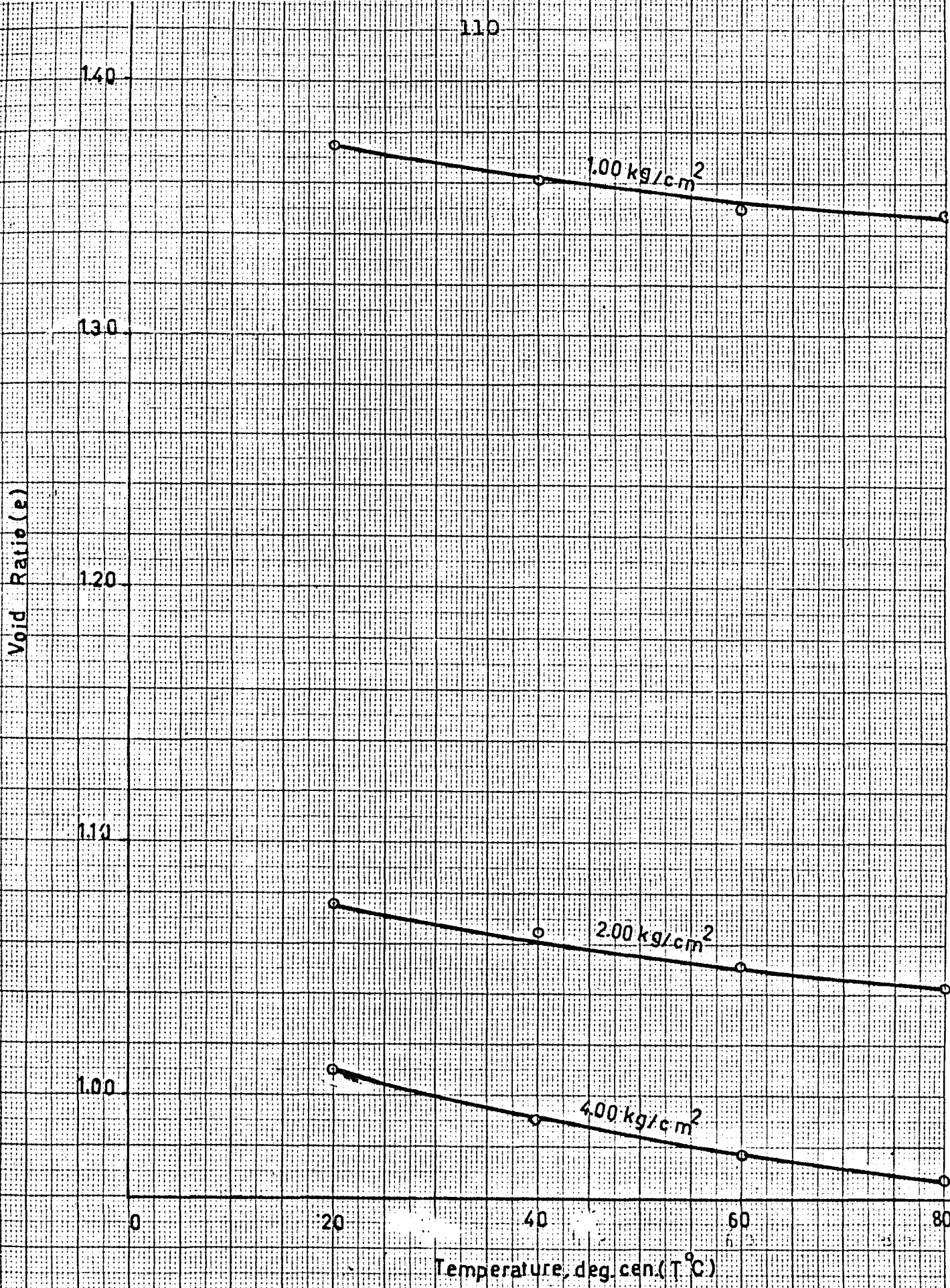


Fig: 4. 45. The Family of Temperature-Void Ratio Curves, for Boğazköy Grey.

DATA SHEET NO. 50. LOGARITHMIC $\times 2$ M.M (4 CYCLE)

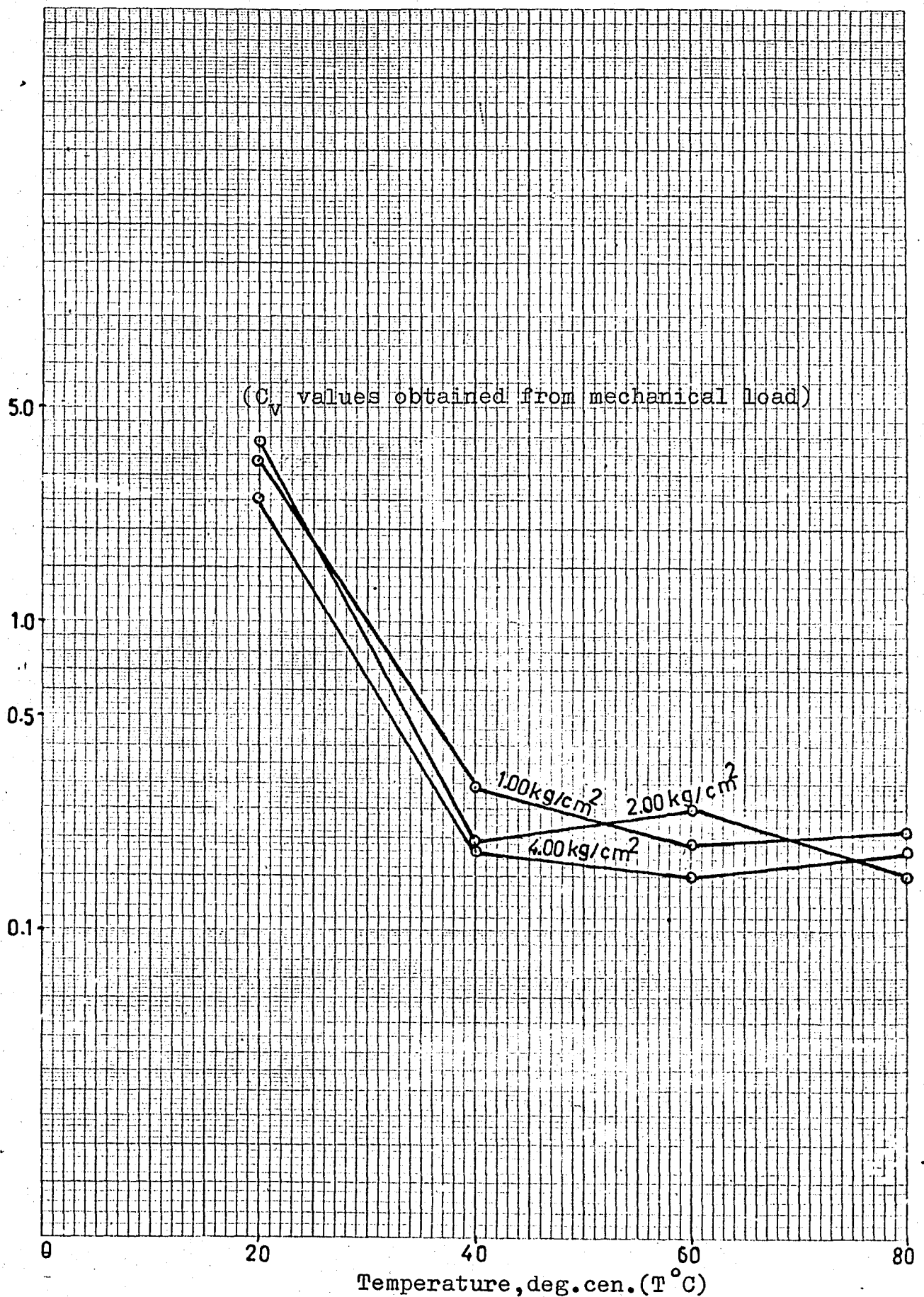


Fig:4. 46. The Family of Temperature-Coefficient of Consolidation for Bogazköy-Grey.

CHAPTER 5 CONCLUSIONS

A review of the test results indicates that the following conclusions can be drawn:

1 - At a constant stress level, maximum effect of temperature on change in sample height is 40°C . Void ratio is effected by change in temperature between the range of 20°C to 40°C the most. Change between the range of 40°C to 60°C and 60°C to 80°C have lesser effects respectively. Temperature increase causes a decrease in volume for a fully drained soil. The reason for this change of volume is because of the temperature, which causes a flow of water out of the system and also causes an increase in ionic movement at the soil particle-water interface.

2 - The coefficient of consolidation due to the temperature change C_{vt} calculated using the semi-log method is small with comparison to the C_v values obtained from mechanical loading. The value of C_{vt} decreases between 40°C and 60°C , but increases when the temperature is raised to 80°C .

3 - The clay with high plasticity showed greater changes due to temperature changes in comparison with the effect of temperature changes on the clay with low plasticity. So we may conclude that at high constant stress levels, application of temperature increases to improve the mechanical properties of a soil can be applied more successfully on clays with high plasticity.

R E F E R E N C E S

- (6) BOWLES, J.E., Physical and Geotechnical Properties of Soils. Mc. GRAW-HILL BOOK COMPANY, INC, 1979.
- (9) BOWLES, J.E., Engineering Properties of Soils and Their Measurement. MC. GRAW-HILL BOOK COMPANY, INC, 1970.
- (7) FINN, F.N., "The Effect of Temperature on the Consolidation of Soil", Special Technical Publication No.126, ASTM, June 1951, pp. 65-72.
- (5) MEANS, R.E., PARCHER, J.V., CHARLES E. MERRILL, BOOKS INC., COLUMBUS, OHIO, 1963.
- (8) PAASWELL, R.E., "Temperature Effects on Clay Soil Consolidation", Journal of the Soil Mechanics and Foundation Division, ASCE, vol. 93, No.SM3, Proc. Paper 5225, May, 1967, pp. 9-22.
- (10) SEARS, F.W., Mechanics, Heat, and Sound. Addison-Wesley Publishing COMPANY, INC, 1958.
- (11) TAYLOR, D.W., Fundamentals of Soil Mechanics. JOHN WILEY and SONS, INC, 1948.
- (4) TSCHEBOTARIOFF, G.P., Soil Mechanics, Foundations, and Earth Structures. Mc.GRAW-HILL BOOK COMPANY, INC, 1951.

- (2) WILUN, Z. and STARZEWSKI, K. Soil Mechanics in Foundation Engineering, International Testbook COMPANY LIMITED, 1972.
- (3) WU, T.H. Soil Mechanics, Allyn and Bacon, INC, 1966.
- (1) YONG, R.N, and WARKENTIN, B.P. Introduction to soil Behavior. The MAC MILLAN COMPANY, 1966.